

**The role of Cornichon (Cni) in axis formation in  
*Drosophila***

**Inaugural-Dissertation  
zur  
Erlangung des Doktorgrades  
der Mathematisch-Naturwissenschaftlichen Fakultät  
der Universität zu Köln**

vorgelegt von  
Sajith Dass  
aus Thodupuzha, Indien  
Köln 2004

Index

**Berichterstatter: Prof . Dr. Siegfried Roth**  
**PD. Dr. Thomas Klein**

**Tag der mündlichen Prüfung: 10.02.2005**

<b>1 INTRODUCTION.....</b>	<b>6</b>
1.1 AXIS FORMATION .....	6
1.2 OOGENESIS IN DROSOPHILA .....	7
1.3 FIRST ROUND OF GRK SIGNALING FROM THE OOCYTE TO THE OVERLYING FOLLICLE CELLS RESULTS IN THE ASSUMPTION OF POSTERIOR IDENTITIES BY THESE CELLS .....	8
1.4 A SECOND ROUND OF OOCYTE TO FOLLICLE CELL GRK SIGNALING ESTABLISHES THE DV AXIS.....	10
1.5 GRK SIGNALING INITIATES THE PROCESS OF THE DV AXIS FORMATION OF THE EMBRYO .....	12
1.6 THE EGF-EGFR REPERTOIRE OF REGULATORS, THEIR INTERACTION IN LIGAND REGULATION AND ROLE IN PATTERN FORMATION.....	14
1.7 CORNICHON AND INITIATION OF GRK SIGNALING FROM THE GERM LINE .....	19
1.8 CELLULAR EXOCYTOSIS, A BRIEF OVERVIEW .....	21
1.9 OBJECTIVES .....	23
<b>2A RESULTS - CORNICHON (CNI).....</b>	<b>24</b>
2A.1 SUB-CELLULAR LOCALISATION OF CNI .....	24
2A.2 EXCESS GRK SIGNAL FROM THE GERM LINE DORSALISES THE EGG SHELL .....	26
2A.3 PATTERNING OF THE EMBRYO AFFECTED WHEN GRK OVEREXPRESSED IN DfH60SCO HETEROZYGOUS BACKGROUND .....	29
2A.4 TIMING OF ONSET IS DIFFERENT BETWEEN NANOSGAL4VP16 AND TUBGAL4VP16 .....	30
2A.5 MIS/OVER-EXPRESSION OF GRK BY TUBGAL4VP16 BUT NOT NOSGAL4VP16 CAN RESCUE CNI FUNCTION.....	32
2A.6 PROTEIN PROFILE OF THE OVARIES USING WESTERN BLOT ANALYSIS .....	35
2A.7 EXPRESSION OF A GRK VERSION THAT LACKS THE CNI INTERACTION DOMAIN AND ITS CONSEQUENCES .....	39
2A.8 ROLE OF JMD IN REGULATION OF GRK TRANSIT TO THE MEMBRANE.....	41
2A.9 EXPRESSION OF ANTI SENSE STAR IN THE GERM LINE.....	42
2A.10 WESTERN BLOT ANALYSIS OF GrkDC5MYC,CNI/CNI, Grk $\delta$ TCMYC AND Grk $\delta$ CMYC.....	44

<b>2B RESULTS - CORNICHON-RELATED (CNIR).....</b>	<b>46</b>
2B.1 ORF CG17262 IS CNIR.....	46
2B.2 VAN EEKENS LINES .....	47
2B.3 L(2)(A1-7) IS A PUTATIVE ALLELE OF CNIR.....	50
2B.4 P ELEMENT INSERTION LINES CLOSEST TO CNIR.....	51
2B.5 MOLECULAR ORGANIZATION OF THE GENOMIC REGION NEAR CNIR: .....	52
<b>2C RESULTS – ENHANCER/ SUPPRESSOR SCREEN.....</b>	<b>55</b>
2C.1 CHROMOSOMAL REGIONS THAT INTERACT WITH CNI (ENHANCERS OR SUPPRESSORS) .....	55
2C.2 CNI ALLELES AND PHENOTYPES .....	55
2C.3 THE SCREEN LOGISTICS .....	59
THE SCREEN .....	59
2C.4 TIER 1: PRIMARY SCREEN .....	59
2C.5 TIER 2 : RETESTING PUTATIVES .....	60
2C.6 TIER 3: SECONDARY SCREEN (INDEPENDENT CONFIRMATION) .....	64
2c.6.1 Suppressor region: <i>Df(3L)VW3 (76A3- 76B2)</i> .....	64
2c.6.2 <i>The 62; 63 region contains two Synthetic lethals and one enhancer region.</i> ..	67
2c.6.3 <i>The Lyra/ senseless region Df42/ 70A2-3;70A5-6</i> .....	70
2c.6.4 <i>The enhancer region (Df99 /86F1;87A9)</i> .....	71
<b>3A DISCUSSION- CORNICHON .....</b>	<b>72</b>
3A.1 CNI IS AN ER TO GOLGI TRANSPORT PROTEIN .....	72
3A.2 GRK TRANSPORTED VIA THE BULK FLOW MODE OF EXOCYTOSIS CAN OVERCOME CNI REQUIREMENT AND PRODUCES ACTIVE GRK .....	73
3A.3 GRK SIGNALING CAN BE RESCUED BUT THE REGULATORY FINE TUNING IS LOST ....	75
3A.4 CNI AND STAR, ARE BOTH INVOLVED IN THE ER TO GOLGI TRANSPORT OF GRK ...	76
3A.5 CLEAVED FORMS OF GRK ARE OBSERVED IN CNI HOMOZYGOUS BACKGROUND .....	77
3A.6 REGULATION MAY ALSO BE AT THE LEVEL OF PROTEIN STABILITY .....	78
3A.7 CNI MEDIATED GRK TRANSPORT PREVENTS HYPERACTIVATION OF EGFR .....	79
3A.8 HYPOTHETICAL MODEL .....	80

<b>3B DISCUSSION – CORNICHON RELATED (CNIR)</b> .....	<b>82</b>
<b>3C DISCUSSION – ENHANCER/ SUPPRESSOR SCREEN</b> .....	<b>83</b>
3C.1 SCREEN COVERAGE .....	83
3C.2 THE SUPPRESSOR WAS IDENTIFIED AS PIPE (PIP) .....	84
3C.3 SALLIMUS (SLS) AND SPROUTY (STY) ARE AMONGST THE LIKELY CANDIDATES ....	84
<b>4 MATERIALS AND METHODS</b> .....	<b>86</b>
4.1 FLY HUSBANDRY .....	86
4.2 FLY LINES USED .....	86
4.3 PREPARATION OF EGG SHELL AND EMBRYONIC CUTICLE .....	87
4.4 FIXATION OF OVARIES FOR IMMUNOSTAININGS .....	87
4.5 ANTIBODY STAINING OF OVARIES .....	87
4.6 IN SITU HYBRIDISATION OF OVARIES .....	88
4.7 ANTIBODIES USED FOR IMMUNO-STAINING .....	89
4.8 PROTEIN EXTRACTION FROM OVARIES FOR IMMUNO BLOT ANALYSIS.....	89
4.9 GLYCOSIDASE ASSAYS .....	90
4.10 WESTERN BLOT ANALYSIS OF PROTEINS .....	90
4.10.1 Electrophoresis and transfer of proteins onto the membrane .....	90
4.10.2 Processing of the transferred membrane and gel.....	90
4.10.3 Primary and secondary antibody treatments.....	91
4.10.4 Detection of western blots.....	91
4.11 ANTIBODIES USED FOR IMMUNO-BLOTS .....	91
4.12 GENOMIC DNA EXTRACTION FROM LARVAE .....	92
<b>5 BIBLIOGRAPHY</b> .....	<b>93</b>
<b>6 SUMMARY</b> .....	<b>101</b>
<b>7 ZUSAMMENFASSUNG</b> .....	<b>103</b>
<b>8 ERKLÄRUNG</b> .....	<b>105</b>
<b>9 LEBENSLAUF</b> .....	<b>106</b>
<b>10 ACKNOWLEDGEMENTS</b> .....	<b>107</b>

# 1 Introduction

## 1.1 Axis formation

One of the primary requirements for a bilaterally symmetric body plan is two perpendicular axes, namely the **Anterior-Posterior (AP)** axis and the **Dorsal-Ventral (DV)** axis. The determination of the two axes is one of the earliest decisions which must be taken for most bilaterian body plans. In the dipteran, *Drosophila melanogaster* both AP and DV decisions are made before the egg is laid. In the eggs both axes can be recognised by distinct egg shell structures which also serve as markers for these axis decisions. The anterior end (where the head of the future embryo would develop) of the egg consist of the micropyle and the operculum (Fig.1A&B). The micropyle is a small pointed structure which functions as a channel for the entry of sperm, associated with the micropyle is a collar structure on the anterior end of the egg shell (Fig.1B). The embryonic larvae hatches out of the egg shell through a structure called the operculum. It is at the anterior of the egg between the micropyle and the **dorsal appendages (DAs)**. The most obvious structures on the egg are the pair of DAs (Fig1.A&B), which are respiratory structures. The posterior of the egg is marked by the aeropyle (Fig1.A&B) which is a structure required for exchange of gases. There is also a subtle difference in the curvature between the dorsal and ventral sides, the ventral side is slightly more convex than the dorsal side (Spradling, 1993).

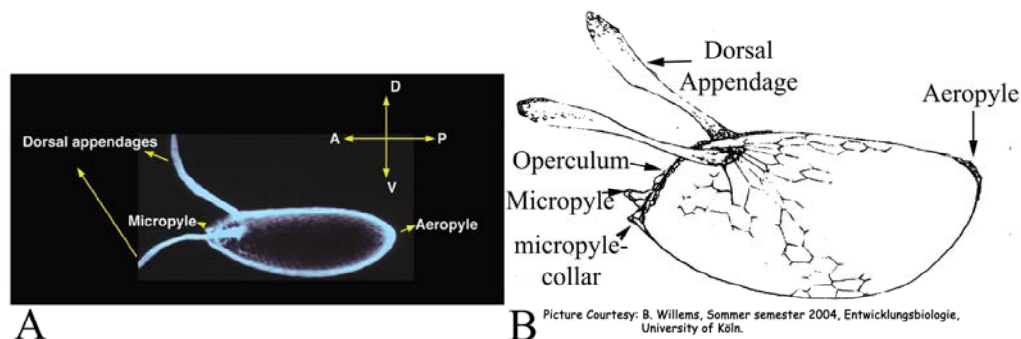


**Fig. 1** The egg of *Drosophila melanogaster*, indicating the egg shell structures which can be used as markers for the morphogenetic processes which patterned the egg. (A) A photograph of an egg laid by wild type female with the AP and DV egg shell structures labeled. (B) A schematic drawing of the wild type egg with the egg shell structures labelled.

## Introduction

Within the egg cytoplasm mRNAs are localised to the anterior and posterior during mid oogenesis where they stay latent until the beginning of embryogenesis. *bicoid* mRNA, responsible for head and thorax development is localised to the anterior cortex and *oskar* mRNA, responsible for the the formation of the primordial germ cells (PGCs/ Pole cells) and the abdomen, is localised to the posterior cortex (for a review see(Riechmann and Ephrussi, 2001).

Therefore, to understand the process of axis initiation it is pertinent to study the processes during oogenesis that initiate these patterns.

### **1.2 Oogenesis in *Drosophila***

Each female fly has a pair of ovaries within which the process of oogenesis occurs. Each ovary is composed of independent chains of structures called ovarioles (Fig.2). Each ovariole consists of the germarium (Fig.2B&C) at the anterior tip, which houses the germ line and somatic stem cells. The germ line stem cell in the niche, at the anterior tip of the germarium undergoes unequal cleavage followed by mitotic amplification. After mitotic amplification, clusters of 16 interconnected germ cells get ensheathed by a monolayer of somatic follicle cells to form an egg chamber (Morgan and Mahowald, 1996; Ray and Schupbach, 1996). As these cells exit from the germarium as egg chambers, one of the germ line cells has been determined by germ line-somatic communication to be the oocyte and the remaining 15 germ line cells develop as nurse cells. The oocyte nucleus is almost transcriptionally quiescent and therefore is dependent on the polyploid nurse cells, for transport of materials required for its growth. The egg chamber is usually arranged in such a manner that the oocyte is positioned posterior to the nurse cells (Godt and Tepass, 1998; Gonzalez-Reyes and St Johnston, 1994; Gonzalez-Reyes and St Johnston, 1998). The egg chambers then go through 14 morphologically distinct developmental stages before the egg is laid (King, 1970; Spradling, 1993). Both the germ line cells and the somatic follicle cells undergo a series of differentiation steps during the transit of the egg chamber through the developmental stages.

This initial polarity which is brought about by the oocyte-nurse cell arrangement is finally converted into both the axes of the egg and embryo by reciprocal communication between the oocyte and the overlying follicle cells. This involves two rounds of signaling

## Introduction

by the TGF- $\alpha$  like ligand, Gurken (Grk), emanating from the oocyte and signaling to the *Drosophila* Epidermal growth factor Receptor (DER/EGFR), Torpedo (*top*), on the follicle cells (Gonzalez-Reyes et al., 1995; Gonzalez-Reyes and St Johnston, 1994; Roth et al., 1995).

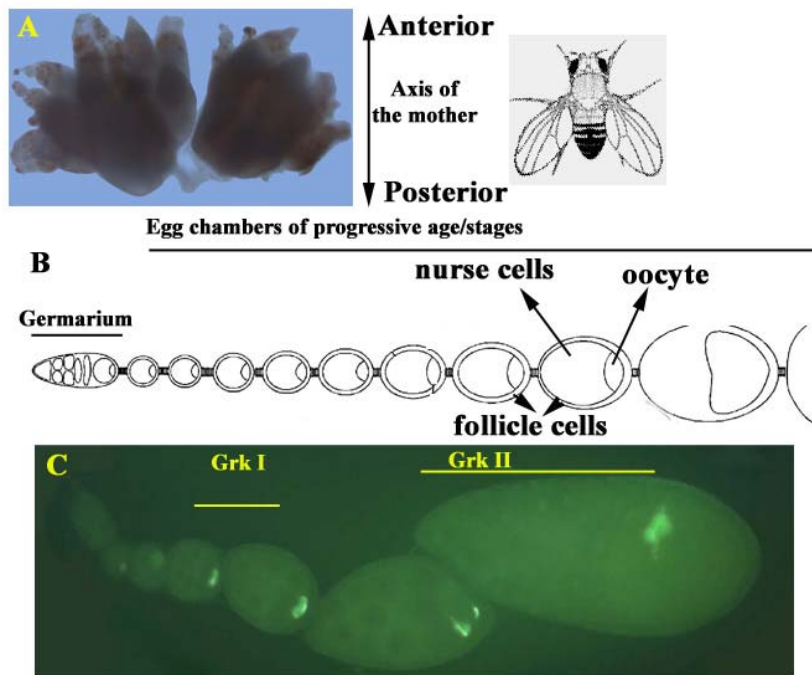


**Fig. 2** *Drosophila* ovary (A) and the organisation of ovarioles which make up the ovary. Each ovariole (B&C) has the germarium which is at the anterior end and consists of the germ line and somatic stem cells. Egg chambers of progressive stages are pushed out of the germarium as the somatic follicle cells ensheath the 16 germ cells. One of the germ line cells is also determined to be the oocyte as the cells exit the germarium. The egg chambers have been categorised into fourteen distinct morphological stages before the egg is laid (King, 1970). Picture C is an RNA *in-situ* for *gurken* (*grk*) indicating both the Grk signals in a fixed tissue (ovariole), the *in-situ* is visualised using a fluorescent TSA substrate and HRP reaction.

### 1.3 First round of Grk Signaling from the oocyte to the overlying follicle cells results in the assumption of posterior identities by these cells

Grk signals at mid oogenesis (stage 6/7) from the oocyte to the abutting follicle cells, where the signal is perceived by the DER. The oocyte nucleus at this stage is located at a symmetric position towards the posterior of the oocyte. The follicular epithelium at this stage is divided into main body and terminal follicle cells. Both populations of the terminal follicle cells, at the anterior and posterior ends of the egg chambers respectively,

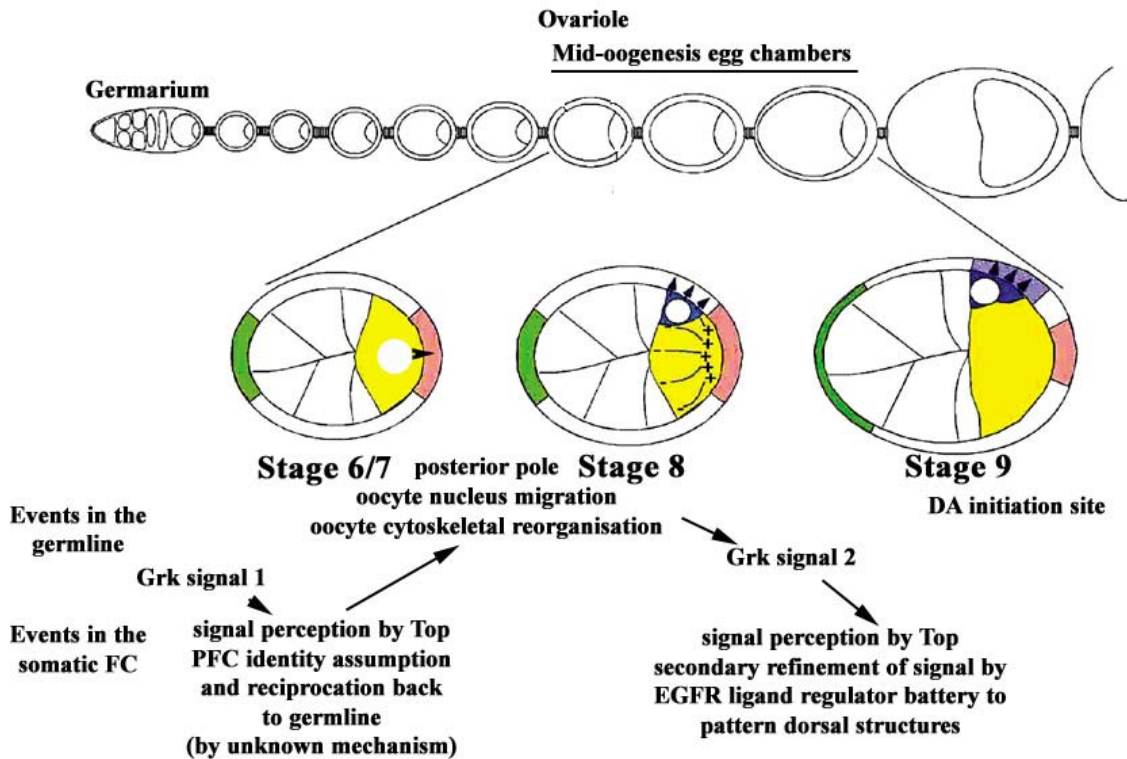


Fig. 3 Schematic representation of the two rounds of Grk signaling from the oocyte to the overlying follicle cells. The first round of Grk signaling from the oocyte (yellow shaded) to the follicle cells via DER, resulting in the assumption of posterior fates by the signal receiving cells (pink shaded), which reciprocate the signal by an as yet unknown mechanism back to oocyte. On perception of the cue from the posterior follicle cells (PFC), the oocyte nucleus migrates from its erstwhile symmetric posterior position to a corner of the anterior cortex. From its new residence, the oocyte now starts second round of Grk signaling, thus initiating the dorsal side of the egg (and future embryo). Dorsal egg shell structures are patterned on the dorsal sides by secondary signal refinement in the receiving cells which involves a highly regulated process involving a number of EGF pathway components to pattern the DAs. In the picture, the follicle cells shaded green are the anterior follicle cells, which is the default identity of these cells in the absence of both rounds of Grk signal. Picture modified from (Roth, 2003).

differ from the main body follicle cells, in their competence to respond to the Grk signal. The two terminal follicle cell populations also contain a symmetric prepattern which is independent of Grk signaling (McGregor et al., 2002; Xi et al., 2003). Grk signals directly to about 200 cells, which extend 10-11 cell in diameter from the posterior pole, via the DER to induce posterior fates in these cells. Both terminal follicle cells can be induced to assume posterior fates by Grk signaling, as has been shown by the assumption of posterior fates by anterior terminal cells in *dicephalic* mutants where the oocyte position is altered without affecting detectable Grk signaling (Gonzalez-Reyes and St

## Introduction

Johnston, 1998). Further, in the absence of Grk signaling both the populations of terminal follicle cells develop as anterior follicle cells, as has been observed in conditions where Grk signaling is compromised. This property of assumption of the default anterior fates in the absence of Grk signal results in eggs which are symmetrical in appearance and have anterior egg shell structures at the posterior end of the egg i.e., two micropyles on either end. (Fig.8B) (Gonzalez-Reyes et al., 1995; Roth et al., 1995).

The posterior follicle cells then communicate back to the oocyte by an as yet unknown signal (back signal), resulting in a cytoskeletal reorganisation in the oocyte. In early stages of oogenesis the microtubules (MTs) are nucleated from a **microtubule organizing centre** (MTOC) present at the posterior of the oocyte (Theurkauf et al., 1992). From the posterior MTOC microtubule projections pass through the ring canals into the nurse cells to function in nurse cell to oocyte transport. The signal from the PFC destabilises the posterior MTOC and at the same time a diffuse anterior MTOC emerges, resulting in the reversal of the polarity of the oocyte microtubule network.

Concurrent and/or consequent to these cytoskeletal reorganisation also the oocyte nucleus which was at a symmetrical position at the posterior of the oocyte now appears at a corner at the anterior cortex of the oocyte. The oocyte begins a second round of germ line to follicle cell signaling, which initiates the dorsoventral axis of the egg and embryo.

### **1.4 A second round of oocyte to follicle cell Grk signaling establishes the DV axis**

That the migration of the oocyte nucleus is not just a correlation but indeed establishes DV polarity, has been shown by laser ablation studies of the oocyte nucleus which resulted in the loss of dorsal chorion structures (Montell et al., 1991). In the absence of nuclear migration as in *mago nashi* (*mago*) mutants (Micklethwait et al., 1997) and in cases where Grk signal is delayed (Peri and Roth, 2000), eggs develop that have a normal AP axis but lack the DV axis. The position at the anterior cortex to which the oocyte nucleus migrates is not predetermined by extracellular processes. In alleles of *spaghetti squash* (*sqh A21*), which have binucleate oocytes, both nuclei move to the anterior cortex and induce dorsal chorion fates independently. The choice of the position occupied by each of these oocyte nuclei is random and there has been no statistical correlation observed, with

## Introduction

respect of the position of one with the other (Roth et al., 1999). Although, the anterior asymmetrical positioning of the oocyte nucleus is necessary for the establishment of the DV axis it does not define the dorsal side of the egg. It has been observed that in 21% of the late egg chambers of *cornichon (cni)* mutants the oocyte nucleus has migrated but the eggs laid are still asymmetric and lacking any sign of DV polarity (Roth et al., 1995).

The oocyte nucleus initiates a second Grk signaling from its new location at the anterior cortex, to initiate the process of DV axis formation of the egg shell and the future embryo. In the dorsal follicle cells the initial paracrine signaling event triggers an autocrine amplification by two other EGF ligands, Spitz (*spt*) and Vein (*vn*), resulting in the formation of the twin DAs. This patterning mechanism is initiated by a positive feedback on DER signaling. Grk induces the expression of *rho* in dorsal follicle cells. Spi only becomes an effective ligand, due to the cleavage of the full length Spi by Rho, which is a seven transmembrane Golgi resident serine protease (Urban et al., 2001). The production of activated Spi leads to increased EGFR signaling and thus to an autocrine self-amplification of the signal. Spitz is diffusible and thus this signal amplification has the potential to spread throughout the follicular epithelium. This spreading is prevented in two ways. First, *rho* can be induced only in anterior follicle cells since its activation requires both TGF- $\alpha$  and TGF- $\beta$  signaling (Peri and Roth, 2000). The TGF- $\beta$  ligand, Dpp, is produced from an anterior ring of follicle cells (Twombly et al., 1996) and spreads only upto a certain distance towards the posterior. This sets the field where *rho* can be activated and in turn, prevents Spi autoactivation from spreading to the posterior pole. The threshold to initiate autoactivation is high and thus remains critically dependent on a certain level of Grk signaling. This is supported by observations from the phenotypic series of *grk* alleles and from the fact that reducing the dose of *grk* by half, leads to a fusion of the DAs (Neuman-Silberberg and Schupbach, 1994; Peri et al., 1999). The dependency on Grk signaling restricts Spi autoactivation to the dorsal side of the egg chamber. A consequence of the high-level EGFR activation is the localised expression of the diffusible inhibitor Argos (*aos*), which alters the profile of signaling. This sequential activation, amplification, and local inhibition of the EGFR forms an autoregulatory cascade that leads to the splitting of an initial single peak of signaling into two, thereby patterning the DAs (Wasserman and Freeman, 1998).

## Introduction

The oocyte nucleus besides migrating to the anterior dorsal cortex of the oocyte has to be maintained in that position for considerable time to bring about DV polarity. In *cap'n*

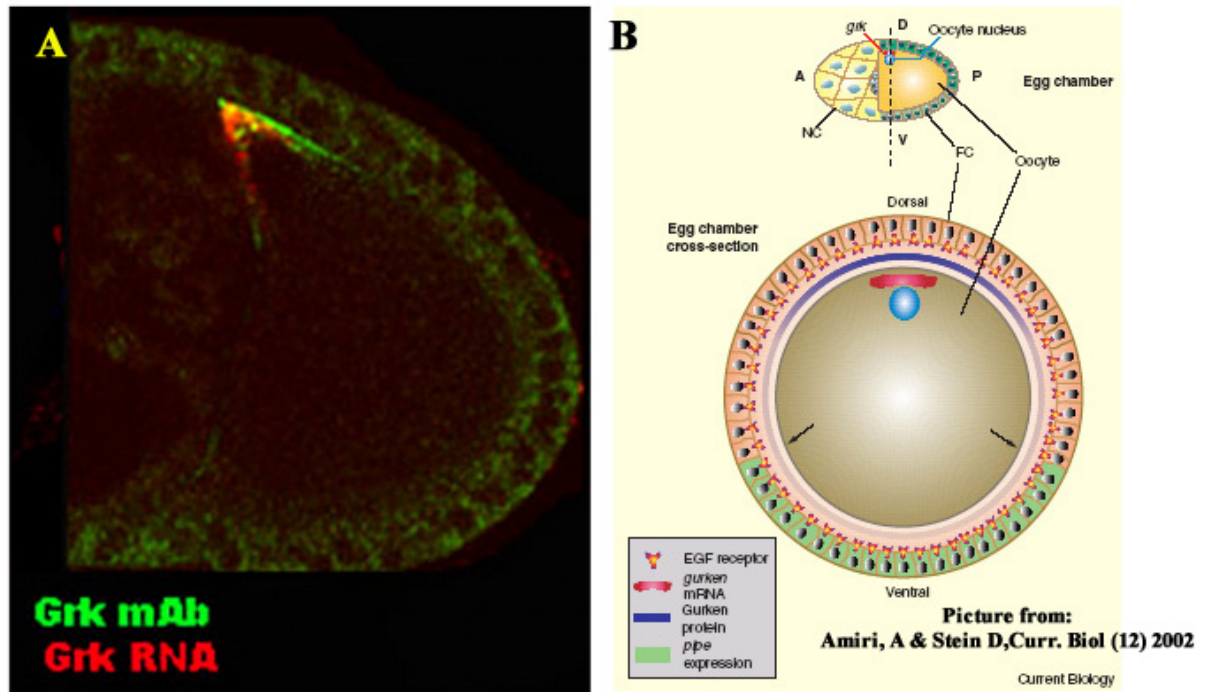


**Fig. 4** Second round of Grk signal and its consequences. In A is a picture of a combination of FISH (in red) and immunostaining for the anti-Grk 1D12 (in green) monoclonal antibody to show the tight localization and restriction of the signal. In B is a schematic representation from a review ((Amiri and Stein, 2002) to indicate the restriction of the ventralising signal (green in B), pipe (pip), by the Grk gradient which is initiated from the oocyte.

*collar (cnc)* alleles, where the oocyte nucleus initially migrates correctly but then slides back to the posterior pole, the eggs exhibit no DV polarity (Guichet et al., 2001).

*grk* RNA and protein are detectable tightly localised to the oocyte nucleus in wild type and in most conditions where the RNA and/or protein are detectable (see Fig.4A).

See Fig.3, for an overview of these processes.

## 1.5 Grk signaling initiates the process of the DV axis formation of the embryo

There are at least three types of follicle cells that can be distinguished by their gene expression pattern, by the eggshell structures they secrete and by the function they fulfil

## Introduction

for embryonic axis induction along the DV axis of the egg chamber. These are the dorsal cells that express *kekkon* (*kek1*) (Ghiglione et al., 1999) and are responsible for dorsal chorion structures including the dorsal appendages, the ventral cells that express *pipe* (*pip*) and contribute the cues for the embryonic DV axis (Sen et al., 1998) (Nilson and Schupbach, 1998) (Fig.4B) and the lateral cells that neither express *kek1* nor *pip*. Grk signaling induces secondary signaling cascades that define these expression domains, as in the patterning of the DAs. Being present in a concentration gradient Grk might act as a morphogen, i.e. *kek1* and *pip* could be direct target genes whose activation or repression depends on particular concentration thresholds of Grk. Genetic mosaic studies support the latter view (James et al., 2002; Pai et al., 2000) (Peri et al., 2002). Analysis of mutant follicle cell clones that are incapable of transmitting the Grk signal (e.g: clones of mutations in downstream components of DER signaling, like *Ras* or *Raf*) show ectopic expression of *pip* in a cell-autonomous manner. Conversely, if the DER pathway is ectopically activated in cell clones, autonomous activation of *kek1* as well as autonomous repression of *pip* is observed.

The expression of *pip* in the ventral follicle cells is necessary for the establishment of embryonic DV polarity (Nilson and Schupbach, 1998; Sen et al., 1998) (See Fig.4B). *pip* mutant females produce eggs with normal eggshells, the embryos that develop in these eggs however are completely dorsalized. The embryos are dorsalised because they lack DV polarity during gastrulation and produce dorsalmost cell fates around the entire embryonic circumference. *Pip* encodes a heparin sulphate 2-*O*-sulphotransferase and is probably involved in the modification of glycosaminoglycans of the extra cellular matrix (ECM) (Sen et al., 2000). The exact nature of the ECM components modified by Pipe is not yet known, but irrespective of the identity of these components, the *pipe* expressing cells secretes the activated ECM component into the space between oocyte and follicle cells before the latter starts producing the inner (vitelline) and the outer (chorion) eggshell membranes, respectively. Consequently, after egg deposition the modified ECM components are present on the vitelline membrane facing the embryo or on the surface of the embryo itself. They initiate a proteolytic cascade that comprises a chain of four serine proteases that culminates in the activation of the extracellular ligand Spaetzle (*spz*) (Morisato and Anderson, 1995; Schneider et al., 1994). Spz has structural similarities to

## Introduction

nerve growth factors (DeLotto and DeLotto, 1998; Mizuguchi et al., 1998; Morisato and Anderson, 1994).

Spz activates the transmembrane receptor Toll which is uniformly expressed on the surface of the embryo (Hashimoto et al., 1988). Activated Toll relays the extracellular signal to the embryonic nuclei by regulating the nuclear import of the NF- $\kappa$ B transcription factor Dorsal (*dl*).

### **1.6 The EGF-EGFR repertoire of regulators, their interaction in ligand regulation and role in pattern formation**

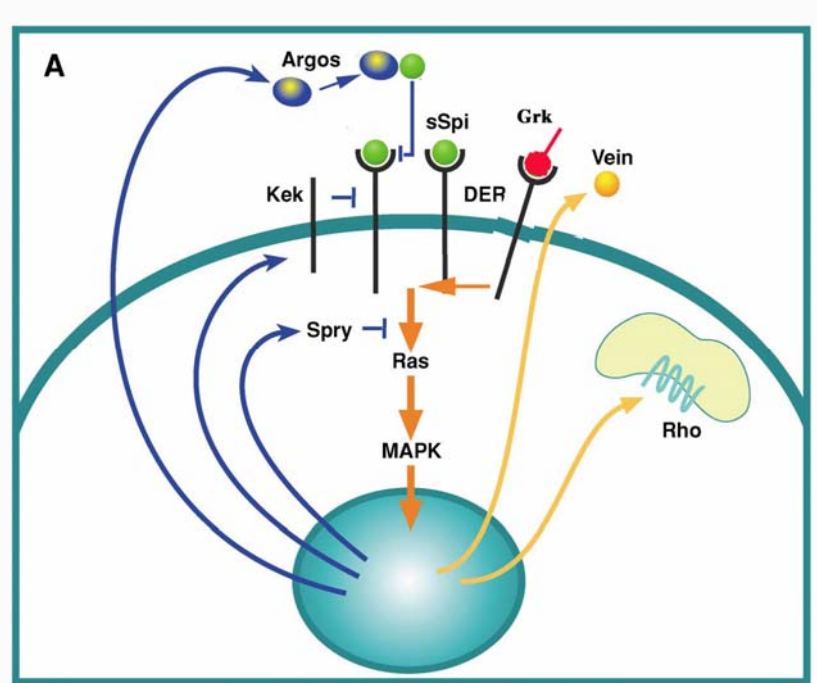
Grk is one of the four ligands in the fly that is capable of activating the DER. There is only one DER in *Drosophila*. DER belongs to the EGFR/ErbB family of receptor proteins and is similar to the mammalian family members in overall structure. The extracellular region has the typical four domains, including two cysteine-rich domains, required for ligand binding (Livneh et al., 1985). There are two different splice variants encoding two different protein isoforms and it is not clear whether there is a distinct role to each of the forms (Schejter et al., 1986). The regulation of the receptor is not via differential tissue specific expression as it is broadly detected in diverse tissues during development (Zak et al., 1990). The wide array of roles played by DER during development in different tissues have complicated the identification of its developmental roles by simple analysis of loss of function phenotypes during embryonic or postembryonic stages (Clifford and Schupbach, 1989). The use of dominant negative receptor constructs, temperature sensitive or hypomorphic mutations in the receptor, or mutations in distinct ligands, have been instrumental in identifying discrete roles for DER in different developmental processes. (For a list of all the different developmental processes that DER has been implicated in, see Table 1 of review(Shilo, 2003).

During oogenesis, the removal of DER from the follicle cells using mitotic clones results in eggs laid which lack both AP and DV polarity (Gonzalez-Reyes et al., 1995). Expression of a constitutively active version of the receptor in the follicle cells using the UAS/Gal4 systems results in dorsalised eggs. Expression all along the follicle cells of the constitutively active construct in a background where the germ line is mutant for the ligand responsible for the initiation of the pathway, Grk, results in eggs which lack all

## Introduction

polarity but have DA material deposited all along the anteroposterior axis of the egg (Queenan et al., 1997). Removal of the ligand from the signal emitting cell (oocyte) during oogenesis results in eggs which lack both DV and AP polarity (Neuman-Silberberg and Schupbach, 1993; Roth et al., 1995).

In order to understand the roles of the DER in initiating the two axes and patterning of the egg shell it is important to know the current state of knowledge as to how the different components interact with each other. Although a lot is known about the activation of the MAPK pathways downstream of the receptor, emphasis will be laid here only on the events upstream of these pathways which are responsible for ligand regulation and the receptor occupation by these ligands.



Picture modified from (Shilo, 2003)

**Fig. 5: Overview of the DER pathway. Grk (red) signal from the oocyte to the follicle cells activates the pathway during oogenesis. Secondary signal amplification and refinement of the pattern formed is brought about by the interaction of several DER components, which in clued another ligand Spi (green) which has to be cleaved to form the active moiety sSpi (green), at least three inhibitors Aos, Kek1 and Sprouty (sty) which act at different levels in the pathway. Two proteins, Star (S) and Rhomboid (Rho) are required for the activation of EGF ligands, esp Spi, via the regulated intermembranous proteolysis (Rip) pathway.**

Besides Grk, there are three other activating ligands for DER, they are Spi, Vn and Keren (*krrn*). Vn is an atypical EGF ligand because it is more similar to the neuregulin type than to EGF type of ligands. It is also the ligand which shows a weaker activation capacity and

## Introduction

is required in tissues where low level activation is required (Schnepp et al., 1998; Schnepp et al., 1996).

Spi, Krn and Grk are produced as precursor molecules with transmembrane domains (Fig.6A&B). Processing of these molecules to produce a secreted ligand was shown to be a key regulatory step in DER activation. This mechanism was first established for Spi and subsequently been also applied to the other two ligands (Schweitzer et al., 1995). The spatio-temporal pattern of Spi-induced DER activation is thus dependent upon regulated processing of Spi.

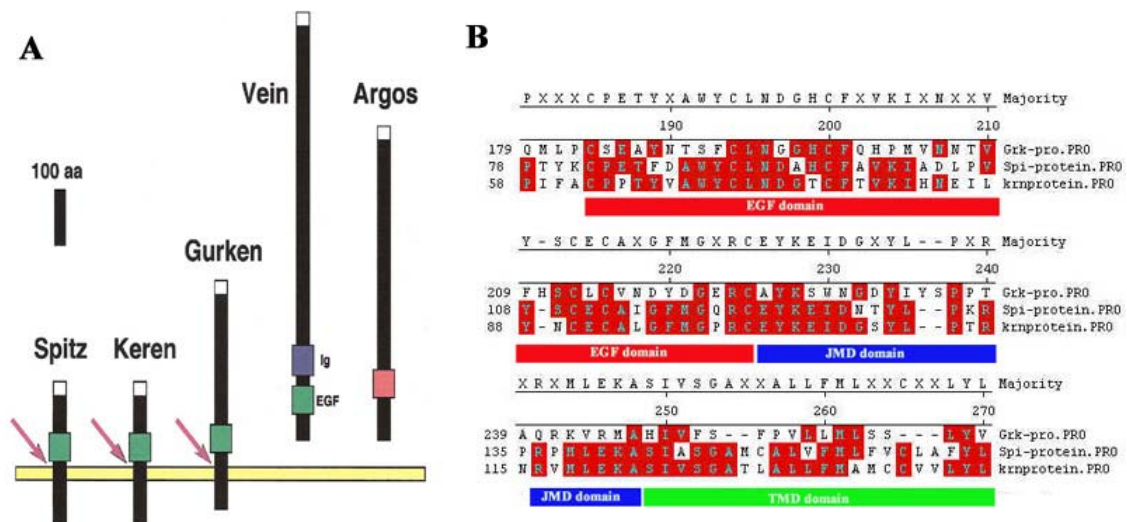


**Fig. 6 Comparison of the EGF ligands in *Drosophila*.** (A) Comparison of the protein domains and domain architecture between the different ligands. A red arrow indicates the position where the ligands are cleaved to form the active moiety by Restricted intermembranous proteolysis (RIP) mechanism. Vein the only secreted ligand is also shown. Argos, an inhibitor which functions by a ligand sequestering mechanism, and possess a region which show low level similarity with the EGF domain (pink bar) also is included. (B) Alignment of the EGF (red line below), Juxta membrane domain (JMD) (blue line below) and Transmembrane domain (TMD) of Grk, Spi and Krn indicate that Spi and Krn (65% similar in EGF domain) are more similar to each other than Grk (Grk and Krn, 35% similar).

Spi, rho and Star(S), along with single-minded (*sim*) and pointed (*pnt*) belong to the zygotc spitz group of genes due to the similarity in embryonic phenotypes between them. Spi, rho and S have been genetically shown to be required in the same cell for the production of the active ligand (Mayer and Nusslein-Volhard, 1988). The biochemical nature of the regulation of EGF ligands by S and Rho has been investigated. The first step

## Introduction

of regulation in Spi processing is the trafficking of the protein from the endoplasmic reticulum to the Golgi compartment. This step is carried out by S, a novel type II transmembrane protein (Kolodkin et al., 1994; Pickup and Banerjee, 1999), that serves as a cargo receptor and associates with Spi (Lee et al., 2001; Tsruya et al., 2002). The exact region on Spi that interacts with Star has not been mapped, although a few amino acids immediately after the transmembrane region leads to highest retention in the ER, when removed (Lee et al., 2001).

In the Golgi, the membrane bound ligand is cleaved by a Golgi resident seven membrane pass serine protease, Rho-1 (Bier et al., 1990). *rho-1*, is one of the four rhomboids found in the fly genome. *rho-2* /Brother of Rhomboid (*brho*) / Stem cell tumour (*stet*), *rho-3*/roughoid (*ru*) and *rho-4* are the other three members (Guichard et al., 2000; Schulz et al., 2002). Rhomboid is essential for Spi cleavage. The catalytic domain of Rho resides within its conserved transmembrane domains and the substrate domain on the ligand also is in the transmembrane domain. Hence Rho gives rise to intramembrane proteolysis of the ligand whose transport to the Golgi is regulated by Star, so this mechanism of regulation of EGF ligand activity has been termed the **Regulated Intramembraneous Proteolysis** (RIP) (Lee et al., 2001; Urban et al., 2001). (See Fig.7 for a schematic representation of the RIP paradigm). *spi* and *S* are broadly expressed where as the expression of *rho* is extremely dynamic (Bier et al., 1990). *rho* pattern is almost identical to the pattern of DER-induced MAPK activation (Gabay et al., 1997). *rho* expression is thus one major limiting step in DER activation. Intriguingly, in some tissues DER activation induces *rho* expression. In tissues where multiple cycles of DER activation are required, the induction of *rho* expression in the responding cells leads to additional rounds of ligand processing (Sapir et al., 1998; Wasserman and Freeman, 1998).

*krr* is the last identified of the EGF ligands and although there has been no loss of function analysis done so far, expression studies have shown that Krn goes through S-Rho mediated cleavage/activation and is independent of S-Rho at low level activity/cleavage (Reich and Shilo, 2002).

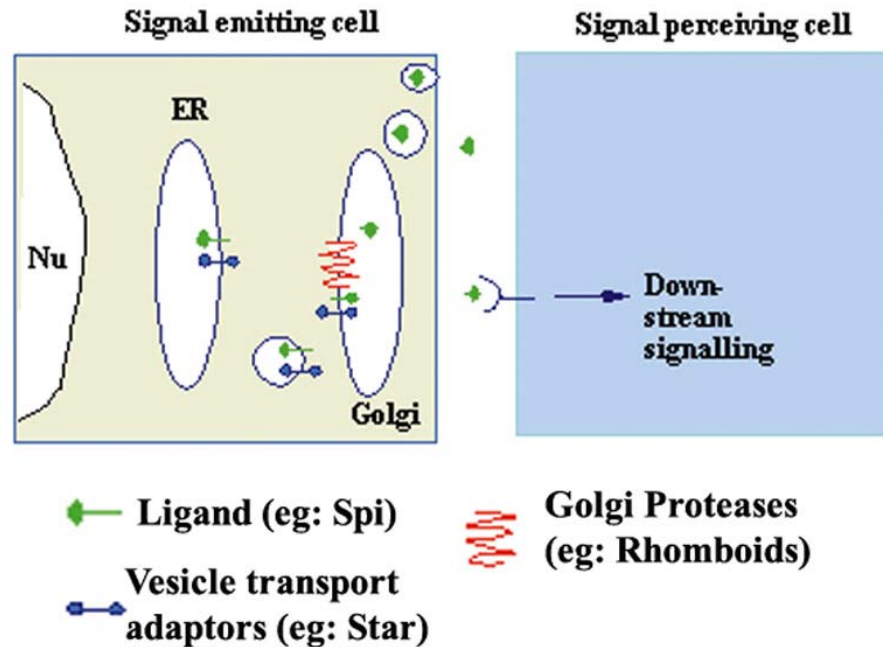


Fig. 7 The Rip pathway of EGF ligand regulation. Star (in blue) functions to ferry the unprocessed Spi (green) from the ER to the Golgi. In the Golgi, it is cleaved in the transmembrane region by Rhomboid (red), a seven membrane pass serine protease, so that active Spi can now be secreted to initiate down stream signaling via DER.

Elucidation of the mechanisms regulating Spi processing has led to insights regarding the other two transmembrane ligands. It was shown that Grk can undergo cleavage that is Rho and S dependent in cell culture. Further, in culture the full length and secreted forms (lacking the TMD and cytoplasmic domains) of Grk have been shown to have differential cell adhesion properties. While cells expressing the full length form adhered together, in case of cells expressing the secreted form no adhesion was observed (Ghiglione et al., 2002). In the ovary, Grk is found predominantly in the cleaved form and is endocytosed by the follicle cells receiving the signal (Peri et al., 1999). A member of the *rho* family (*brho*, *rho-2* or *stet*) that is expressed in the oocyte may carry out Grk processing (Guichard et al., 2000; Schulz et al., 2002). Genetic interactions show that Star may also be required (Ghiglione et al., 2002).

However several questions are still not clear regarding EGF ligand production from the germ line. Germ line clones of *spi*, has absolutely no effect on the egg shells structure. So

## Introduction

though there can be very regulated refinement after DER has been activated, there must be some other mechanisms to initiate the signal.

Cornichon (*cni*), a small hydrophobic protein, is absolutely required for Grk signaling from the germ line. The role of *cni* in initiating the Grk signal has not been understood so far.

### 1.7 Cornichon and initiation of Grk signaling from the germ line

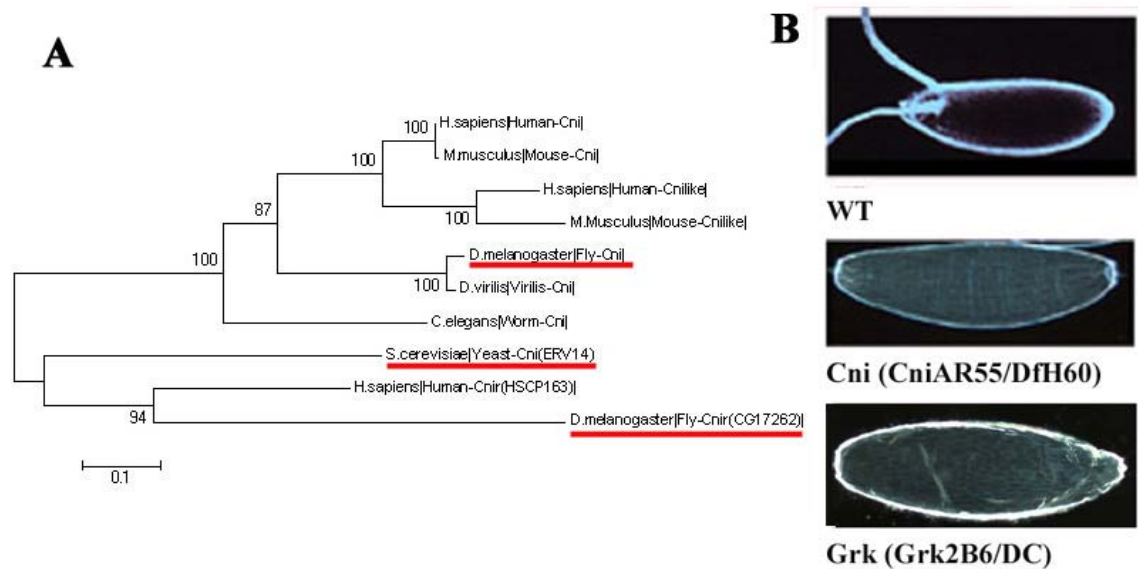


**Fig. 8** Cornichon is one of the founding members of a family of small hydrophobic proteins found across a number of species. **A:** is a dendrogram representing the known *cni* members from the Swiss-prot data base. Underlined with a red line are the two members of *cni* in flies and the yeast member Erv14p. **B:** The eggs laid by *grk* amorphic mothers are identical to the eggs laid by *cni*.

Cni is a small hydrophobic protein of 144 amino acids and is required in the germ line for the correct DV axis initiation in *Drosophila*. Cni is absolutely required for the initiation of Grk signaling from the oocyte to the overlying follicle as can be seen by the fact that eggs laid by *cni* amorphic mother exactly phenocopy the Grk amorphic egg shell phenotype (Fig.8B). The expression levels of *cni* is low and does not show any specific mRNA localization patterns (Roth et al., 1995). *cni* members are present all across the animal kingdom and show varying degrees of similarity with each other (Fig.8A). Cnih, the mouse homologue of Cni shows 93% similarity (68% identity) with the *Drosophila*

## Introduction

protein (Hwang et al., 1999). Although, Cni homologues from systems as varied as humans (Utku et al., 1999) to ascidians (Davidson and Swalla, 2001) have been reported, very little is understood about the cellular and biochemical roles of these proteins in different systems.

ER-vesicle protein of 14 kD (Erv14p) is the Cni homologue of *S. cerevisiae*. It is one of the components of the COP-II-coated ER derived transport vesicles in yeasts. COP-II mediated vesicle transport is responsible for the ER to Golgi anterograde transport of proteins in the cell. Erv14p is required for the polarised transport of Axl2p, a protein responsible for selection of axial sites and which normally localises to nascent bud tips or the mother bud neck. In the *erv14* mutants Axl2p accumulates in the ER, while other secretory proteins are transported at wild type rates. Haploid cells that lack *erv14p* are viable but display a modest defect in bud site selection (Powers and Barlowe, 1998). The membrane topology of Erv14p was shown to be three membrane pass structure by factor XA cleavage assays. Erv14p has been proposed to coordinate COP-II vesicle formation with incorporation of specific cargo (Powers and Barlowe, 2002).

In flies *cni* has been shown to interact with *grk* and *sec23* in yeast two hybrid assays. The interaction with Sec23 was not reproducible with protein-protein interaction assays. Grk and Cni interacts with each in protein-protein interaction assays. The luminal side of Cni interacts with the JMD region of Grk (C. Boekel, Ph.D work) (Fig.9B).

Based on these data the working hypothesis is that this interaction between Cni and Grk specifically enriches Grk into COP-II vesicles on its route of transit from the ER to Golgi (Fig.9A).

CG17262 is an open reading frame in the fly genome which shows highest similarity to *cni*, hence called *cornichon related (cnir)*. There is no loss of function alleles of *cnir* and absolutely nothing is known about the cellular function of the protein coded by this ORF. *cni* and *cnir* are synthetically lethal (C. Boekel, Ph.D work). The only other closely related member to *cnir* is one of the three hundred ORFs of undefined genes expressed in human CD34+ Haematopoietic Stem/Progenitor Cells (HSPC), namely HSPC163 (Zhang et al., 2000).

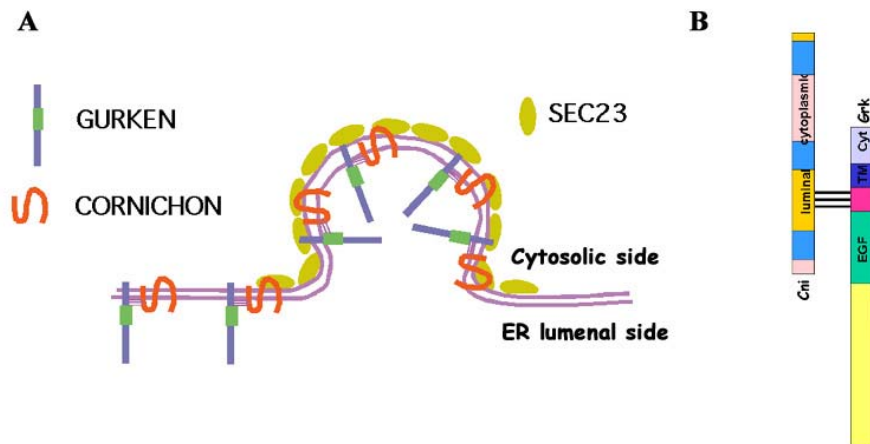


**Fig. 9 Hypothetical model for the interaction between Cni and Grk. A: Shows a model for the interaction between Grk and Cni at the COP-II budding sites of the ER. B: Scheme representing the regions luminal region of Cni (yellow) interacting with the JMD (pink) domain of Grk.**

## 1.8 Cellular Exocytosis, a brief overview

Glycosylation is a characteristic post-translational modification in eukaryotic cells. There are two types of glycosylations namely N-glycosylation and O-glycosylation based on the amino acid side chain on the protein onto which the sugar residues are added. The two types of glycosylations differ from each other with respect to both, the subcellular location where the sugars are added and also the mode in which they are added. As the freshly translated protein leaves the ribosome and enters the ER a multi branched high mannose containing sugar structure is added onto the N-side chains of Asn/Gln acids from dolichol phosphate in a single step reaction. The high mannose branched sugar chain is differentially modified through its exocytic route from the ER to the cis-Golgi structures. Endoglycosidase H (Endo H) is an enzyme which can remove the initial branched high mannose sugar moiety that is added onto the N-amino acid. But as this branched structure matures through its exocytic transit it becomes resistant to Endo H. Very few proteins retain their Endo-H sensitivity in the mature form that has undergone the transit through the Golgi and hence, Endo-H sensitivity in most cases acts as a litmus test for proteins retained in the ER.

O-glycosylations on the other hand, are the stepwise addition of sugar moieties onto the OH-side chains of Ser/Thr amino acids that takes place in the cis and trans-Golgi

## Introduction

structures. In the case of O-glycosylation reaction it is carried out as a single sugar is added by a single enzyme catalysed reaction, there is no transfer of large branched sugar structures as in the case of N-glycosylation reactions (Lodish et al., 1999).

The ER is the entry point into the secretory pathway for newly synthesized proteins. Ribosomes dock onto a protein pore in the ER membrane, thereby releasing the nascent polypeptide into the lumen of the ER. The primary role of the ER is to provide a milieu that facilitates protein folding. Besides the addition of N-linked glycan chains, post-translational modification of nascent chains, including addition of and hydroxylation of proline residues, first occurs in the ER. The next region in the exocytotic transit of the protein is the Golgi apparatus, a series of cisternae housing enzymes that function in glycan side chain modification and proteolytic cleavage. Transport of proteins between these various compartments of the secretory pathway occurs via small vesicles that are generated at a donor compartment and fuse with a downstream acceptor compartment. COP-II coated vesicles are the vesicles that have been associated with ER to Golgi anterograde transport of proteins (Lee et al., 2004). An important aspect of vesicular transport is that only designated cargo proteins are packaged into a nascent vesicle, organelle resident proteins fail to be incorporated (Malkus et al., 2002). The ER is not a homogenous environment, regions dedicated to generating COP-II vesicles have been variously designated as ER exit sites (ERES) or transitional ER (tER). The precise mechanism by which these distinct zones are maintained, the full complement of proteins that mark these sites and the functional significance of these privileged budding sites is not yet fully clarified (Malkus et al., 2004; Pagano et al., 1999).

The ER-Golgi intermediate compartment (ERGIC), also known as vesicular tubular clusters (VTC), is a compartment thought to arise from the homotypic fusion of COP-II vesicles and is the main sorting station for the retrieval of escaped ER resident proteins (Martinez-Menarguez et al., 1999). ERGIC vesicles may represent a functionally distinct budding zone similar to that of the ERES/ tER sites (Lee et al., 2004).

The correctly folded and processed proteins exiting the ER are of two very broad categories:

- a) Proteins that are capable of entering transport vesicles at their prevailing concentrations in the ER. These proteins are thought to passively enter the

## Introduction

transport vesicles and this mode of ER exit, believed to be used by protein produced in high quantities is called the “Bulk flow” mode of exocytosis.

- b) Proteins that have to enter the transport vesicles at concentrations significantly higher than those in the general ER. Specific enrichment of both membrane and soluble cargo proteins in transport vesicles occur at concentrations ~3-50 fold higher than the bulk flow mode of transport. This enrichment is achieved by interaction of the cytoplasmic coat with distinct sorting signals on cytoplasmic segments of membrane cargo proteins. To be recognized by the coat machinery, these signals must be accessible and in an appropriate conformation that maybe influenced by a number of factors, including the folding status of the protein, interactions with accessory proteins or transport receptors, and/or oligomerisation state that may influence the presentation of positive sorting signals or masking of retention signals. This mode of exocytosis is termed the “specific enrichment of cargo” mode of transport.

There are several open questions in the regulation of both modes of protein transit (Lee et al., 2004).

## 1.9 Objectives

The broad objectives of the following study can be listed as follows:

- i) Understanding the cellular and biochemical role for Cni in the initiation and subsequent Grk mediated patterning of the two axes in *Drosophila*.
- ii) Identifying a loss of function allele of *cnir*, which is an ORF similar to *cni* in the fly genome, to better understand the cell biological role of this family of proteins.
- iii) Identify other regions/genes in the genome that have a so far unknown role in axis polarization and/or EGFR signaling using an enhancer suppressor screen.

## 2a Results - Cornichon (Cni)

### 2a.1 Sub-cellular localisation of Cni

Erv14p, the yeast homologue of Cni has been shown to be a protein required for ER to Golgi transport of Axl2p, another protein involved in axial budding of yeasts, (Powers and Barlowe, 1998). To investigate a similar cellular function for Cni, we studied the subcellular localization of Cni. A Myc tagged version of Cni was misexpressed in the follicle cells using the *UAS/Gal4* system (Fig.10), originally from yeasts. Although *cni* is expressed and required in the germ line, the reason for using the follicular epithelium as the system of choice for studying co-localisation of Cni-Myc with subcellular markers are two fold. First, the follicular epithelium is a *bona-fide* polarised epithelium with a basal and an apical side unlike the oocyte in which the subcellular organization is atypical and not pliable with most of the known subcellular markers. Second, *pUAST* vector based constructs can be driven only in somatic tissue whereas to drive expression in germ line tissue constructs have to be based in pUASp vectors (at present we do not have a *UASpcni* construct in hand).

A monoclonal antibody, against the immunoglobulin heavy chain **binding protein** (Bip) was used as a marker for the **Endoplasmic Reticulum** (ER). Bip is an ER resident protein (Steiner and Smolen, 2002; Vaux et al., 1990). Monoclonal anti-Bip antibodies showed the maximum colocalisation with Anti-Myc polyclonal antibodies, indicating that most of Cni is present in the ER. The distribution of Cni-Myc was very characteristic for an ER localised protein (Fig.11A-C). Besides ER structures which showed colocalisation with both Bip and Myc antibodies, there were also structures solely positive for the individual markers. This indicates not only that Cni is not present in all structures of the ER but also, that it is present in other subcellular structures, besides the ER.

MAC 256 is a rat monoclonal antibody against the KDEL-peptide. We used this as a marker for the **Endoplasmic Reticulum Golgi Intermediate Compartment** (**ERGIC**). MAC256 and Anti-Myc showed some colocalisation indicating that Cni was also present in subpopulations of the ERGIC vesicles (Fig.11D-F). However, the amounts, distribution and colocalisation of MAC256 and Myc was to a lower extent than that seen

in Bip/Myc experiments. This indicates not only that the ERGIC is a much smaller subcellular structure than the ER but also that Cni is more in the ER than in the ERGIC. Both the ER and the ERGIC colocalisation experiments were done in the Stretched Follicle Epithelium (SFE), which are very flat cells overlying the nurse cells (Fig.11A-F & Fig.10,yellow arrowheads). A commercially available monoclonal raised against Drosophila embryonic Golgi membranes was used to assay colocalisation of Cni-Myc with Golgi stacks. Experiments for colocalisation with Golgi apparatus marker were done in the Cuboidal Follicular Epithelium (CFE) (Fig.10,red arrowhead), because of difficulties to visualize the Golgi apparatus in the SFE. Cni and the Golgi marker colocalised in a few Golgi vesicles too, although the least amount of Cni appeared to be in the Golgi structures/ vesicles (Fig.11,G-I).

These experiments indicate that Cni can be detected in the ER, ERGIC and Golgi structures of the follicular epithelium, hence validating a ER to Golgi transport function for Cni.

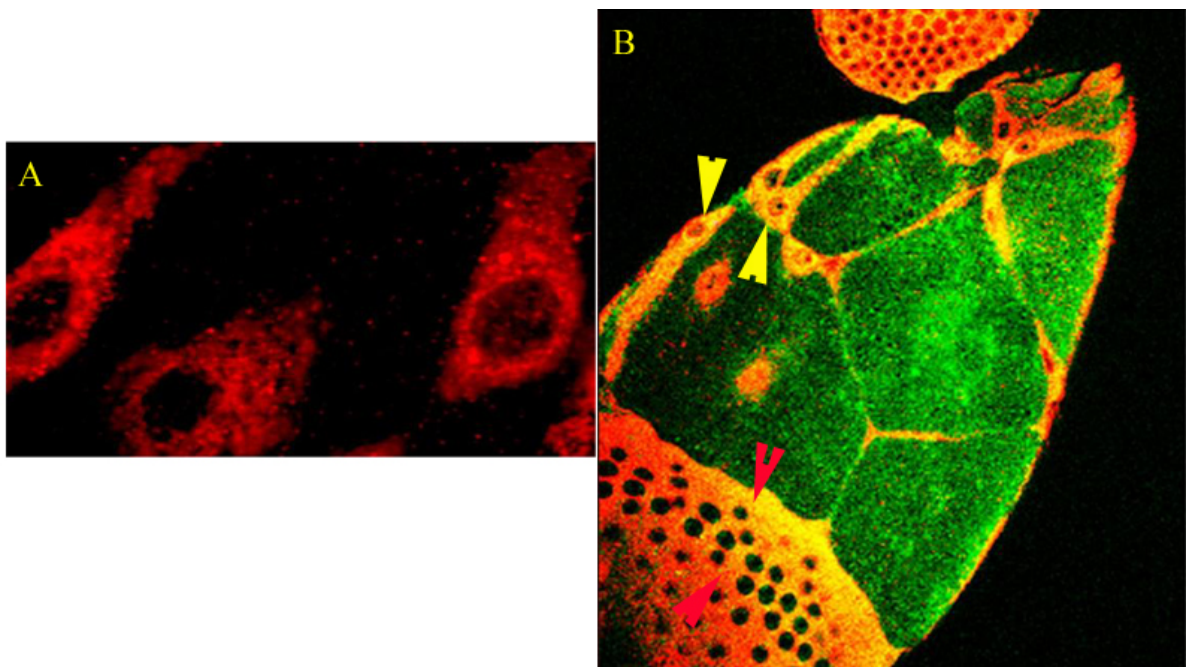


**Fig. 10** Distribution of Cni in the follicular epithelium. (A) The distribution of Cni-Myc expressed with follicular drivers and detected using an anti-Myc polyclonal antibody. The picture shows the distribution of Cni in an SFE (indicated with yellow arrowheads in B) (B) In Green are the nurse cells (germ line) which lie beneath the SFE. Red arrowheads indicate the CFE whereas the yellow arrowheads indicate the SFE.

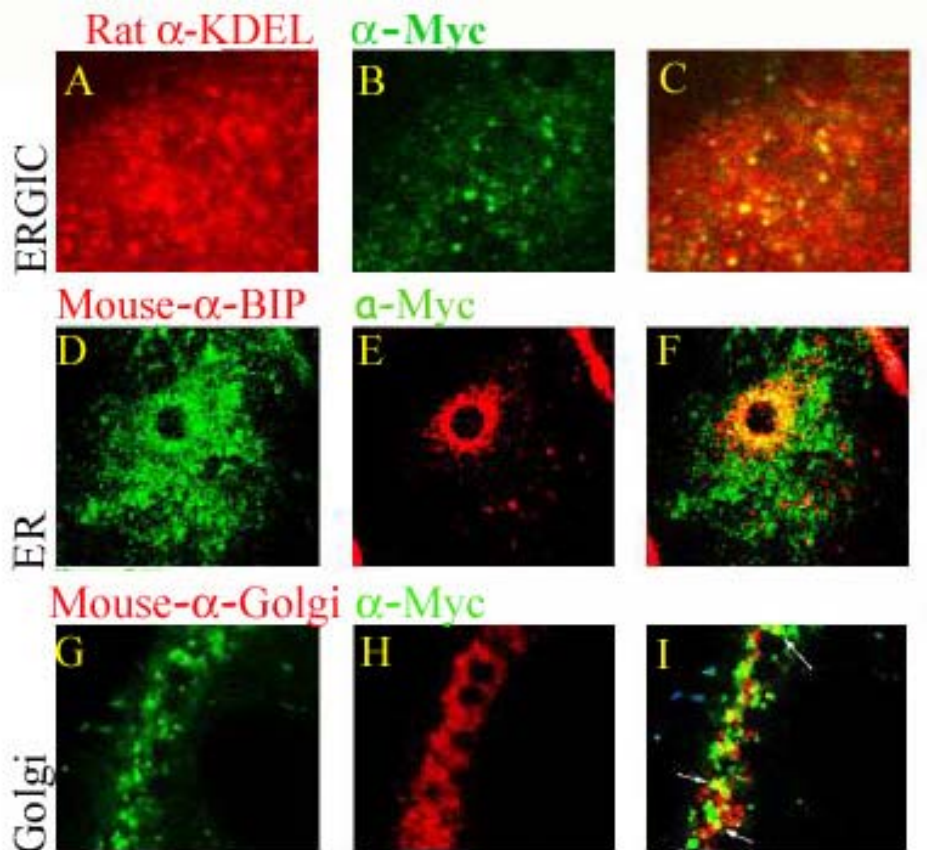


Fig. 11 Sub-cellular localization of Cni. Distribution of MAC256 in SFE (A), anti-Bip in SFE (D) and anti-Golgi in CFE (G) B, E & H are the distribution of Cni indicated by anti-Myc antibodies. C, F and I are the colocalisation of the respective markers with the anti-Myc antibodies. White arrows in I indicate Golgi vesicles which were found to be real colocalisations by taking optical sections to check whether the apparent localization was due to vesicles with the individual markers lying over each other. The colocalisation was found to be real with the resolution of the confocal microscope we used.

## 2a.2 Excess Grk signal from the germ line dorsalises the egg shell

The UASp/Gal4 system was used to overexpress *Grk* in the germ line. The effect of increased Grk was assayed by the dorsalisation of the egg shells. Two Gal4 drivers, namely, *TubulinGAL4VP16* (*TubGal4VP16*) (a tubulin which is restricted to oogenesis) (Source: St.Johnston lab) and *Nanos GAL4VP16* (*NosGal4VP16*) (Source: Ephrussi lab), were used in the study. Both Gal4 drivers, had the ability to increase *Grk* expression from the germ line, as was evidenced from the resulting, dorsalised egg shells. The dorsalisation of the egg shells in case of both Gal4 drivers was never a single phenotype, rather a spectrum starting from the wild type egg shell with the two dorsal appendages at

the end of the operculum (anterior end). And at the other end of the spectrum was the most dorsalised egg shell, characterised by an enlarged operculum. The characteristic twin dorsal appendages in this case, are replaced by dorsal appendage material distributed all around the circumference of the enlarged operculum.

The dorsalisation scale is an arbitrary scale we devised to assay the spectrum of egg shells that were produced. The basis of this scale is the visual examination of the egg shells. The spectrum of the egg shell phenotypes can be classified in three broad categories.

- a) Wild type to very slight dorsalisation: This corresponds to the first two egg shells from the left in Fig.12a&b. The slightly dorsalised eggs are almost identical to wildtype eggs but the dorsal appendages and operculum are pushed from their normal dorsanterior asymmetric location to a more symmetric anterior location.
- b) Intermediate to strong dorsalisation: Eggs in this category, the next two pictures in the Fig.12c&d, are characterised by the loss of the asymmetric position of the dorsal appendage material. The dorsal appendages are transformed into a ring of dorsal appendage material, and the operculum circumscribed within the ring, are both pushed to a symmetric anterior position instead of their characteristic dorsal asymmetric location. The eggs with a perfect ring of dorsal appendages (Fig.12c) can be considered to be less dorsalised in comparison to those where the dorsal appendage material protrudes at out at the ventral side of the egg (Fig.12d).
- c) Extreme dorsalisation: The last two pictures on the scale represent the maximum dorsalisation observed (Fig.12e&f). The operculum is extremely enlarged and the dorsal appendage material is almost absent in extreme cases but when present is present in patches all along the rim of the enlarged operculum.



**Fig. 12 The dorsalisation scale: Egg shell phenotypes representative of the degrees in dorsalisation observed due to overexpression of Grk from the germ line. (a) and (b) indicate the wildtype to weak dorsalisation, (c) and (d) the intermediate to strongly dorsalised egg shells and finally (e) and (f) represent the transition to extreme dorsalisation.**

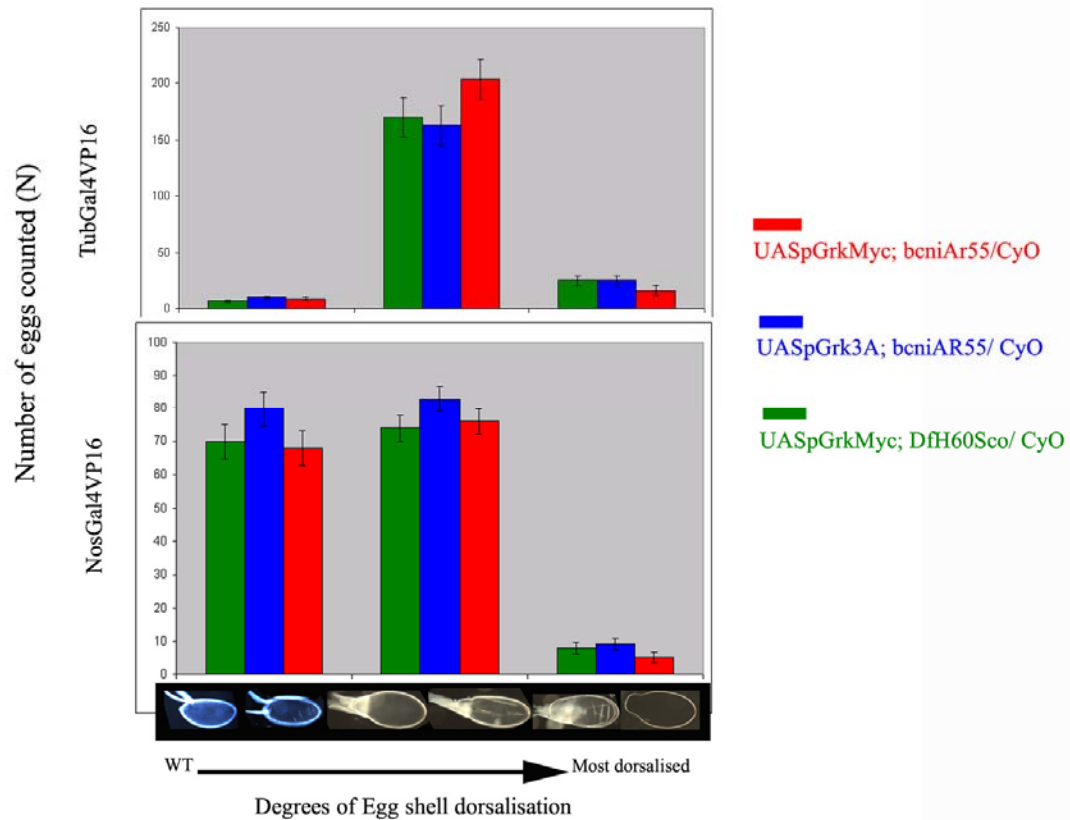


**Fig. 13** Excess *Grk* from the germ line results in the dorsalisation of the resultant egg shells. In both graphs the Y axes represents the number of the eggs that were considered for analysis, the X axes gives the dorsalisation scale. The panel above is the distribution of egg shell phenotypes using *TubGal4VP16* driving different *UASpGrk* constructs (*Myc* tagged/ non tagged, with *bniAR55/CyO* or *DfH60Sco/CyO* on the second chromosome). The panel below indicates similar distribution using *NosGal4VP16* as the driver with different *UASpGrk* versions.

The spectrum of egg shell dorsalisation is not changed irrespective of whether the *UASpGrk* construct is a C-terminal *Myc* tagged version or an untagged version (Fig.13). In general, egg shell dorsalisation due to *Grk* mis/overexpression using *NosGal4VP16* as the driver, was weaker than *Tubgal4VP16*. This is based on the fact that the dorsalised egg shell spectrum is spread more widely in case of *NosGal14VP16*, with the distribution frequency peaking at the intermediate to strong range in dorsalisation. The spectrum in case of using *TubGal4VP16*, on the other hand, is narrower and the peak frequency being pushed further towards the extreme dorsalisation phenotypes.

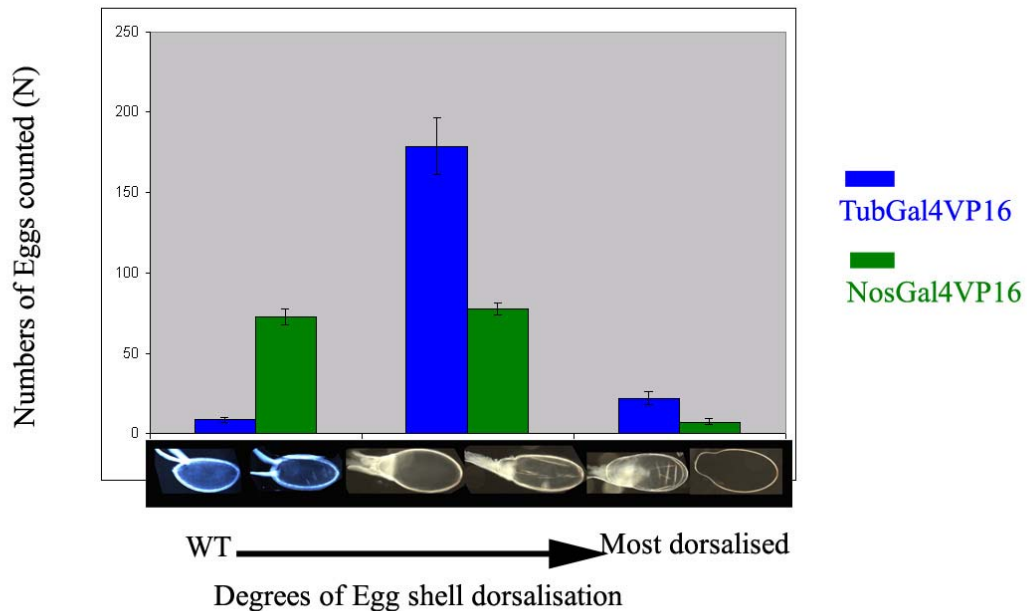


Fig. 14 Comparison of egg shell dorsalisation using different germ line Gal4 driver lines.

### 2a.3 Patterning of the embryo affected when Grk overexpressed in DfH60Sco heterozygous background

There is a significant number of apparently wild type egg shells laid when Grk is overexpressed using *UASpGrk* and using *NosGal4VP16* as the driver (46%, N=152). The number of wild type egg shells were considerably less in the case of overexpression using *TubGal4VP16* (5%, N=198). In both cases there were no embryonic cuticles visible in dorsalised eggs shells, indicating that these eggs could not even be fertilized. In case of the egg shells, which were wildtype in appearance, from the cross in which *Grk* was overexpressed using *NosGal4VP16* as the driver in a heterozygous amorphic *cni* background (*bcniAR55/CyO*), insignificant number with embryonic cuticles observed (5%, N=36). Intriguingly, when the same experiment was done using the deficiency of the *cni* (*DfH60Scob/CyO*) region in heterozygous condition on the second chromosome, significant number of egg shells with embryonic cuticle phenotype were observed (39%, N=57) (Fig.15A). The cuticles phenotypes varied from subtle phenotypes such as the fusion of ventral denticle belts, missing denticle belts and gaps in denticle belts to a strong phenotype such as entire anterior segments being misformed, missing terminal segments and complete absence of dentilce belts (Fig.15B). *DfH60Scob*, besides

removing *cni* also removes *cactus* (*cact*) and *fizzy* (*fzy*). This indicates that the removal of one copy of *cact* has a small suppression effect, which makes the dominant maternal phenotype of *cact* visible in these embryos. It is probable that a similar phenomena happens with the *TubGal4VP16*, *Grk* overexpression too, but it is difficult to quantify this due the lower numbers of the wild type eggs laid in this case. We did observe a few c very strong cuticle phenotypes in this case, too (Data not shown).

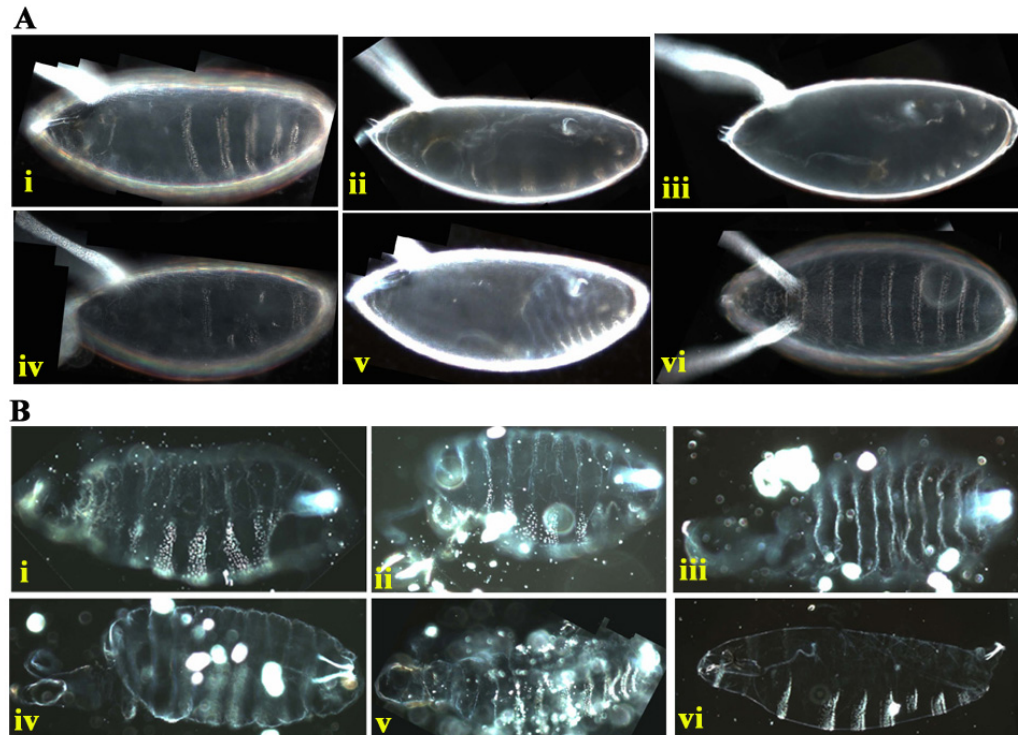


Fig. 15 Egg and cuticles from the wild type egg shell fraction laid by *UASpGrk; DfH60Scob/CyO; NosGal4VP16* mothers. (A) i-vi Apparently wildtype eggshells in which the misinformed embryonic cuticles are visible. (B) i-vi Range of cuticle phenotypes from these eggs.

## 2a.4 Timing of onset is different between *NanosGal4VP16* and *TubGal4VP16*

*TubGal4VP16* and *NanosGal4VP16* were the drivers of choice because they were germ line specific Gal4 drivers. To ascertain whether these are strict germ line drivers or they also expressed the overlying somatic follicle cells, we expressed an *UASpEGFP* construct (*UASp* constructs should be expressed in the soma and germa) using the two Gal4s as drivers. While the two drivers are strictly germ line restricted as visualised by

the complete absence of GFP from all somatic follicle cells and presence in nurse cells and oocyte. However, there was a dramatic difference between the two Gal4 drivers as to the stages of the egg chambers where GFP could be first detected. In case of *TubGal4VP16*, GFP expression could be detected as early as in stage 4 and stage 5 egg chambers. In these stages the oocyte nucleus is still in a symmetric posterior location. These are stages before the first round of Grk signaling occurs. In case of the *NosGal4VP16*, GFP could be detected only in stages as late as stage 6 or stage 7 egg chambers. Not a single egg chamber was detected in which the oocyte nucleus was still in the posterior symmetric position and expressed GFP. Hence, *NosGal4VP16* is active between the two Grk signals from the germ line (Fig.16).

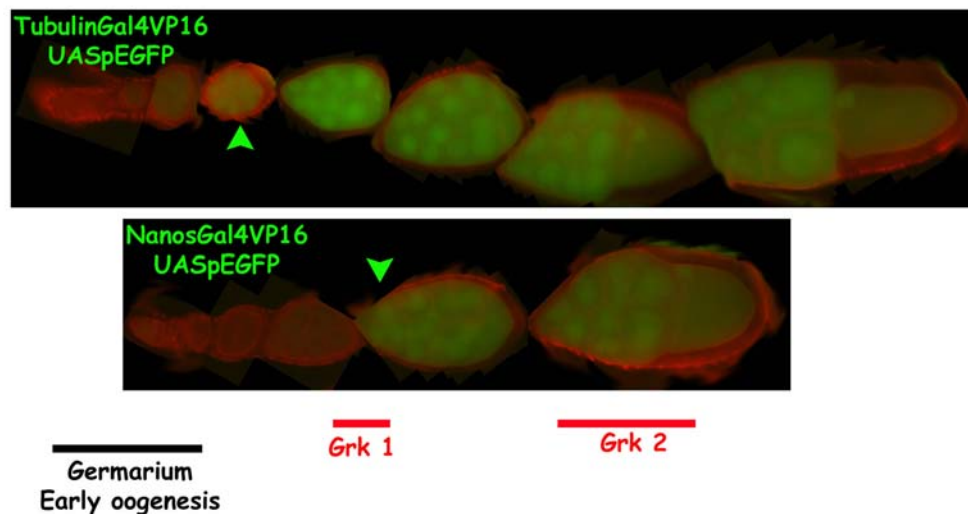
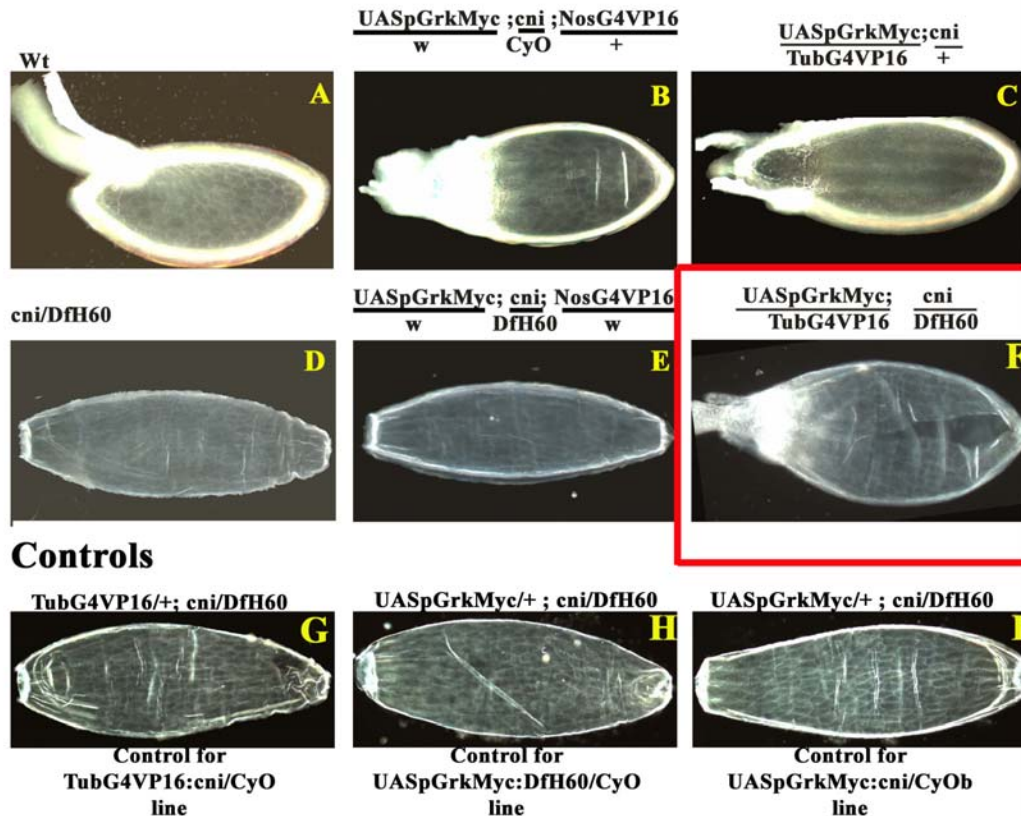


Fig. 16 Comparison of the expression profile between *TubGal4VP16* and *NanosGal4VP16*, using an UASpGFP reporter. The GFP signal could be detected in much earlier stages of oogenesis (stage 4-5) in case *TubGal4VP16* (upper panel) than in case of *NanosGal4VP16* (lower panel). Green arrowheads in either panels indicate the earliest time point where GFP was detectable in either of the drivers. Red line, below the two panels, indicate the approximate time window of the two Grk signals. Black line is to indicate the time window of early oogenesis events.

In both the Gal4 drivers no GFP expression was observed in any follicle cell at any stage of oogenesis, ascertaining the fact that the drivers used are both strictly germ line drivers (Fig.16).

Although, from the egg shell dorsalisation assays *TubGal4VP16* appeared stronger than *NosGal4VP16*, this issue could not be clarified by differences in GFP signal. GFP was not detected in early germarium of both drivers, although *NosGAL4VP16* is supposed to have early germarium function/expression (P. Filardo, personal communication).

## 2a.5 Mis/over-expression of Grk by TubGal4VP16 but not NosGal4VP16 can rescue Cni function



**Fig. 17** Egg shells indicating that mis/over expression of Grk with TubGal4VP16 can overcome Cni requirement for realisation of the active Grk ligand. The wild type egg shell (A) has clearly patterned dorsal appendages and anterior and posterior structures, whereas the egg shells laid by *cni* amorphic mothers (D), is dorsoventrally symmetric with anterior structures on either ends. While both *NosGal4VP16* and *TubGal4VP16*, overexpressing Grk in a *cni* heterozygous background results in dorsalisation of the egg shells to different degrees (B&C), the same experiment in a *cni* homozygous background does not show any rescue of the *cni* egg shell in case of *NosGal4VP16* (E), but both AP and dorsoventral patterning are rescued in case of *TubGal4VP16* (F). Appropriate controls of the *TubGal4VP16* with *cni* homozygous background (G), and the UAS constructs in a *cni* homozygous background (H&I) all result in *cni* amorphic egg shells.

If the biological function of Cni is the enrichment and/or giving a subcellular vectoriality to Grk containing vesicles en-route its exocytotic transit from the ER to Golgi, could it be possible to overcome Cni requirement by overloading the system with Grk. From the egg shell dorsalisation assays it is already obvious that higher amounts of Grk from the germ line is produced in case of both *TubGal4VP16* and *NosGal4VP16*. To test whether Grk produced in bulk and passing through the exocytotic route can replace the requirement

for Cni in enriching and targetting the Grk containing vesicles, we over/misexpressed in a amorphic *cni* homozygous background using these two drivers. Overexpression using *NosGal4VP16* did not result in any change in the *cni* amorphic egg shells (Fig.17E). Overexpression using *TubGal4VP16*, on the other hand, resulted in rescue as can be seen from the resultant egg shell with posterior structures resembling an aeropyle and also with dorsal appendages deposited on the egg shell giving the egg shell a dorsalisied appearance. Rescue in case of *Tubgal4VP16*, and not *NosGal4VP16* indicate that both the amounts and timing of Grk are critical for the patterning events as similar amounts of Grk was detected in case of both drivers using Western blot analysis (see Fig.20).

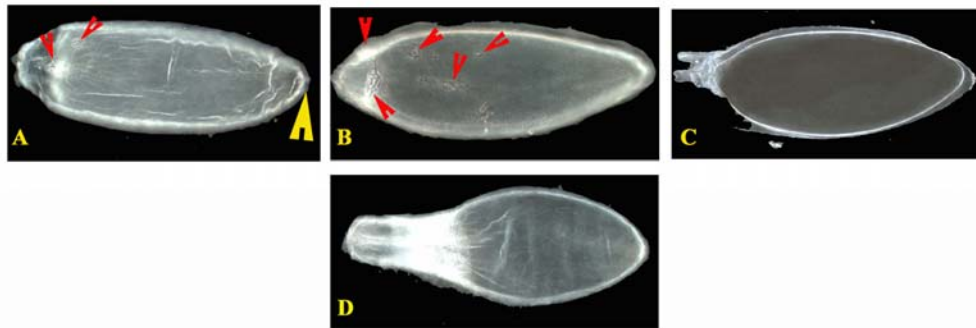


**Fig. 18** The range of phenotypes amongst the *TubGal4VP16* rescue egg shells. We observed egg shells, where the AP axis was not rescued (by the presence of a posterior micropyle (yellow arrowhead), but multiple Dorsal appendage material deposition (red arrowheads) on the egg shell (A), egg shells where the AP axis was fine but there was dorsal appendage material deposited at several points (red arrowheads) on the egg shell (B), and egg shells where the dorsal appendages were pushed very close to the anterior micropyle showing almost a complete absence of an operculum (C). The most commonly observed rescue phenotype was the dorsalisied one (D).

The extreme pertinence of Cni-mediated Grk transport regulation for patterning the egg shell can be seen by the fact that among rescued egg shells there were none with wild type dorsal appendage pattern. Among the rescued egg shells were also those with very striking patterns like, eggs where there were micropyle like structures on both ends of the egg shells but also multiple dorsal appendage initiations on the egg shell (Fig.A). Also eggs with both micropyle and aeropyle but with multiple dorsal appendage material deposited all across the egg shell (Fig.18B) and egg shells with dorsal appendage pushed very close to the anterior (Fig.18C). These egg shells underline the importance of Cni in patterning the invariant and determinate pattern of the egg shell. Both the semi-lethality and low egg lay frequency also associated with *cni* mutations were not rescued by this rescue assay. The most commonly occurring phenotype resembled a dorsalisied egg,

because the dorsal appendage material seemed to form a constricting ring at the anterior of the egg (Fig.18D).

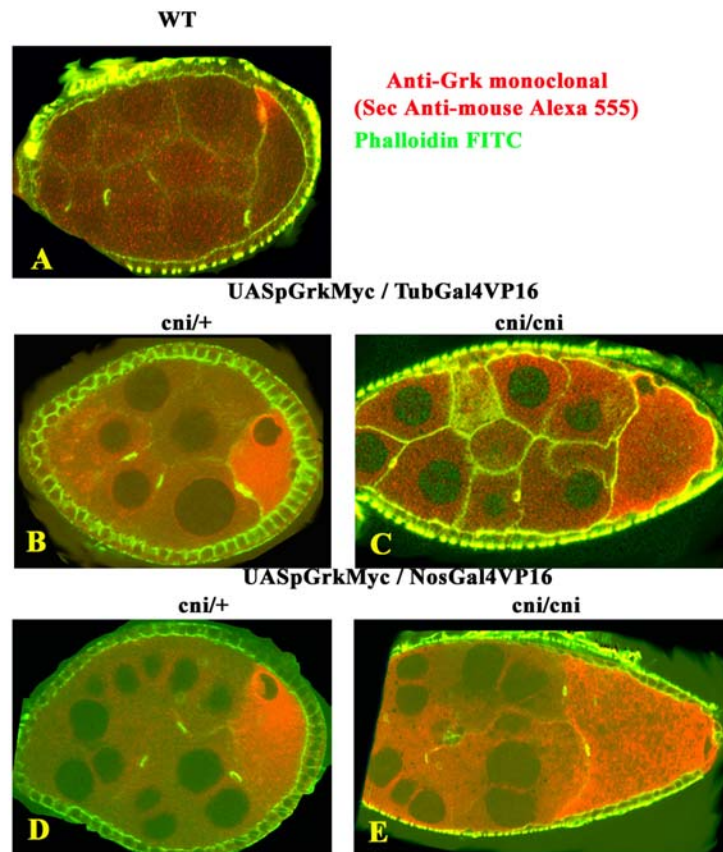


**Fig. 19** Grk protein distribution in wild type and mis/overexpression conditions. The wild type Grk protein is present at the anterior rim of the “future” dorsal cortex of the oocyte (A). In case mis/overexpression of UASpGrk using either Gal4 drivers, TubGal4VP16 (B) and NosGal4VP16 (D), in *cni* heterozygous back ground higher amounts of Grk can be detected in the oocyte. In case of mis/overexpression in a *cni* homozygous background with these drivers, TubGal4VP16 (C) and NosGal4VP16 (E), although massive amounts of Grk can be detected in the oocyte also there is an increase in signal from the nurse cells too. Grk monoclonal 1D12 primary antibody was detected with goat anti-mouse Alexa555 (red) and actin was detected using Phalloidin-FITC (green).

Grk protein distribution was checked by using immunostaining assays. The wild type Grk protein is restricted to the “future” dorsal anterior corner of the oocyte (Fig.19A) and is associated with the oocyte nucleus. In case of both, *TubGal4VP16* (Fig.19B) and *NosGal4VP16* (Fig.19D) Grk mis/overexpression in *cni* heterozygous background, the characteristic pattern of protein restriction to the corner of the oocyte nucleus was lost and also there higher amounts of Grk protein detected in oocyte. Mis/overexpression in a *cni* homozygous background using both drivers (Fig.19,C&E), also detected massive amounts of Grk in the oocyte, despite patterning defects in the follicle cells and

mispositioning of the oocyte nucleus. In the *cni* homozygous mis/overexpression assays there was more Grk detected in the nurse cells than in both the *cni* heterozygous overexpression case and the wild type situations. All of the immunostaining reactions were done with the same conditions and same microscope settings (i.e: gain and offset), as far as possible, to avoid variations due to these parameters.

## 2a.6 Protein profile of the ovaries using Western blot analysis

To better understand the role of Cni in regulation of Grk ligand production western blot analysis of protein extracts from *Drosophila* ovaries was standardized. A monoclonal antibody (1D12) raised against the extracellular EGF domain of Grk was used as the primary. Despite several different variations of conditions and methods in extracting the protein, different modes of transfer of the proteins onto the membrane and using detection kits with different sensitivities wild type amounts of the protein was never detectable, beyond very faint bands (Fig.20, lane4&5). It was possible to detect Grk easily in the over expression conditions.

The amounts of Grk protein detected in case of overexpression with both Gal4 drivers in a *cni* heterozygous background (Fig.20, compare the biggest bands in lanes 1&2 with that of those in lanes 6&7) were comparable on visual examination. Besides, the bigger band (between 60 and 70 Kd), a smaller band (between 40 and 25 Kd) was also detected in case of the overexpression (Fig.20, lanes3,4&8) in a *cni* homozygous background with both Gal4 drivers. The bigger band can be presumed to be the unprocessed full length form of the ligand and the smaller bands the processed form. This indicates that Grk processing by the S-Rho pathway is inhibited by Cni, which transports the full length form of the ligand.

There is no difference in Grk activity between the Grk-Myc tagged UASp line and the one without the tag, as degree of dorsalisation patterns of the eggs laid by flies carrying either of these constructs and driven by either Gal4 indicates (Fig.13). There is however, a major difference in the ease with which they could be detected in western analysis. *UASpGrkMyc* could be detected much more easily (0.5-1 hours of exposure using ECL-plus detection) than the *UASpGrk* versions (3hrs- overnight exposure using ECL-plus

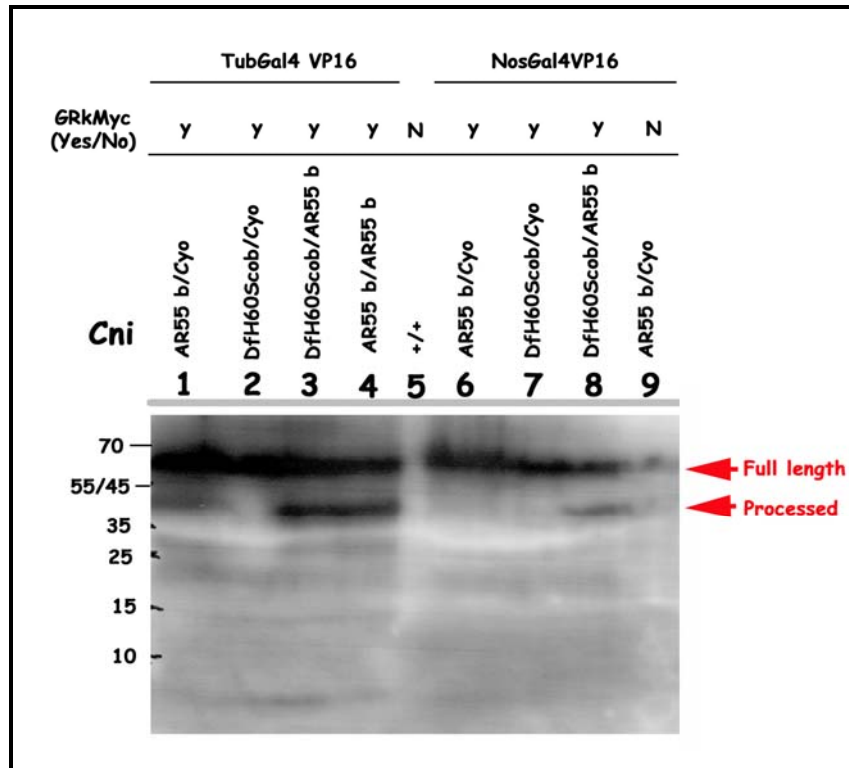


Fig. 20 Western blot analysis of protein extracts from ovaries, where Grk was mis/overexpressed with different germ line Gal4 drivers in *cni* heterozygous and homozygous backgrounds. Processed forms of Grk could be detected only in *cni* homozygous conditions in case of expression with both of the drivers (lanes 3,4 & 8). A Monoclonal antibody (1D12) raised against Grk was the primary used. Wild type grk was not detectable (lane5) and non-Myc tagged Grk weakly detected (lane9). Only full length Grk was detected on over-expression in *cni* heterozygous background with both drivers (lanes 1,2,6&7).

detection). The smaller processed form of the ligand was very faint and almost not detectable in case of the experiments with the *UASpGrk* constructs (Fig.21, lane 1).

In experiments with the *UASpGrk* constructs driven by *NosGal4VP16*, in a *cni* homozygous background, the full length form of the protein was detected as a distinct doublet band (Fig.21, lane1). Expression in a *cni* heterozygous background on the other hand showed a single band only (Fig.21, lanes 2&3). The formation of the doublet could be due to a post translational modification of Grk only in the *cni* homozygous condition. One possibility is that in a *cni* loss of function situation the exocytic machinery is compromised and the doublet is due to some of the higher amounts of Grk being trapped in its exocytic route, unable to be secreted. Testing the glycosidase (esp., EndoH) sensitivity of these proteins is the way to test this scenario.

## Results - Cornichon

Endoglycosidase H (EndoH) and Peptide N-Glycosidase (PNGase), act on N linked glycosylations, while O-Glycosidase acts on O-linked glycosylations. While PNGase removes all mature N-linked glycosylation events that had passed through the cellular exocytotic machinery and reached the plasma membrane, EndoH removes only the huge branched high mannose type of glycosylation initially added onto the protein in the ER. The high mannose type of glycosylation is trimmed gradually through the exocytotic route of proteins to form the mature PNGase sensitive glycosylations on the protein. So usually proteins retained in the ER are EndoH sensitive. O-glycosidase on the other hand removes the “one sugar, one enzyme” mediated glycosylations predominantly carried out in the cis and trans Golgi regions of the cell.

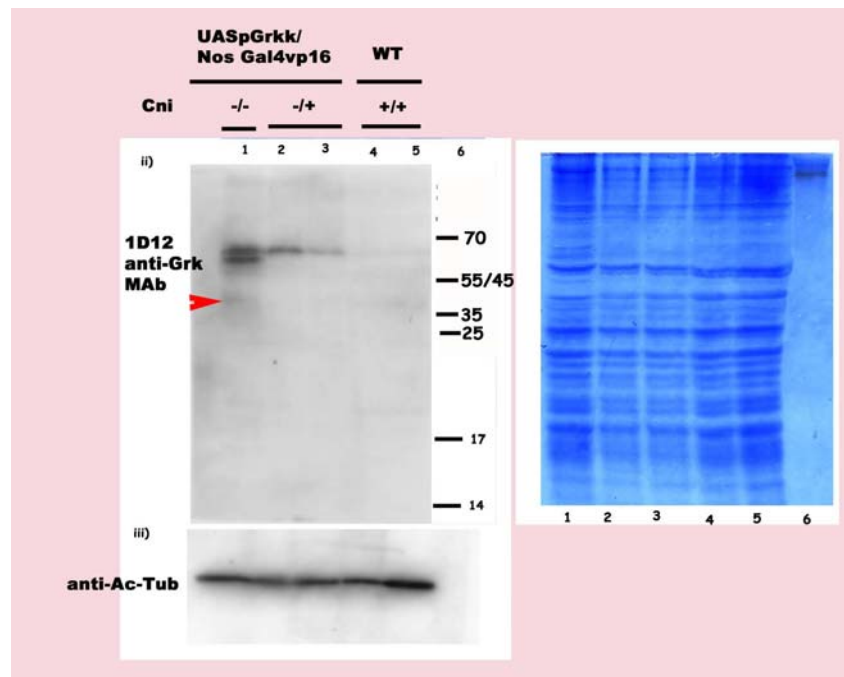


**Fig.21** Grk overexpressed with NosGal4VP16 in a *cni* homozygous (ii, lane 1) and heterozygous condition (ii, lane 2 and 3) compared to the wild type ovarian protein extracts (ii lane 4 and 5). The processed form can be detected very faintly (red arrowhead) in the *cni* background. Adjacent is the -10% SDSAcrylamide gel stained with coomassie staining after the transfer of the proteins. (iii) Below is the same membrane as in (ii) but detection using mouse anti-acetylated tubulin antibody as primary antibody to show that equivalent protein amounts were loaded in each of the wells.

Protein extracted from ovaries overexpressing Grk was treated with the different glycosidases at 37°C for 45 minutes before the protein extracts were heat inactivated and electrophoresed on 10% SDS-PAGE gels. The proteins were then transferred onto Immobilon-P Nylon membrane by semi-dry mode of transfer. Monoclonal 1D12 Grk anti

bodies were then used to assay the effect of the glycosylations on Grk. Glycosylation assays using individual glycosidases and with glycosidases in combination with each other did not remove the doublet band of Grk overexpression in a *cni* homozygous background. The doublet band could therefore, be due to some other post translational protein modification, eg., phosphorylation.

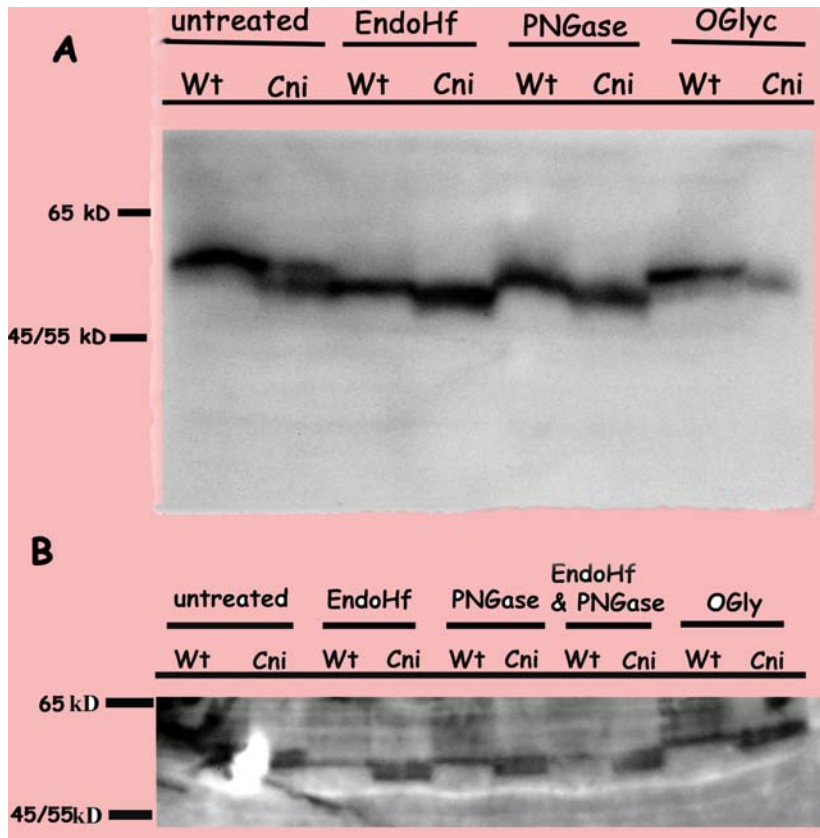


**Fig. 22** Glycosidase assays on Grk proteins over expressed in *cni* heterozygous (lanes labelled as Wt in both panels) and *cni* homozygous (lanes labelled as Cni in both panels) conditions. (A) The treatment of the protein extracts with the individual glycosidases. (B) Indicates the the treatment with individual and combinations of glycosidases. Though the doublet pattern in a *cni* homozygous background is not lost due to any of the treatment, both Grk in homozygous and heterozygous Grk protein retains the ER type high mannose glycosylations aseedenced by the decrease in size of both Cni and Wt Grk due to EndoH treatments.

The glycosidase assays however indicated that the mature protein in both homozygous and heterozygous *cni* background retained the ER type hi-mannose glycosylations which was detected by the Endo-H sensitivity (note the decrease in size in both wt and *cni* Endo-H lanes in Fig.22).

## 2a.7 Expression of a Grk version that lacks the Cni interaction domain and its consequences

The hypothesized region of interaction between Grk and Cni is between the **Juxta-Membrane Domain (JMD)** of Grk and the N-terminal luminal end of Cni (C.Bökel, Ph.D work). The JMD (amino acids Y 224 to A 245) is the region between the EGF domain (C 183 to I 223) and the **Trans-Membrane Domain (TMD)** (A 245 to A 265) of Grk. A construct ( UASpδ19aaMyc ) which deletes 19 amino acids ( Y 224 to V 242 ) which consists of most of the JMD including the dibasic cleavage signal R240 and K241) has been shown to result in very weak ventralisation of the egg shell when overexpressed in the oocyte (Ghiglione et al., 2002).

The ultimate objective of the following series of experiments is to test whether overexpression of this construct in a *cni* amorphic background could rescue any of the early or late Grk activities. Driving the construct in a wild type (heterozygous) backgrounds, as a preliminary test before driving expression in a *grk* and *cni* heterozygous backgrounds, already show intriguing phenotypes. An antimorphic phenotype, indicated by a weakly ventralised egg shell with a single DA, was seen in 7% of the egg shells laid when this construct was driven by *NosGal4* (Ghiglione et al., 2002). The weak egg shell phenotype (Fig.23iiA) was visible in upto 27% (N=30) of the eggs, when the construct was driven with *NosGal4VP16*. Further, these eggs and the eggs which had wild type dorsal appendages enclosed embryos which had patterning defects (Fig.23iiB,iiC&iiD). All the cuticles defects affected the patterning of the structures at the anterior end of the embryo, the most common and striking of these patterns were once in which the entire head patterning was affected, although (Fig.23,iiC &iiD), the thoracic and abdominal segments were present and patterned normally. In case of overexpression of the same construct with *TubGal4VP16* there were no egg shells with the weak ventralisation phenotypes. All eggs showed wild type DAs (N=30) (Fig.23,iiE), although the cuticle phenotypes were present (Fig.23 iiF, iiG and iiH). The cuticle phenotypes were comparable between expression using *NosGal4VP16* and *TubGal4VP16*, although in case of the latter there were cuticles with very little ventral denticle belt material (Fig.23 iiF) or no denticles belt material at all (Fig.23,iiG) besides the ones with the missing head structures (Fig.23,iiH).

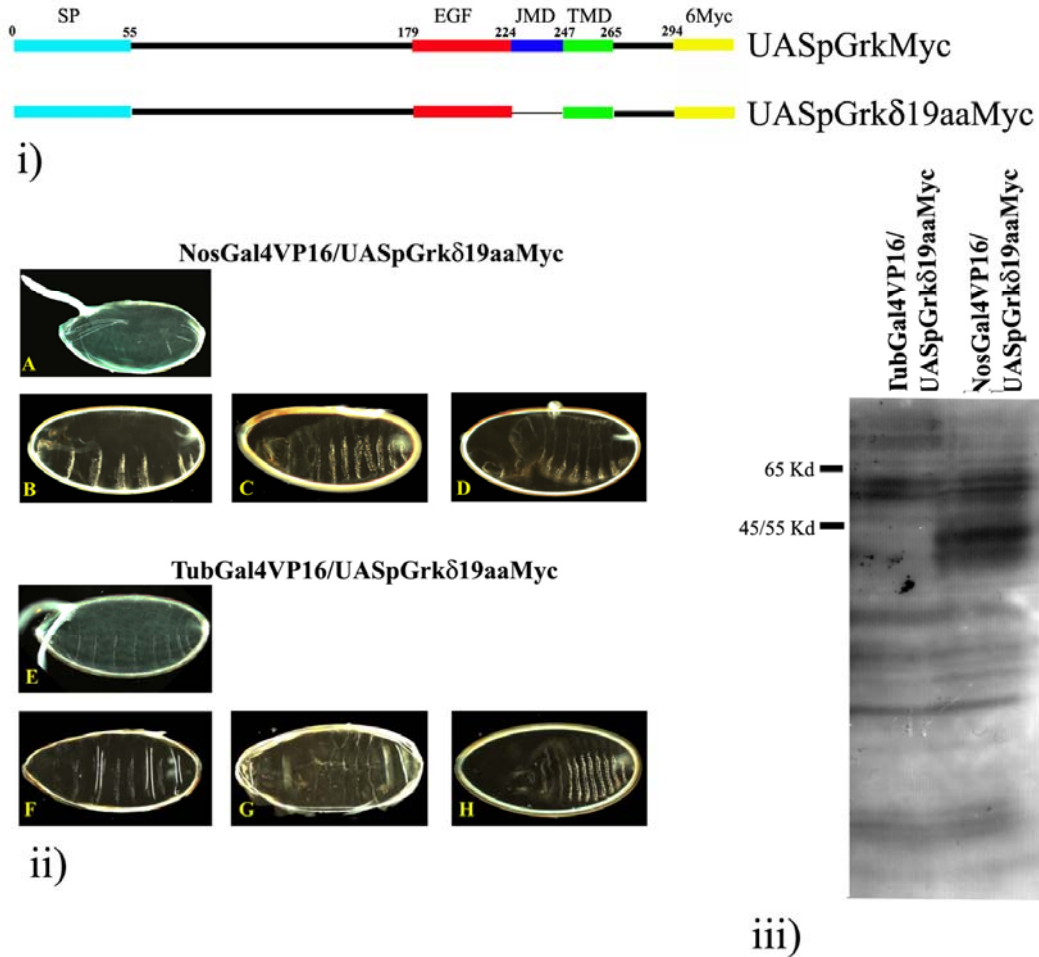


**Fig. 23** Overexpression of the *UASpΔ19aaGrkMyc* constructs using *NosGal4VP16* and *Tubgal4VP16* drivers. Schematic representation of the 19aa JMD (blue block) missing (replaced by thinner black line) compared to the *UASpGrkMyc* (i). The weak ventralisation of the egg shell with *NosGal4VP16* (iiA), the eggs have cuticle phenotype (iiB, iiC and iiD). Overexpression with the *TubGal4VP16* did not result in the egg shell ventralisation (iiE), but the cuticles were mis-patterned (iiF, iiG and iiH). Protein profiles of the two overexpressions were also different (iii) as indicated by Western analysis with anti-Grk 1D12 monoclonal antibody. The smaller cleaved band was missing in the *Tubgal4VP16* condition (iii middle lane).

The analysis of Grk profiles by using protein extracts from the two drivers and using 1D12 monoclonal showed differences between *UASpGrkΔ19aaMyc* driven by the two drivers. While in the case of the *NosGal4VP16* the *UASpGrkΔ19aaMyc* construct showed the presence of a smaller/processed band which was absent in case of expression with *TubGal4VP16* (Fig.23,iii first lane, on the left) constructs. The processed band seen in case of the *NosGal4VP16 /UASpGrkΔ19aaMyc* was a doublet (Fig.23iii,second lane

on the right). In *TubGal4sGal4VP16 /UASpGrk $\delta$ 19aaMyc* (Fig.23iii,first lane) case this processed smaller band was not detected at all.

## 2a.8 Role of JMD in regulation of Grk transit to the membrane

Constructs lacking the JMD, TMD and cytoplasmic regions are unable to rescue Grk function when expressed from the germ line using the endogenous *grk* upstream region. The inability to rescue is because the TMD/JMD domains are necessary for the proper membrane targeting of Grk in the oocyte (Queenan et al., 1999). A construct lacking only the TMD and the cytoplasmic region termed, *UASpSecGrk*, when expressed using germ line Gal4 drivers resulted in a small frequency of weakly dorsalised eggs (Ghiglione et al., 2002). These studies indicate the importance of the JMD in the production and regulation of the active Grk signal from the germ line.

Expression of *UASpSecGrk* in the germ line using *NosGal4VP16* and *TubGal4VP16* resulted in contrasting outcomes. In the case of expression using *NosGal4VP16*, the eggs laid were wild type in appearance. These eggs however did not hatch and also in most if the egg shells (85%) there was no cuticle present. The few fertilised egg shells (15%) enclosed embryonic cuticles which indicated extreme patterning defects (Fig.24ii, A,B,D and E). The range of the cuticles were from a phenotype where the ventral denticle belts were pushed up on to the top due to a huge hole in the posterior end (Fig.24,iiD) to a strongly dorsalised cuticles with one to two ventral denticle belts (Fig.24,iiE). Expression with *TubGal4VP16* resulted in no eggs being laid. The ovaries of these flies were dissected and although indicated no sign of regression as seen in most situations where egg lay is obstructed eg: Cni amorph, the egg chambers were all arrested at stage6-7. There were no egg chambers which were beyond Stag6-7, as estimated by visual examination under the dissecting binocular microscope. Immunostaining analysis with anti-Grk 1D12 antibodies indicated that there was Grk detectable in earlier (stages 2-5) in oogenesis, but in later stages (stage5 and later) there was no Grk detectable in the oocyte, although it could be detected in the nurse cells (Fig.iiC&F).

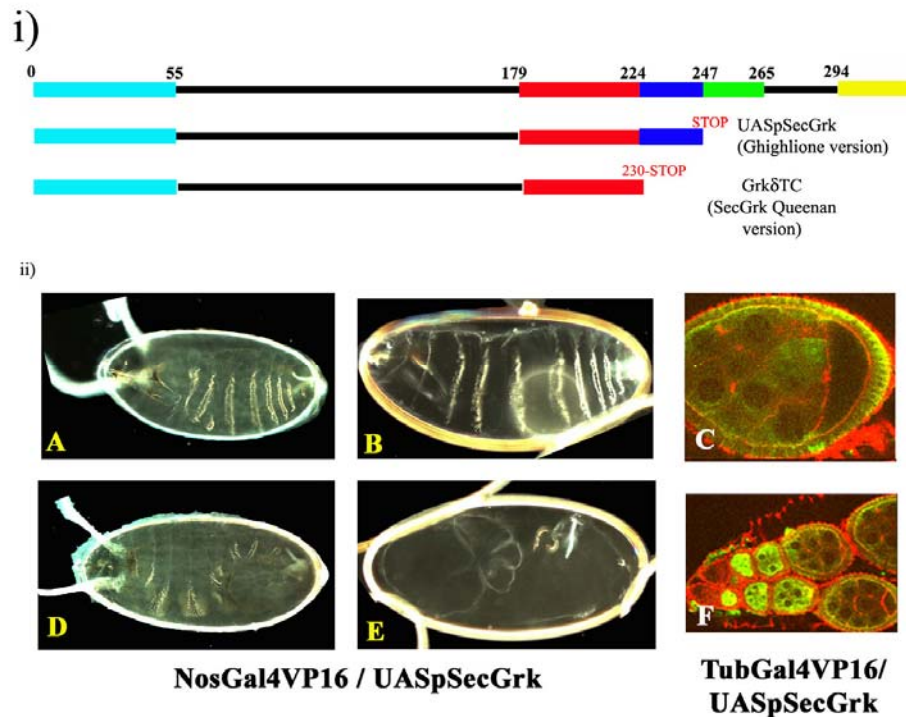


**Fig. 24** Expression of *secGrk* in the germ line using UASp/Gal4 system. Schematic representation of the Grk deletions used in previous studies, while Queenan et al., used a construct (Grk $\delta$ TC) lacking the JMD (blue block), TMD (green block) and the cytoplasmic domain (black line between blue and yellow blocks) driven by Grk upstream regulatory region, Ghiglione et al., have used a version of Grk (UASpSecGrk) lacking only the TMD (green block) and the cytoplasmic domain (black line between blue and yellow blocks) and expressed it using germ line Gal4 drivers. Expression of UASpSecGrk using NosGal4VP16 resulted in eggs with wildtype egg shells, however most of the eggs remained unfertilised (no hatchers and no embryonic cuticles within the egg shells). Few of the egg shells which had cuticles indicated extreme patterning defects (ii A,B,D&E). Flies UASpSecGrk was expressed using TubGal4VP16 laid no eggs. Ovaries from these flies showed egg chambers till Stage 6-7 (visual estimation) but not beyond. Grk was produced in the germ line of these egg chamber (green in iiF) but was absent from the oocyte of older eggchambers (ii C&F). In figures iiC&F, the red channel indicates Actin-Phalloidin Rhodamine and Green is the Grk 1D12.

## 2a.9 Expression of anti sense *star* in the Germ line

*Star* (*S*) is involved in the ER to Golgi traffic of full length EGF ligands. It is difficult to address the role of *S* in Grk signaling, because *S* germ line clones result in very early arrest in oogenesis. A *UASpStar-AntiSense* (*UASpStar-AS*) is an useful tool in understanding the germ line role of *Star* in the production of the active Grk ligand. Expression of this construct in the germ line has been shown to ventralise the egg shell (Ghiglione et al., 2002).

Expression of this construct in the germ line using *NosGal4VP16* resulted in the same egg shell phenotype as reported earlier, namely ventralisation (90%, N=30)

(Fig.25,A&B). In addition there was a series of cuticle phenotypes which have not been reported earlier (Fig.25,C,D,E&F).

Expression using *TubGal4VP16* on the other hand resulted in wild type egg shells (Fig.25G). There was however, a range of cuticle phenotypes (Fig.25,H,I,J&K) comparable to the range observed with the expression using *NosGal4VP16*. There were two notable differences in the range of cuticles between expression using the two drivers. One was the presence of extremely dorsalisated cuticles with *TubGal4VP16* (Fig.H&I). Second was the higher incidence of denticle belt fusions observed in these embryos (Fig.25, G, I and J). A few of the larvae which hatched from these eggs also showed a fused denticle belts (Fig.25, K) phenotype.

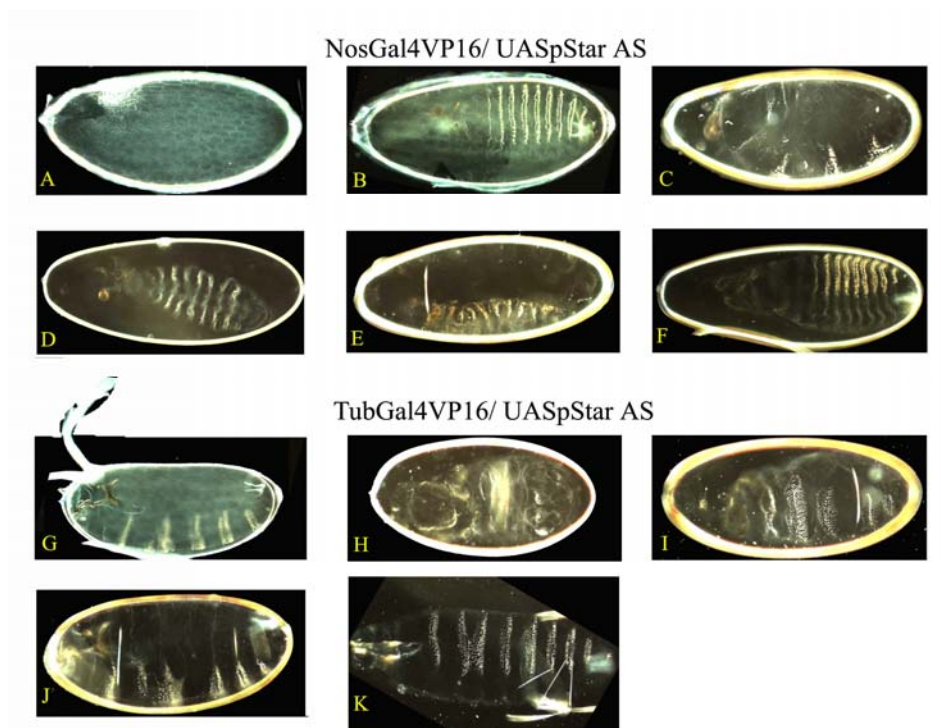
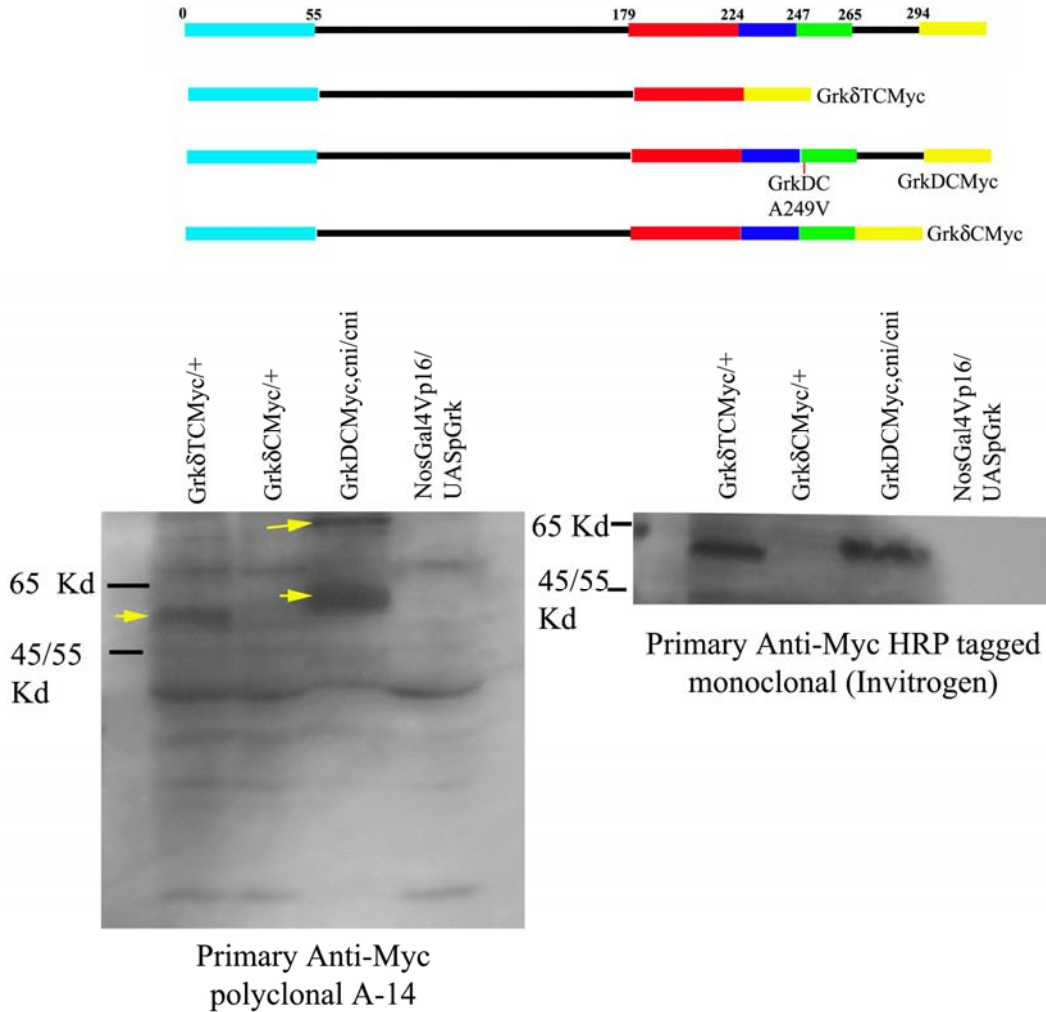


Fig. 25 Egg shell and embryonic cuticles observed on expression of the UASpStar-AS using the germ line drivers.

## 2a.10 Western blot analysis of *GrkDC5Myc,cni/cni*, *Grk $\delta$ TCMyc* and *Grk $\delta$ CMyc*



**Fig. 26** Protein profiles of *GrkDC5Myc,cni/cni*, *Grk $\delta$ TCMyc* and *Grk $\delta$ CMyc* using different anti-Myc primary antibodies. i) Schematic representation of the *Grk $\delta$ TCMyc*, which lacks the JMD, TMD and cytoplasmic domains of *Grk*, *GrkDC5Myc*, which besides the AtoV substitution at position 249, also has a c-terminal Myc tag and *Grk $\delta$ CMyc*, is a version of *Grk* where the cytoplasmic end has been replaced by the Myc tag. Analysis using a rabbit polyclonal antibody indicated a band at around 60-70 kD (yellow arrowheads) region in both *GrkDC5Myc,cni/cni* and *Grk $\delta$ TCMyc* situations (ii, lanes 3&1 respectively), *GrkDC5Myc,cni/cni* also had a much higher band. In *Grk $\delta$ CMyc* there was no new band detectable (ii lane two). The rabbit polyclonal antibody produced some cross reacting back ground bands as was evidenced by these bands also being present in the protein extracts from a NonMyc tagged construct (ii lane 4). The higher bands detected in *GrkDC5Myc,cni/cni* and *Grk $\delta$ TCMyc* were also detected using an Anti-Myc monoclonal (iii).

## Results - Cornichon

GrkDC is an allele of Grk where the alanine 249 is mutated to valine. This single amino acid substitution results in a loss function allele of Grk. The position of the ala 249 is interesting because it is in the TMD and is included in the conserved domain which is essential for the Rho mediated cleavage of EGF ligands. Anti-Myc primary antibodies were used for these western blot analyses because all constructs in these experiments were driven by the Grk upstream regulatory sequences. Attempts to detect these constructs using the anti-Grk 1D12 monoclonals were not made. In both GrkDC and Grk $\delta$ TC we were able to detect a band in the region of 60-70 kD region which is presumably the non cleaved version of Grk (Fig.26,ii&iii). This was tested by two different Anti-Myc antibodies, a rabbit polyclonal (Fig.26,ii) and a mouse monoclonal with covalently linked HRP (Fig. 26,iii). The rabbit polyclonal detected some cross reacting background bands, in addition to the specific bands. The cross reacting bands were present in case of aversion of Grk without Myc tag. There was no cross reacting bands detected in the case of the monoclonal antibody. Using both Anti-Myc antibodies no band was detected in the Grk $\delta$ CMyc lanes indicating that constructs lacking the cytoplasmic tail was too unstable to be detected. The cause of this instability is not understood.

## 2b Results - Cornichon-related (*Cnir*)

### 2b.1 ORF CG17262 is *cnir*

CG17262 is an Open reading frame (ORF) in the fly genome whose predicted translation product shows highest similarity (45%) and identity (25%) with Cni. Cytologically CG17262/*cnir* maps to the region 23D1 on the left arm of the second chromosome.

A

```

Cni  TYIVALIGDAFLIFFAIFHVIAFDELKTDYKNPIDQCNSLNLPLVLPEYXXXXXXXXXXXXX 68
     T+ + L+ ++ I++V+ +L+ DY N + C LN V+P++
Cnir TFCITLLVYGAILLLLIIYVVLTLADLECDYLNQAQCCRRLNFWVIPKFGSHALLCVLLLL 67

Cni  CGEWFSLCINIPLIAYHIWRY--KNRPVMSGPGLYDPTTVLKTDTLRYNMREGWIKLAVY 126
     G W +N+P++ IW + +R G+YDP + L ++R I L Y
Cnir GGHWVMFLLNLPV---IWLFEYELHRQRDSLGVYDPVDIHSRGLLKVHLRNCMIYLGYY 124

Cni  LISFFYYIYGMVYSLI 142
     + FF +Y ++ SLI
Cnir FVMFFVGLYCLISSLI 140
    
```

B

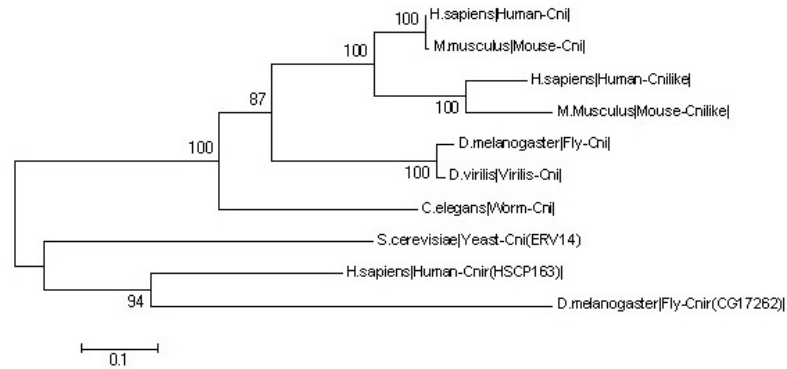


**Fig. 27 Similarity between Cni and Cnir. (A) Cni and cni share 25% identity and 45% similarity. Shown here is the resultant alignment of Cni and Cnir using the blast2p services of the NCBI BLAST. Identical aa are mentioned by the single letter amino acid code in the middle-consensus line whereas similar aa are marked by a “+”. Score = 61.2 bits (147), Expect = 7e-09. Identities = 35/136 (25%), Positives = 63/136 (45%), Gaps = 5/136 (3%). (B) Cladogram of Cni proteins that were available in Swissprot. Cladogram was created using MEGA3 software and is a boot strapped neighbour joining tree (A bootstrapped UPGMA tree (data not shown) had similar branching characters).**

To check whether this open reading frame has any role, either in conjunction with or independent of Cni, it would be desirable to have a “loss of function” allele for this gene. The smallest chromosomal deficiencies of this region are *DfJS17*, *DfC28* and *DfJS7*. *DfC28* and *DfJS7* are smaller deficiencies which are included in *DfJS17* (Fig.28). Using

these deficiencies we tried to identify a mutant line for *cnir* from the Van Eeken lines (VE lines)

## 2b.2 Van Eekens lines

Eighteen EMS generated mutant lines, probable alleles of genes in the region near CG17262, were available from the lab of Late Prof. Van Eeken (VE lines). Some of these lines were also independently obtained from the Bloomington stock centre (Table 1). These lines were initially screened on the basis of their inability to complement *DfJS17* (23C1-2;23E1-2).

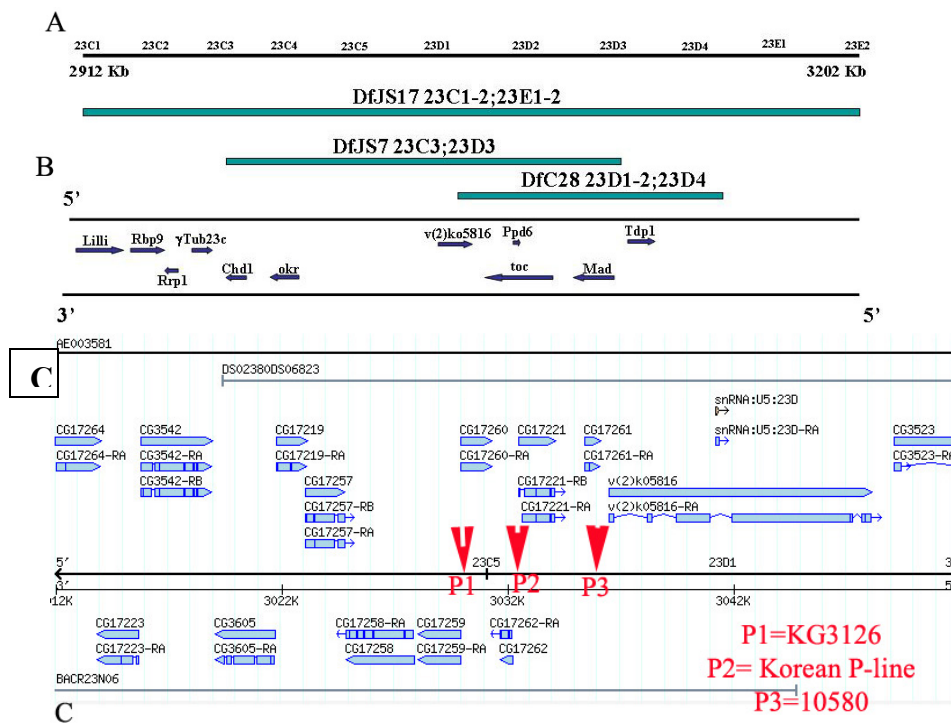


**Fig. 28** Genomic organization of the region around *cnir* (A) Schematic representation of the regions removed by the various deficiencies mentioned in the text. (data for regions removed by the deficiency lines from Flybase) (B) Schematic representation of the identified genes in the region (C) Magnified scheme of the transcript map of 23C4-23D1. CG17262/*cnir* and the P element insertions closest to it (in Red arrowheads pointing to approximate insertion sites) are also shown.

The lines were subsequently classified based on their inability to complement *DfJS7* or *DfC28* or both the deficiencies, which are smaller deficiencies in the DFJS17 region (Flybase Reports Van eeken 2000, FBrf01205088).

The strategy was to screen this collection of EMS mutant line for mutations in *cnir*.

<i>SLNo</i>	<i>Genotype description (Nomenclature from Eeken)</i>	<i>Bloomington line No. (If line available from Stock centre also)</i>	<i>VE Line No (version of the line Over CyOK-GFP balancer : to aid screen/sequencing homozygotes)</i>	<i>Included in Deficiency</i>	<i>Other information</i>
<b>1</b>	L(2)23CDa[A1-6]cn[1]bw[1]	BL-5718	VE-1	JS7 but not C28	
<b>2</b>	L(2)23CDb[A1-15]cn[1]bw[1]	BL-5719	VE-2		
<b>3</b>	L(2)23CDc[A1-4]cn[1]bw[1]	BL-5720	VE-3	JS7 but not C28	
<b>4</b>	L(2)23CDd[A9-3]cn[1]bw[1]	BL-5721	VE-4 \ VE-10	JS7 but not C28	
<b>5</b>	L(2)23CDe[A8-1]cn[1]bw[1]	BL-5722	VE-5 \ VE-15	JS7 but not C28	
<b>6</b>	L(2)23CDf[A13-1]cn[1]bw[1]	BL-5723	VE-6 \ VE-9	JS7 but not C28	
<b>7</b>	toc[A1-1]cn[1]bw[1]	BL-5737	VE-7	JS7 but not C28	Toucan (toc) allele
<b>8</b>	L(2) [A3-2]cn[1]bw[1]	-	VE-8	JS7	
<b>9</b>	L(2)Ce [A15-2]cn[1]bw[1]	-	VE-17	JS17	
<b>10</b>	L(2)CDc [A14-4]cn[1]bw[1]	-	VE-16	JS7	
<b>12</b>	L(2) [A14-9]cn[1]bw[1]	-	VE-18	JS17	
<b>13</b>	L(2)CDa [A4-3]cn[1]bw[1]	-	VE-14	JS7	
<b>14</b>	L(2)CDd [A19-9]cn[1]bw[1]	-	VE-12	JS7	
<b>15</b>	L(2)23Db[A18-1]cn[1]bw[1]	-	VE-20	C28 but not JS7	
<b>16</b>	L(2)23Da[A9-4]cn[1]bw[1]	-	VE-21	JS17	was semi-lethal with C28 (Eeken data)
<b>17</b>	L(2)23Cb[A20-2]cn[1]bw[1]	-	VE-13	JS17	
<b>18</b>	L(2) [A1-7]cn[1]bw[1]	-	VE-19	JS7	Chir allele
<b>Df</b>	Df(2L)JS17dppHOD[Pry+]	BL-1567			Used as negative control in screen

Table 1: Details of the EMS lines and Deficiencies from Van eeken collection and Bloomington Stock centre.

Results – Cornichon related

A) Tester line Candidate lines

$$\frac{w}{w}; \frac{DfJS17}{CyO}; \frac{Pswapcni:Cnir[w+]}{TM2} \times \frac{+}{y}; \frac{VE-X}{CyO}$$

▼

$$\frac{w}{y}; \frac{DfJS17}{VE-X}; \frac{Pswapcni:Cnir[w+]}{+}$$

Scored for straight winged males with w+ eyes

---

B)

Sl. No	VE Lines (candidates) tested (Stock no of ♂)	Tester line	F1 Progeny	
		w/w;DFJS17/CyO; PswapCniCnir (5 ♀ taken per cross)	Curly (CyO) wings (Non-complementation) N (♀ + ♂)	Straight wings + w+(in ♂) (complementation) N (♀ + ♂)
1	L(2)23CDb[A1-15] cn[1] bw[1] (BL-5719)		79 (33 + 47)	3 (1+2)
2	L(2)23CDc[A1-4] cn[1] bw[1] (BL-5720)		55 (29 + 26)	0
3	L(2)23CDd[A9-3] cn[1] bw[1] (BL-5721)		43 (26 + 17)	0
4	L(2)23CDe[A8-1] cn[1] bw[1] (BL-5722)		14 (7 + 7)	0
5	toc[A1-1]cn[1]bw[1] (BL-5737)		124 (66 + 58)	0
6	L(2) [A3-2]cn[1]bw[1]		10 (7 + 3)	0
7	L(2)Ce [A15-2] cn[1] bw[1]		53 (18 + 34)	0
8	L(2)CDc [A14-4] cn[1] bw[1]		85 (41 + 44)	0
9	L(2)23CDe[A8-1]cn[1]bw[1]		120 (61 + 59)	0
10	L(2)CDa [A4-3] cn[1] bw[1]		8 (1 + 8)	2 (2+0)
11	L(2)CDd [A19-9] cn[1] bw[1]		98 (58 + 40)	0
<b>12</b>	<b>L(2) [A1-7]cn[1]bw[1]</b>		<b>63 (33 + 30)</b>	<b>28 (13 + 15)</b>
13	L(2)23Db[A18-1] cn[1] bw[1]		82 (37 + 45)	0
14	L(2)23Da[A9-4] cn[1] bw[1]		51 (22 + 29)	0
15	L(2)23Cb[A20-2] cn[1] bw[1]		21 (13 + 8)	0
Con	Df(2L)JS17dppHOD[Pry+]		66 (39 + 27)	0

Fig. 28 Screening through Van Eeken lines for a *cnir* allele. (A) The genetic designs of the strategy used to screen through the EMS allele collection. (B) Table with the data of the screen. One candidate, *L(2)(A1-7)* was identified.

*PswapcniCnir* (C.Boekel unpublished data) is a construct that uses the 5' cis-regulatory region of *cni* to drive expression of *cnir*. The strategy was to screen through Van Eeken lines to identify a line which would complement *DfJS17* (Fig.28A) when *Cnir* was

expressed using *PswapcniCnir* from the third chromosome. As a negative control to test the efficacy of the strategy, we used the deficiency *DFJS17*, itself as a candidate line and as expected this did not result in rescue.

### **2b.3 *L(2)(A1-7)* is a putative allele of *cnir***

*L(2)(A1-7)* was a line which complemented *DfJS17* using such a strategy. *VE-19* corresponds to the line which carries *L(2)A(1-7)* over the GFP balancer (CyO-KrGFP). The GFP balancer line was created to map the window of lethality and also to sequence the region of and around *cnir* in the *L(2)A(1-7)* homozygous condition.

*L(2)A(1-7)* itself complements *DFJS17* when provided with *Pswapcnicnir* on the third chromosome. There is a significant degree of semi-lethality and the rescue is not absolute as the straight winged flies were only about half the numbers of the curly winged flies (Fig.28B). The straight winged flies also had characteristic “bubbles” on the wings (Fig.29 blue arrowheads), which is due to the improper adhesion of the two epithelial cell layers that form the wing in the fly. These “bubbled wings” were a fully penetrant (100%) phenotype in the rescue flies. Microscopy preparations of these wings also showed aberrations (Fig.29,a&b) in the wing venation patterns. Whether the wing bubbles are the reason or the consequence of these aberrant wing venation patterns is not clear.

The non fluorescent embryos from the *L(2)A(1-7)* lines carrying the GFP balancer died either in late embryonic stage or early (1<sup>st</sup> or 2<sup>nd</sup> instar) larval stage. The embryonic lethals had normal egg shells but the head showed a distinctive embryonic cuticle phenotype (Fig.29c&d). The anterior structures in the embryonic cuticle are missing, and were replaced by necrotic material. The number and pattern of denticle bands, although pushed more to posterior, was normal. The non fluorescent larvae from the few eggs that hatched were wild type in appearance, but they were much slower and uncoordinated in their movement and did not survive beyond early second instar. The sibling fluorescent larvae either survived to adulthood, giving raise to flies with Curly wings, or died at late larval (3<sup>rd</sup> instar) stage or pupal stages, presumably these were the homozygous *CyO* flies. Genomic DNA was extracted from non-fluorescent larvae to sequence the region of and around *cnir*.

## 2b.4 P element insertion lines closest to *cnir*

P element insertion lines closest to *CG17262/cnir* were identified because they could themselves be new alleles of *cnir* or could be used in P element mobilization assays to recover new alleles of *cnir*.

1) G2359 (10534 geneexcel collection): This was the most promising P element insertion line because it is annotated as an insertion in the first intron of *CG17262/cnir*. However, it complemented both *L(2)A(1-7)* and *DfJS17*.

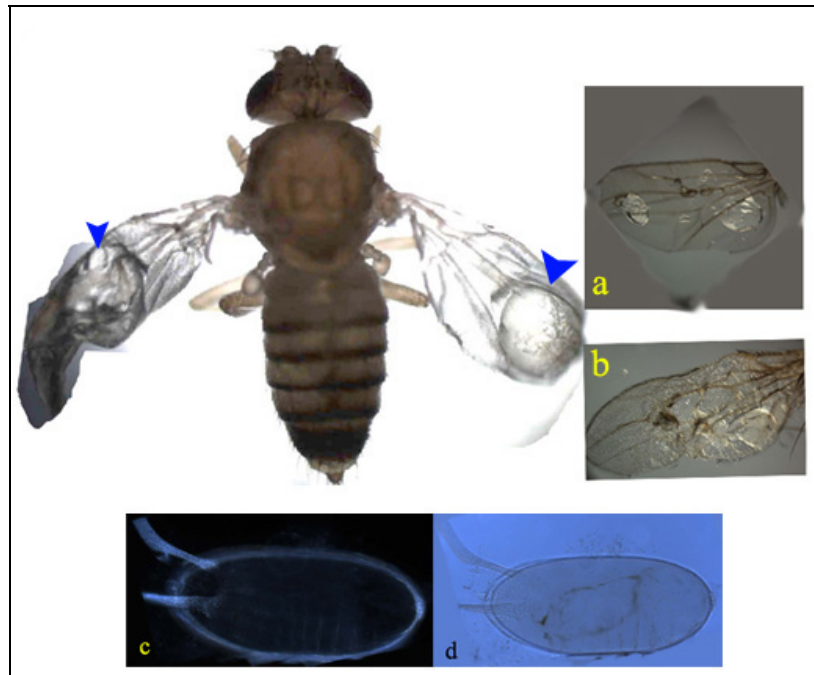
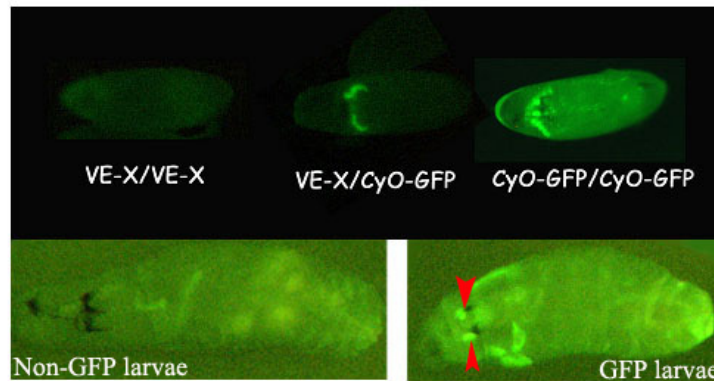


Fig. 29 *A(1-7)* is a probable allele of *cnir*. The “bubble wing” phenotype (arrowhead), which was the result of complementation of *DfJS17* by providing *Cnir* with *cnir* regulatory sequence. a) and b) wing preparations of the “bubble wing”, where as a) is an example with minimum wing venation defect b) is the most severe wing venation defect. c) and d) are the egg phenotypes of the unhatchers from VE-19. c) shows the normal egg shell d) shows the embryonic cuticle defects.

2) KG3126, this enhancer trap line has been mapped to the 5' end of *CG17259* and about 300bp from the 5' end of *CG17260*, which places it around 2 kb downstream of the stop codon of *CG17262/cnir*. This line complements *L(2)A(1-7)* but does not complement *DfJS17*. It is presently the ideal candidate identified, for the P element mobilization assays to generate new alleles of *cnir*.

3) *L(2)P10580*, is a P insertion annotated to be in the gene *l(2)k05816*, which lies about 4 kb upstream of the start codon of *CG17262/cnir*. However, this line complements



**Fig. 30** Egg and larvae from VE-19 flies, VE-19 is L(2)A(1-7)/CyO-KrGFP, to aid in finding the lethal stage of A(1-7) and sequence the alleles responsible for the lethality. The panel above shows the eggs and the presumed genotypes of the embryos based on the amounts of fluorescence. Since analysis of embryos were difficult due due background fluorescence of the yolk and/or maternally loaded GFP, larvae were used for analysis. Lower panel shows a fluorescent and a non fluorescent larvae. (Red arrowheads marks glands which were used as a “landmark” confirmation of fluorescence.

*DfJS17* making further analysis necessary before considering this line suitable for P element mobilization assays.

### 2b.5 Molecular organization of the genomic region near *cnir*:

In order to have the entire transcriptional region of *cnir*, a 2.8 kb region including the region after the 3' end of CG17260 (the ORF 3' of *cnir*) and everything before the ATG of CG17221 (the ORF 5' of *cnir*) was cloned using primers **Rescnir5p** and **Rescnir3p** (see Fig.31b for primer location). These primers were appropriately designed to get the intervening region which included *cnir*/CG17262 and all the sequences upstream and downstream till the next transcription start and end site. This was cloned in Pcasper 2/4, which has only a  $w^+$  gene to assay transgenesis in *Drosophila* and the requisite replication and selection genes to exist as a bacterial plasmid. Such a construct when introduced into flies should be able to complement a *cnir* mutant allele and thus serve as an assay system to check putative *cnir* loss of function mutant alleles.

The 490 bp *cnir* cDNA was cloned from Tolias ovarian cDNA library and the 590 bp *cnir* genomic fragment was cloned using genomic DNA as template. Both fragments were cloned into PCR2 vector. While the cDNA PCR2 construct was used to make sense and antisense probes by using the SP6 and T7 polymerase binding region which flank the multiple cloning site of the vector. These constructs, both the cDNA and the genomic

*cnir* gene will be used to make pUASp/pUAS<sub>t</sub> constructs of *cnir* which will aid in miss/overexpression studies of *cnir*, both in the germa and soma.

Primers were also designed evry 700-800 bp inside the 2.8 kb region, this is to aid in sequencing the *cnir* allele from *L(2)A(1-7)* homozygous larvae. Homozygous non fluorescent larvae were collected fom *L(2)A(1-7)* flies, and genomic DNA prepared. The entire 2.8 kb region was sequenced using the primers designed as in Fig.31B. DNA from fluorescent sibling larvae was used as the sequence for positive controls. PCR2 plasmid containing the 2.8 kb sequence was used as the sequencing reaction control and for reference wild type sequence. Also, DNA sequence of the region from the annotated fly genome was used for reference sequence.

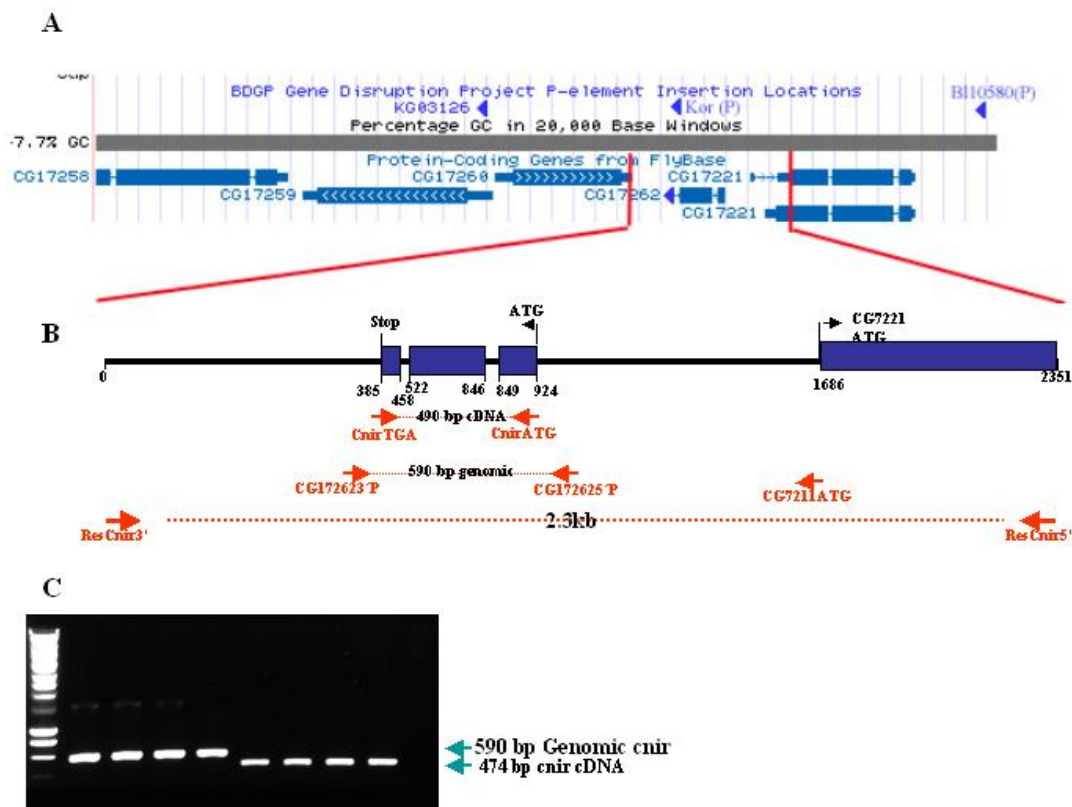
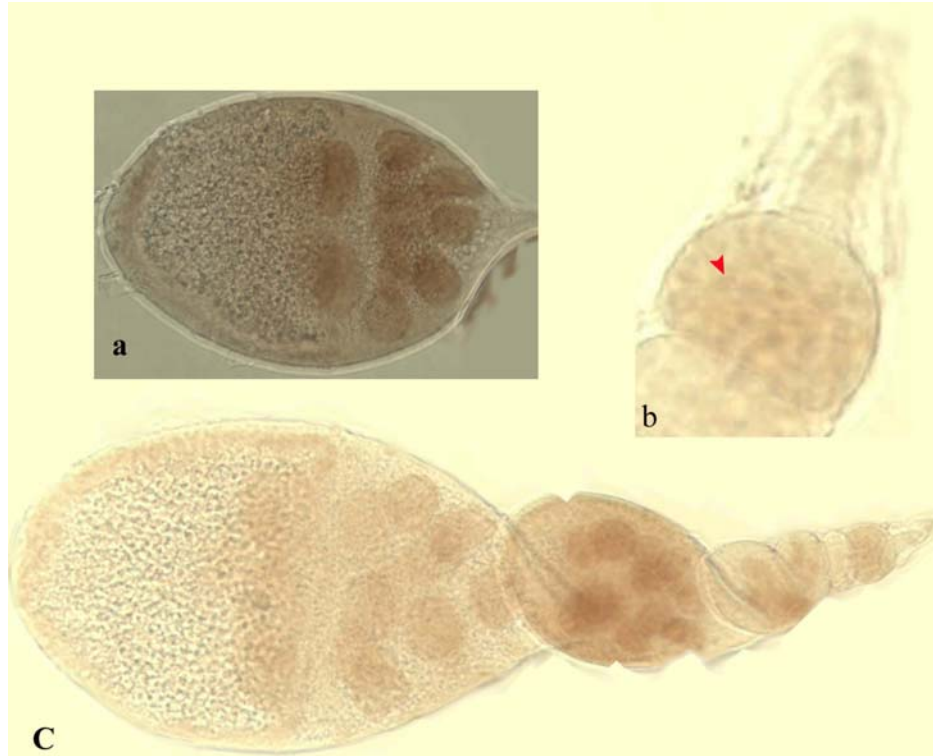


Fig. 31 Molecular organisation of the region around *CG17262/Cnir* (A) Gives the graphical representation of the transcriptional units in the region and the locations of the P insertions in the region as in the annotated genome. (B) A blowup of the region included in the red line boundaries of A. Red arrows indicate PCR/sequencing primers also with corresponding names als in red script below the arrows. Primer pairs joined by dotted red lines indicates the corresponding region has been cloned into bacterial plasmid vector. (C) Indicates PCR products using Genomic DNA or cDNA libraries as template DNA. Four lanes, each lane differs only in the annealing temperatures of the PCR reaction (48°C, 51°C, 53.5°C, 58.0°C in case of both Genomic DNA templates and cDNA library templates each)



**Fig. 32** *cnir* expression is expressed in the germ line. The 490 bp cDNA was used as a probe for *in-situ* in embryos and ovaries. Shown here is the pattern from the ovaries. (a) expression in the nurse cells was detected as late as stage 9 in oogenesis (b) The earliest expression could be detected even before the egg chamber were defined the red arrowhead points to expression in the cystoblast stage. (C) An overview of the temporal pattern of *cnir* expression across oogenesis.

The sequence of the region, except for about 800 bp to 1 Kb 5' of the start site of *cnir*, has been checked. The only sequence difference between the GFP and non-GFP are a couple of single bp changes in the 3' UTR of *cnir*. This has to be reconfirmed. Also the sequencing of the 5' Kb gap in sequence information has to be filled. RNA *in-situ* using the *cnir* anti-sense strand as the probe has indicated low level non specific expression in all germ line cells (Fig 32).

## **2c Results – Enhancer/ Supressor screen**

### **2c.1 Chromosomal regions that interact with *cni* (Enhancers or Supressors)**

The cellular function of Cni can be better understood if components from the cellular milieu, which interact with Cni, can be identified. Distinct egg phenotypes that are associated with different alleles of *cni* and the fact, that there are subtle adult phenotypes also due to *cni* mutations were used as handles to design a genetic screen. The purpose of the screen is to identify regions of the fly genome, which upon dosage reduction, modify (enhance or suppress) the effects caused by a sensitized *cni* background. Gene dosage reduction in flies can be easily brought about by using chromosomal deficiencies whose breakpoints have been cytologically mapped.

### **2c.2 Cni alleles and phenotypes**

The most pronounced phenotypes are those exhibited by the mothers with the amorphic allele (*cniAR55*) over the chromosomal deficiency which includes the *cni* region (*DfH60Scob*) and the eggs laid by them. The eggs laid are completely symmetrical with a micropyle at either end of the egg and no trace of dorsal structures. The amorphic allele (*bcniAR55*) is due to a stop codon at amino acid 44, whereas the hypermorphic allele (*bcniAA12*) is a stop codon at amino acid 87 (Roth et al., 1995)

That the hypomorphic allele, (*cniAA12*), has residual function can be inferred from anterior and posterior egg shell structures i.e: micropyle and aeropyle which is indistinguishable from eggs laid by wild type flies. Also, the hypomorphic allele has a much shorter residual dorsal appendage structure implying that the process of dorsoventral axis specification has also been initiated.

The sensitised background used for the screen was a combination of the hypomorphic allele over the amorphic allele. The egg phenotypes laid by the mothers with one copy of *bcniAA12* over one copy of the *bcniAR55* (Fig.33d) is akin to the halfway point between the extreme amorph/ Df phenotype (Fig.33e) and the comparatively subtler hypermorph

*Df* phenotypes (Fig.33c), namely the eggs have nearly wild type anterior and posterior structures, whereas there is no residual dorsal appendage as seen in the *bcniAA12*.

The adult phenotypes are the head phenotype (ocellar bristles and post vertical bristles absent and slight roughening of the eyes) and wing venation phenotype (shortening of the second vein). The head phenotypes are more consistent and are exhibited by almost all (90%) the flies which have the amorph/*Df* combination. The wing phenotype is erratic and very much dependent on the genetic background of the flies. The loss of function *cni* alleles, are also semi-lethal.

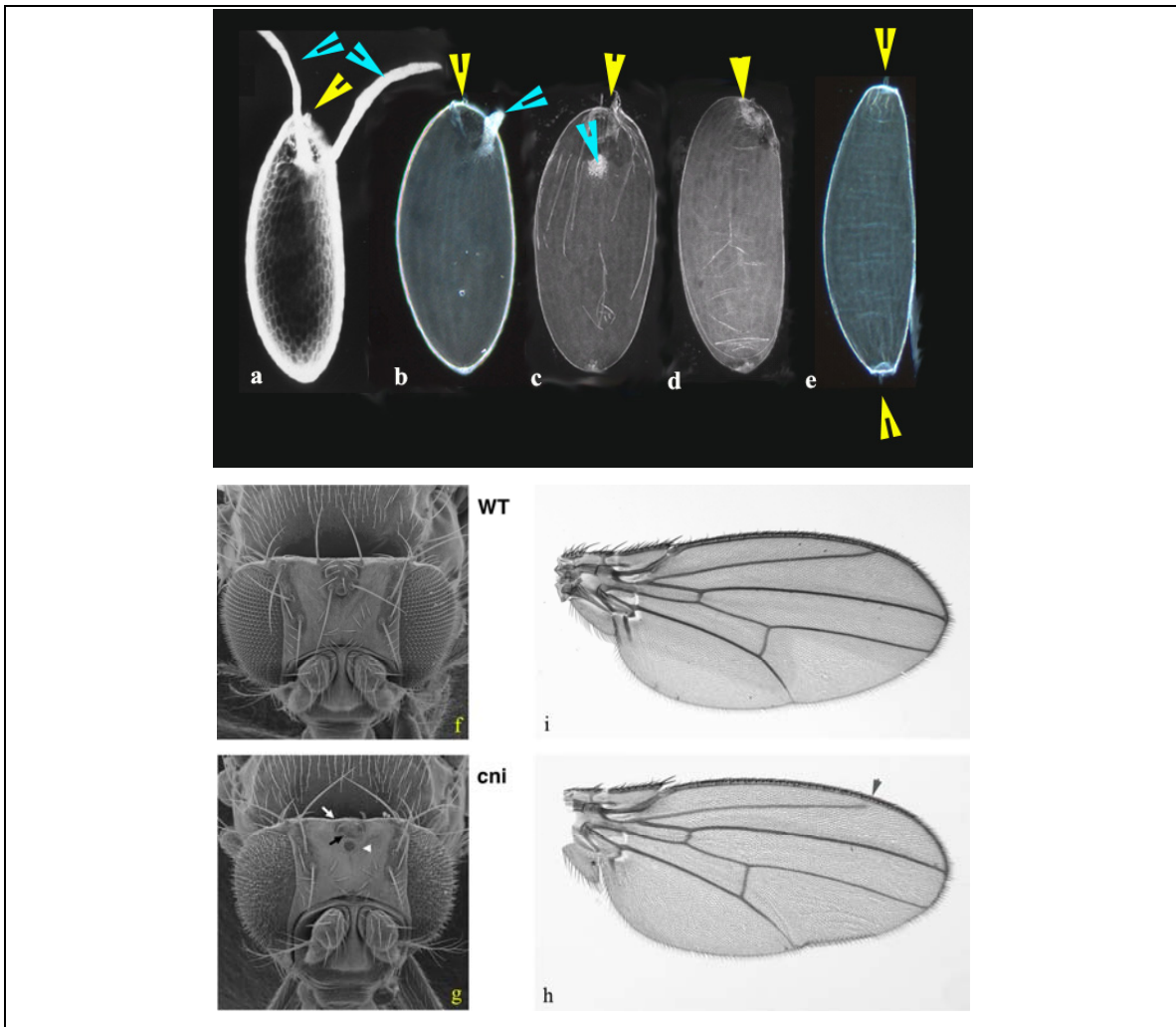


**Fig. 33** *Cni* egg and adult phenotypes. The top panel shows the egg phenotypic series exhibited by flies with different permutations of *cni* alleles. Yellow arrowheads mark micropyle, cyan arrowheads mark DAs/ DA material (a) wild type egg (b) Hypomorph (*cniAA12/cniAA12*) (c) Hypomorph/deficiency(*cniAA12/Dfh60Scob*) (d) Hypomorph/Amorph (*cniAA12/cniAR55*) (e) Amorph/Def(*cniAR55/Dfh60Scob*). The lower panel indicates the adult, head and wing phenotypes, that are present on mothers which lay the *cni* eggs. Note the slight roughening of the eyes, absence of ocellar and postvertical bristles and in the wing the second vein is shortened in the *cni* flies.

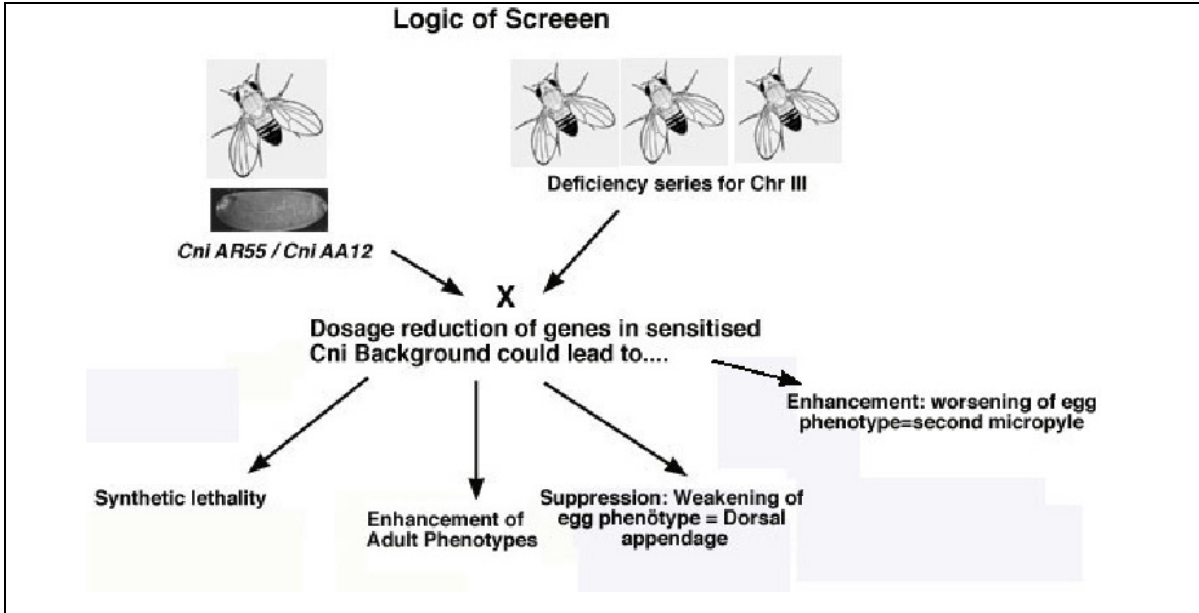


Fig. 34 The scheme of conducting the search for enhancer or supressor regions on the third chromosome in a cni senitised background. The chromosomes deficient in regions are brought into the sensitised cni background by a more elaborate two generation genetic scheme (shown in the picture below), which has been represented here in a simpler single step process for brevity.

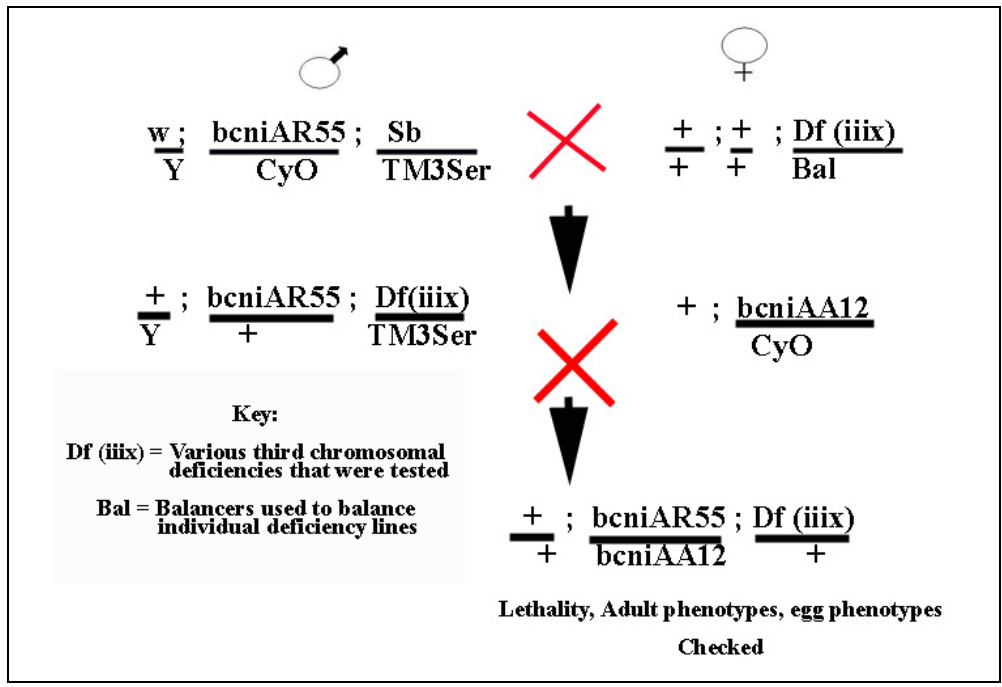


Fig. 35 The genetic scheme of the strategy to identify new cni interacting regions from the third chromosome.

Table 2: Deficiency regions of the third chromosome which were tested for its interaction with cni. The deficiencies which are highlighted in yellow were considered for a secondary test based on the absence of egg preparations but presence of carcasses.

Results – Enhancer / Suppressor screen

Serial no	Bloomington Stock No.	Screen. Code. No.	Breakpoints of the deletion stocks	Egg mounts	Carcass
1		1	61a;61d03	+	+
2		2	61c03-04;61e	+	-
3		3	61c05-08;62a08	+	+
4		4	61c;061f	+	+
5		6	62a2-b1;62c2-d1	+	+
6		7	62a7-b1;62e6-f1	+	+
7		8	62a10-b1;62c2-d1	+	+
8		9	62a10-b01;62c04-d01	-	+
9		10	62a10-b01;62d02-05	+	+
10		13	62b07;62b12	+	+
11		15	62b8-10;62b11-c1	-	+
12		17	63a01;063d01,62a;64c	-	+
13		19	63c01;63d03	+	+
14		21	63d01-02;64b01-02	+	+
15		22	63e01-02;64b17	-	+
16		23	63e06-09;64a08-09	+	+
17		24	63f04-07;64b09-11	+	+
18		25	64a3;64a6	-	+
19		26	63f04-07;64c13-15	-	+
20		28	064f	+	+
21		31	65a;65e	+	-
22		32	65f03;66b10	+	+
23		33	66b01;66b02	+	+
24		34	66c07-10	+	+
25		42	70a02-03;70a05-06	-	+
26		43	70c01-02;70d04-05	+	+
27		45	70c06-15;70e04-05	+	+
28		48	71f01-04;72d01-10	+	+
29		53	72e04;73b04,63b08-11;72e01-02	+	+
30		60	076a03;76b02	-	+
31		62	76f01-03;77d01-02	+	-
32		63	77a01;77d01	+	-
33		67	81f;82f10-11	-	+
34		68	82d03-08;82f	-	+
35		74	84a05;84b01	+	+
36		77	84c01-03;84e01	+	+
37		81	84d03-05;84f01-02	+	+
38		83	84d04-06;85b06,025d;85b06(T)	+	+
39		84	84d08;85b03-05	+	+
40		99	086f01;87a09	-	+
41		102		+	+
42		108			-
43		109	087b15-c01;087f15-88a01,87c02-03;88c02-3;021-040		-
44		110	87d01-02;88e05-06;y	+	+
45		111	87e-f;88b	-	+
46		112	87e01-02;87f11-12	-	+
47		114	88b01;88d03-04	+	+
48		116	89a01-02;89a11-13	-	+
49		118	89b07-08;89e07-08;020	+	+
50		120	89c01-02;89e01-02	+	+
51		124	90c02-d01;91a01-02	+	+
52		128	93c03-06;93f14-94a01	-	+
53		133	95d07-d11;95f15	+	+
54		134	95e08-f01;95f15	+	+
55		136	96a01-07;96a21-25	-	+
56		139	97b;97d01-02	-	-

### 2c.3 The Screen Logistics

As a first step towards identifying chromosomal regions which interact with *cni* we screened through an ordered set of third chromosomal deficiency stocks that were available in the lab. Out of the initial collection of 154 autosomal deficiency stocks of the third chromosome available, we tested 56 stocks (see Table 2) for genetic interactions with *cniAR55/ cniAA12* (sensitized background). The remaining deficiency stocks could not be tested either because of unmarked chromosomal aberrations (duplications/ inversion / transversion) that made unambiguous identification of progeny classes difficult or due lack of a third chromosomal balancer combination in the stock which could make the progeny class identifiable, in the genetic scheme with the sensitized background, or due to inherently high mortality rates of the deficiency stocks themselves. Further, since this was a pilot screen for “proof of principle” of the strategy it was decided to go ahead only with a smaller number of well defined and easily identifiable deficiency stocks and contemplate on a more thorough and complete interaction screen including all three chromosomes only dependent on the results of the “pilot screen”.

### The Screen

The screen itself was conducted in a multi-tiered mode:

#### 2c.4 TIER 1: Primary screen

The first step of the screen, due to the sheer numbers of the deficiencies to be screened (n=56), had to be the simplest with respect to the ease of selecting putative interactors. We decided to look at adult flies and eggs from the second filial generation (F2) of the scheme (Fig.35). We scored for deficiencies

- a) **No Egg category:** F2 flies which had both the *cni* alleles (*black (b)* was used as a visible marker for *cni* besides the absence of balancer (CyO) on the second chromosome) and are heterozygous for the deficiency on the third chromosome were selected. Although the carcasses of these candidates were at hand, the corresponding egg preparations from these flies were absent. One of the reasons for the lack of egg preparations could be that the deficiency enhances the *cni* oogenesis function to such an extent resulting in the inability of these flies to lay

eggs. This assumption was validated by the fact that in the Tier 2 of the screen ovaries from these “no egg category” flies were examined showing the presence of a large number eggs with posterior micropyles “in utero” but were not laid. This was not immediately done with the flies from Tier 1 because in this case the carcasses of the flies were preserved to be examined later. Carcasses of 10-15 adults were preserved for analysis.

- b) No Fly category:** F2 flies with the sensitised *cni* background on the second chromosome and a heterozygous deficiency on the third were detected amongst the siblings. This maybe because the removal of a single copy of genes in the deficiency region may result in synthetic lethality with the sensitised *cni* background. Similarly, the region around *cnir* (*CG17262*) which is included in the deficiency *DfJS17* is known to be synthetically lethal with *cni* (C. Boekel., Ph.D work).

All the egg, wing and head preparations were examined for putative suppressors or enhancers of the *cni* egg, head and wing phenotypes. Sibling controls from the cross with the sensitized *cni* background on the second chromosome and the heterozygous wild type over balancer combination on the third chromosome was used for identifying lethality, enhancement or suppression due to the deficiency.

Sixteen of the fifty six deficiencies were identified as putative interacting regions at the end of Tier 1 (Table 2). These were considered for a more rigorous retesting phase in Tier-2.

### **2c.5 TIER 2 : Retesting Putatives**

The next Tier consisted a rigorous retesting of the sixteen candidates that were selected from the last Tier. Since there were a lesser number of deficiencies to screened in this round, they were checked more thoroughly. The “No egg” flies were maintained overnight in fly media with fresh yeast and their ovaries were examined the next day. Most of the “no egg” lines were enhancers i.e: eggs “in utero” were symmetrical with micropyles at either ends. At the end of the second Tier we had identified 8 deficiencies which were putative candidates for the next Tier.

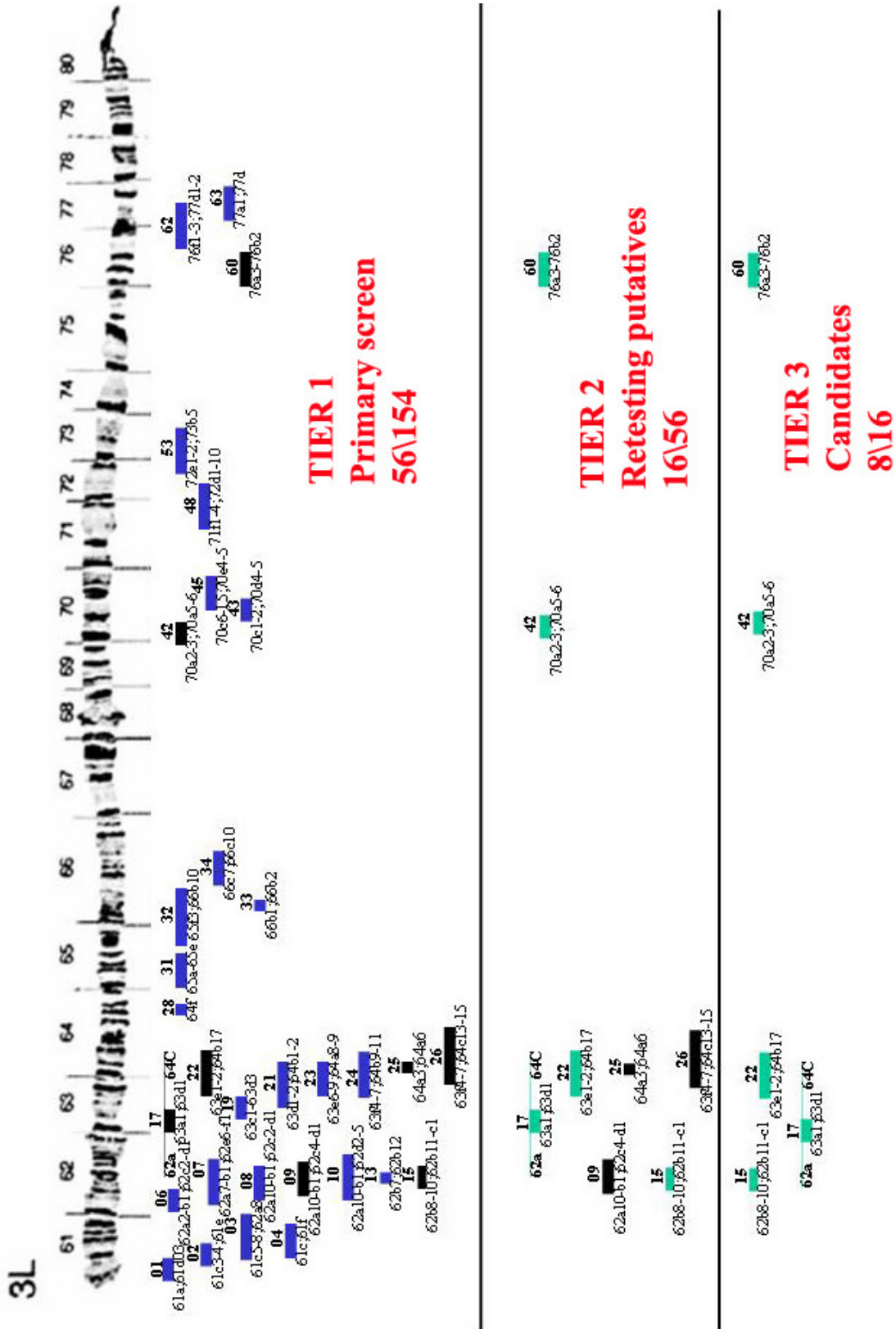


Fig 36: Schematic representation of the deficiencies that were considered for the screen from the left arm (3L) of the third chromosome.

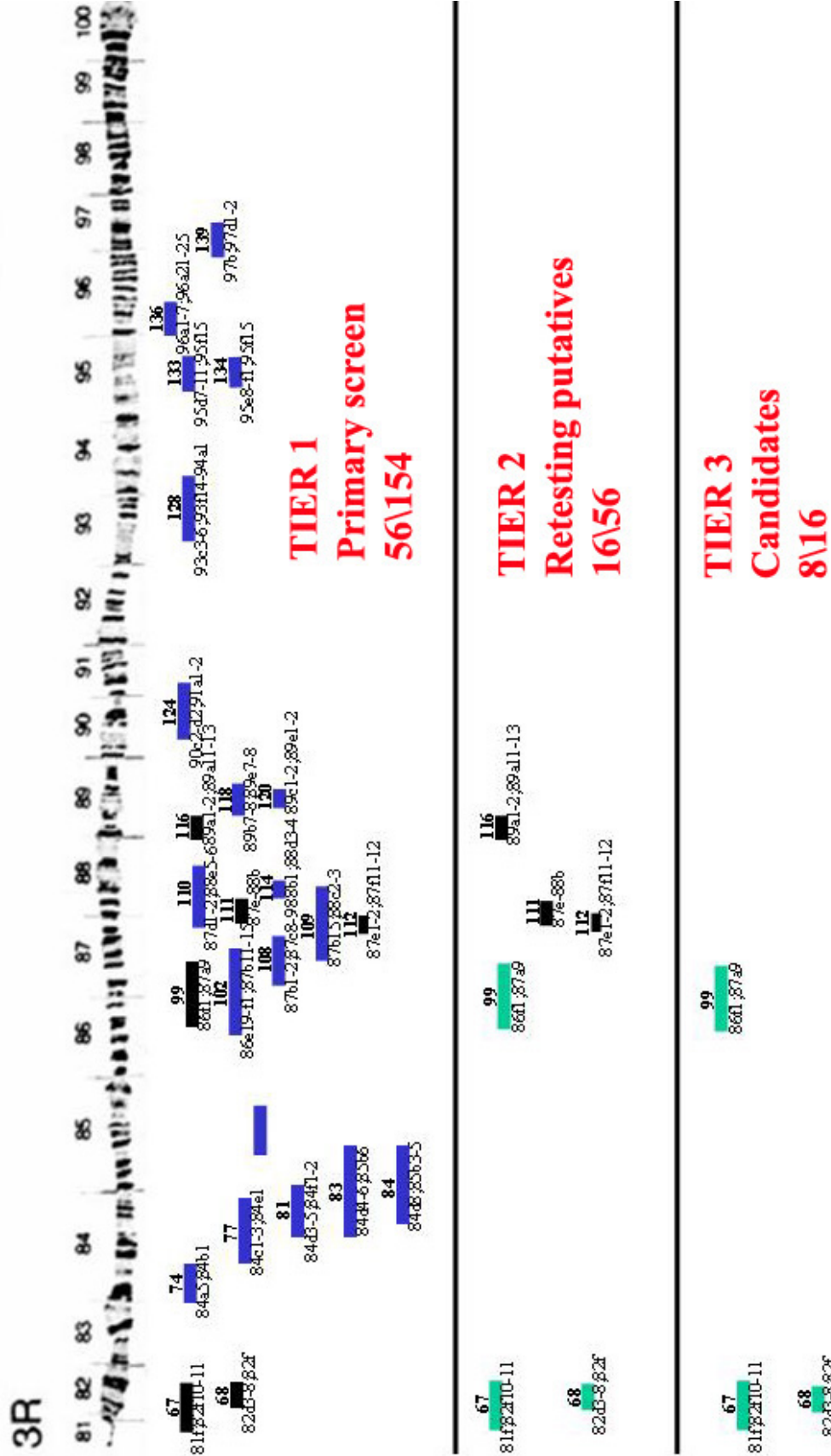


Fig 37: Schematic representation of the deficiencies that were considered for the screen from the right arm (3R) of the third chromosome.

## Results – Enhancer / Suppressor screen

These candidates were composed of one suppressor, three synthetic lethal deficiencies and four enhancer regions (Table 3). Although we identified 8 deficiencies which interact genetically with *cni*, these could be classified into four broad classes dependent on the chromosomal regions.

- 1) Supressor region: A small deficiency region (*Df 60/76A3;76B2*) which includes *pipe (pip)* , *falten (fal)* and *frizzled 2 (fz2)*.
- 2) The 62;63 region: This region contsined two synthetic lethals (*Df15/ 62B8-10; 62B11-C1* and *DF17/ 62A;64C* ) and one enhancer (*Df22/ 63E1-2;64B17*) interactors with the *cni* alleles.
- 3) The Lyra / *senseless (sens)* region: One enhancer (*Df42/ 70A2-3;70A5-6*) in this region which has been attritbuted to be a *sens* allele (Flybase).
- 4) The 86F1/87A region due one enhancer (*Df99 /86F1;87A9*) in this region.

<b>SYNTHETIC LETHALS</b>			
<b>Sl No.</b>	<b>Screen no</b>	<b>Genotype of deficiency</b>	<b>Region covered by deficiency</b>
<b>1</b>	<b>15</b>	<b>Df (3L)9Aprt-53/TM2</b>	<b>62B8-10, 62B11-C1</b>
<b>2</b>	<b>17</b>	<b>Df (3L)HR370/Ln(3LR)T33(L)f19(R)</b>	<b>063A01,063D01,062A,064C(Dp on In)</b>
<b>3</b>	<b>67</b>	<b>Dp (3:192-2, w(118);Df (3R)2-2/TM3</b>	<b>081F,082F 10-11</b>

<b>NO EGG PHENOTYPE</b>			
<b>Sl No.</b>	<b>Screen no</b>	<b>Genotype of deficiency</b>	<b>Region covered by deficiency</b>
<b>1</b>	<b>22</b>	<b>w(1118);Df(3L)GN50/TM8,</b>	<b>063E01-02,064B17</b>
<b>2</b>	<b>42</b>	<b>Df(3L)Ly,mwh(1)7TM1,jv</b>	<b>070A2-03,070A05-06</b>
<b>3</b>	<b>68</b>	<b>w(1110);Df(3R)6-7/TM3, Sb</b>	<b>082D03-08,082F</b>
<b>4</b>	<b>99</b>	<b>Df(3R)T47</b>	<b>086F01,087A09</b>

<b>SUPPRESSOR</b>			
<b>Sl No.</b>	<b>Screen no</b>	<b>Genotype of deficiency</b>	<b>Region covered by deficiency</b>
<b>1</b>	<b>60</b>	<b>Df (3L)VW3/TM3</b>	<b>076A03,076B02</b>

**Table 3: The chromosomal deficiencies which genetically interact with *cni* at the end of the Tier 2 of the screen.**

The deficiencies that were considered for the screen covered 101u (genetic units) as calculated from the breakpoints of the individual deficiencies that is available from

## Results – Enhancer / Suppressor screen

Flybase. This covers roughly 42% of the the third chromosome (240u). 42% of the third chromosome is roughly 17 % (16.8 %) of the entire genome. Hence our “pilot screen” covered about 17% of the fly genome.

56 regions of the third chromosome which were analysed in Tier 1 narrowed down to 14 (25%) and at the end of the second Tier we had further narrowed down the number to 8 (14%).

### **2c.6 TIER 3: Secondary screen (Independent confirmation)**

The objective of Tier 3 was two fold, one was to confirm the genetic interaction of *cni* and the regions identified with independent and overlapping deficiencies and the second was to narrow down the genetic interaction region to as few genes as possible. Confirmation with independent overlapping is crucial because it confirms that the genetic interaction is real and due to the removal of the deficiency region and not due to some inexplicable genetic background.

#### **2c.6.1 Supressor region: Df (3L)VW3 (76A3- 76B2)**

Initially we identified the deficiency called *Df (3L)VW3* as a suppressor of *cni* egg phenotype. Rescue was assayed by the observation of a reduced dorsal appendage (Fig.38 a&b) appearing on the eggs laid by mothers that were heterozygous for the deficiency and in the sensitised *cni* background. The deficiency itself removes a small region of the genome (194 Kb) as calculated from the breakpoint data ascribed to it at Flybase. There are about 19 genes which are in the region that corresponds to *DfVW3*, eight of these are characterised genes (Table4) whereas the other eleven are uncharacterised ORFs named with CG numbers. {CG14084, CG9666, CG9629, CG14088, CG14885, CG14086, CG14089, CG9619, CG32206, CG14087, CG32206}. The most interesting candidate in this region from a dorsoventral patterning perspective is Pipe (*pip*), also *pip* is the only gene in this region that had two EMS induced mutant alleles available from public stock centres. Two deficiencies which remove regions downstream of *pip* including the regions removed by *DfVW3* and also further down stream till 76F were considered for retesting the suppressor, these were the *Df(3l)kto2* and *Df(3l)fln1*. Corresponding deficiencies upstream of *pip* and removing *fz2* and/or *fal* were

St. No.	Genes included in DfVW3	Cytological Location	Kind of Protein Coded / size of Translation product (in aa)	Allele stocks available (Yes/No number of Lines (x))	What kind of mutation is the allele	Other information
1	mRpL21 (mitochondrial ribosomal protein L21)	76A3	mitochondrial large ribosomal subunit (201 aa)	No	-	
2	rept (reptin, Tip48, CG9750)	76A3	DNA helicase activity (481 aa)	Yes (1)	Pelement.BL11706	
3	nes (nessy, CG9655)	76A3	Membrane protein (497 aa)	No	-	Mesoderm
4	Max (CG9648, dmax)	76A3	Transcription factor (161 aa)	No	-	
5	fal (CG9670)	76A5	GTPase (420 aa)	Yes (1)	F element BL12621	Mesoderm
6	pip (pipe-ST2, CG9614)	76A6	hepam-sulfate 2-sulfotransferase activity (413 aa)	Yes (2)	EMS allele BL3110, BL3288	DV axis
7	Chd3 (CG9594, DmCHD3)	76B3	Helicase chromatin binding (892 aa)	No	-	
8	825-Oak	76B3	Unknown (154 aa)	No	-	

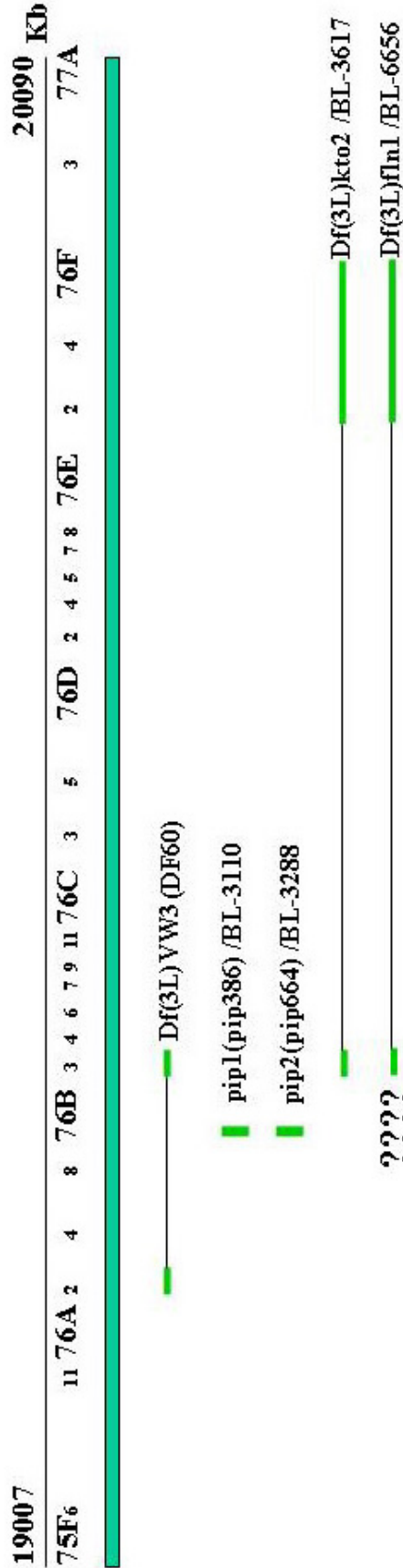


Table 4: The genes that are included in the cni suppressor Df VW3. Fig: Overview of the overlapping deficiencies and the pip alleles used to retest DfVW3.

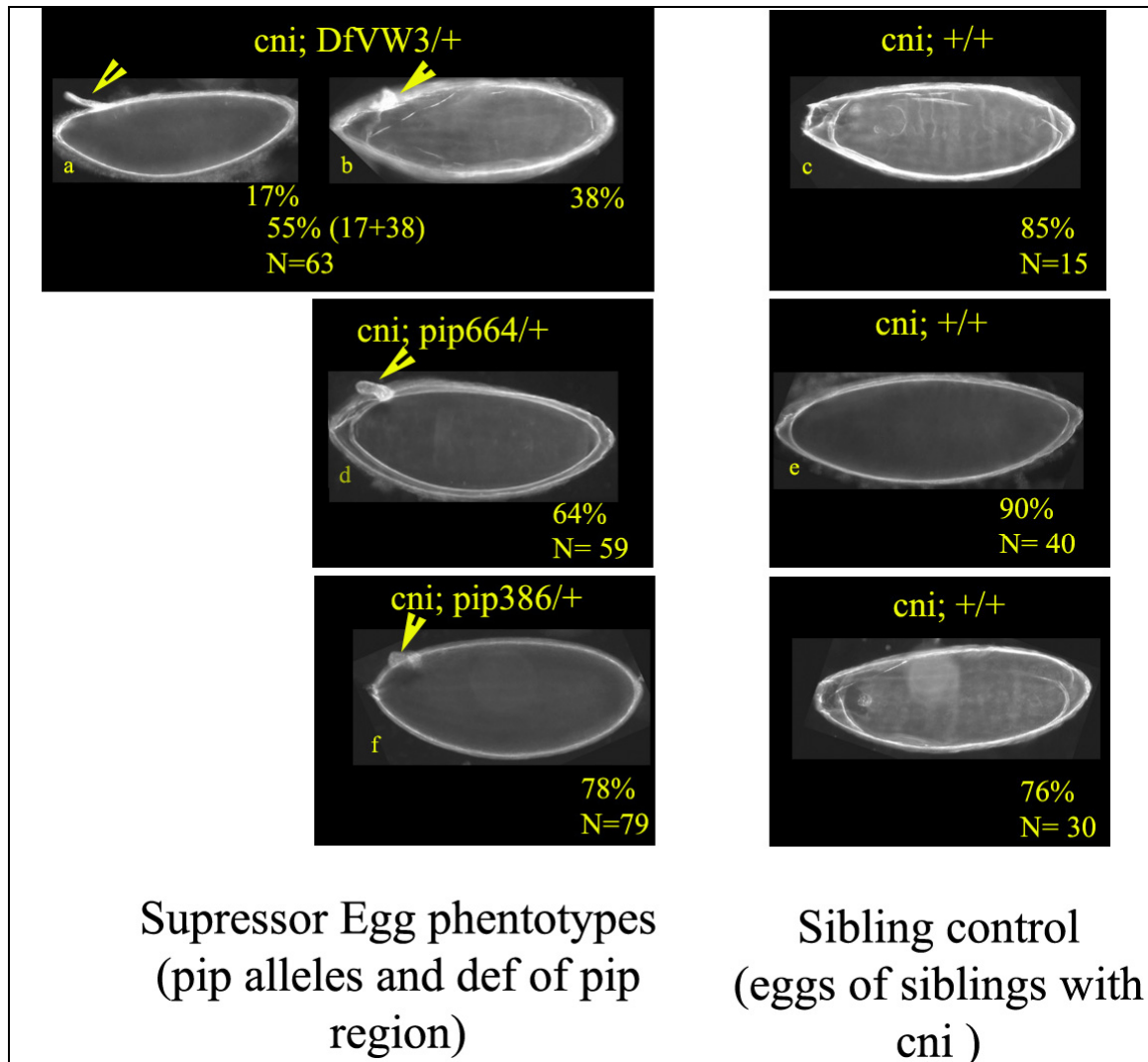


Fig. 38 The egg phenotypes and distribution of the original suppressor *DfVW3* (a,b) and the two pipe alleles (d,f). On the left side are the corresponding egg phenotypes from the *cni* siblings (c,e,g). Egg phenotypes of other deficiencies tested in the region are not shown because they were not significantly different from the *cni* siblings alone. (N= The number of eggs looked at)

considered. Of the two deficiencies used for the confirmation one (*DfFln1*) has to be tested again with the *cni* sensitized background as the genetic cross was not a healthy one and did not give enough offsprings to be considered as successful retest and the other deficiency (*Dfkto2*) was not a suppressor, but exhibited the same egg phenotypes as the siblings with the *cni* background only. The two *pip* alleles tested however, showed significantly higher suppression (Fig.38,d&f) of the *cni* egg phenotypes as against the original suppressor (*DfVW3*) to let us conclude that the suppression is due to *pip*.

### 2c.6.2 The 62; 63 region contains two Synthetic lethals and one enhancer region

This region is complex, as we identified two synthetic lethals (**Df15/ 62B8-10; 62B11-C1 and DF17/ 62A;64C** ) and one enhancer (**Df22/ 63E1-2;64B17**) in close proximity. The enhancer **Df22/ 63E1-2;64B17** is a rather big and not very well defined deficiency which overlaps with regions that are part of both the synthetic lethals, **Df15/ 62B8-10; 62B11-C1 and DF17/ 62A;64C**. We considered the the three candidates in two different data sets.

#### Synthetic lethal 1 Df1562B8-10 (62B11-C1):

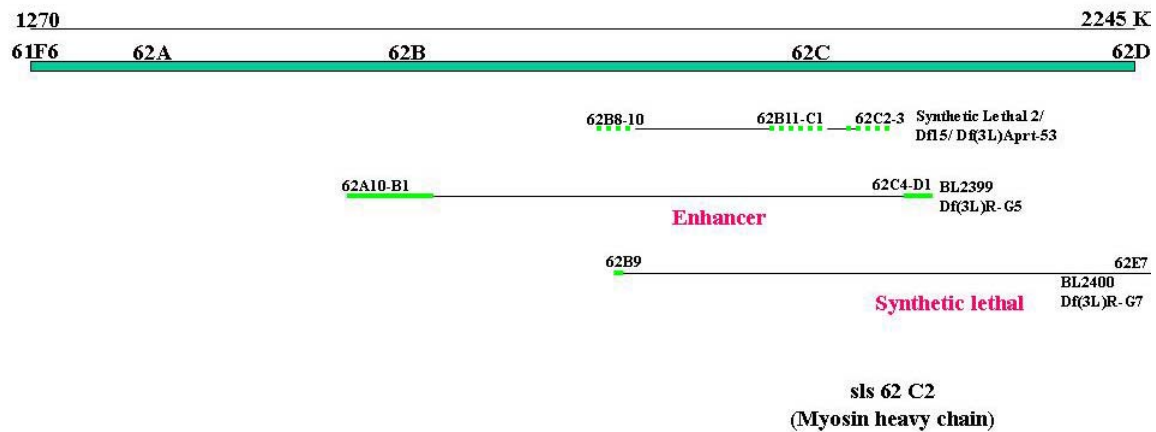


**Fig. 39** The deficiency region included in Df15 and the independent and overlapping deficiencies which were used to reconfirm the synthetic lethality, that was induced by Df15

Although the enhancer **Df22/ 63E1-2;64B17**, is a not well defined and it includes regions that are part of both the synthetic lethals **Df15/ 62B8-10; 62B11-C1** and **Df17/ 62A;64C**, we analysed it as part of the data set that was considered for confirmation of the **Df17**.

**Df15/62B8-10;62B11-C1** was tested using two independent and overlapping deficiencies, **Df(3L)R-G5/62A10-B1;62C4-D1** and **Df(3L)R-G7/ 62B9;62E7**. **Df(3L)R-G5** behaved as a heterozygous enhancer in the *cni* sensitised background, where **Df(3L)R-G7** was another synthetic lethal in a *cni* sensitised background. The only candidate gene which is coincidental in the region which is common to all three of these is a rather large gene called *sallimus* (*sls*), which is described as Myosin light chain kinase (Flybase). *Sls* is known by synonyms such as Kettin, Titin, Mitotic Chromosomal

## Results – Enhancer / Suppressor screen

Protein (MCP), or anon-CREST. There is one available mutant allele of *sIs* from the public stock centre which has to be tested for its effect in a sensitized *cni* background.

### Synthetic lethal, DF17/ 62A; 64C and enhancer, Df22/ 63E1-2;64B17:

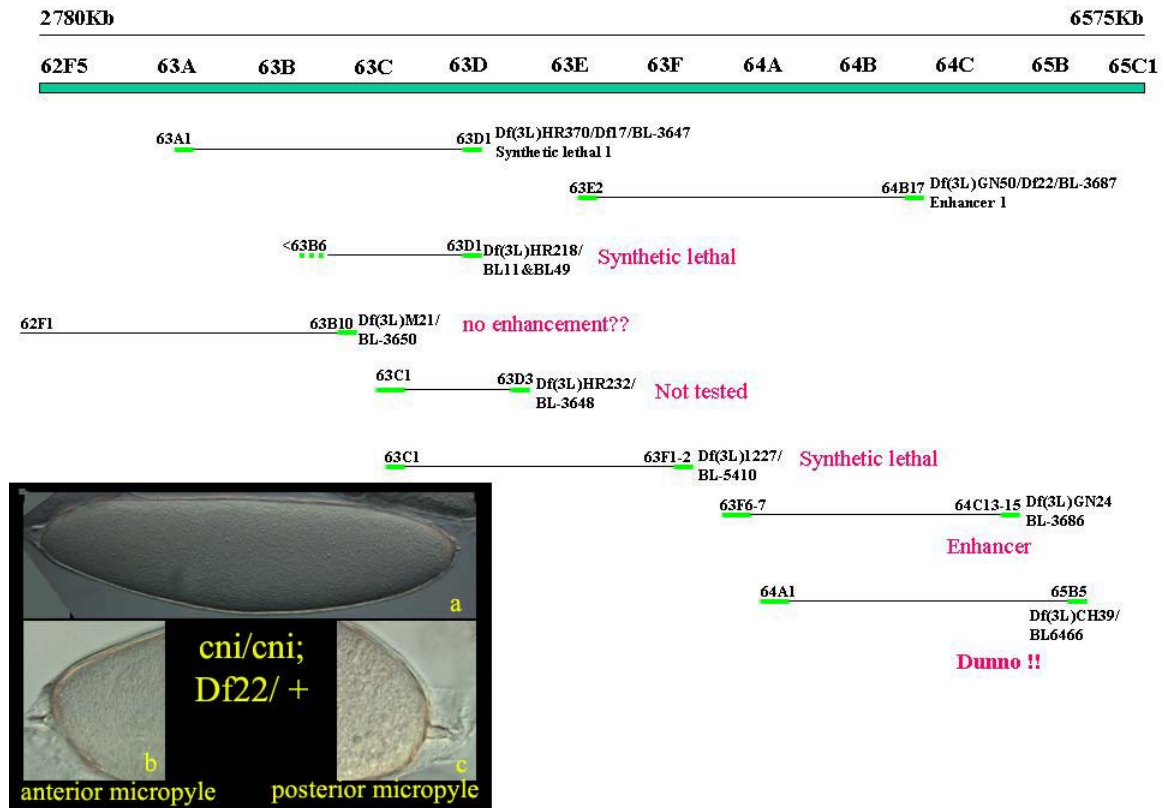


Fig. 40 Schematic representation of the chromosomal region included in the synthetic lethal Df17 and the enhancer Df22. Also represented are the overlapping deficiencies that were used to confirm these interactions. In inset is shown the enhanced egg phenotype that is exhibited by the *cni/cni; Df22/+* combinations. The eggs were not laid but found “in utero” in the ovaries of the mothers.

Synthetic lethal 1 / *DF17/ 62A; 64C* is very interesting because *sprouty (sty) 63D2-3* is one of the genes that is removed by this deficiency. *Sty* is a known inhibitor of EGFR signaling (Kramer et al., 1999). The synthetic lethality was also reproducible by two other independent deficiencies, *Df(3L)HR218/ 63B6;63D3* and *Df(3L)1227/ 63C1; 63F1-2*. All three of these deficiencies remove several other genes in addition to *sty*, so it has to be tested with a loss of function allele of *sty*. The other genes which are in the region *63C1 to 63D3* are:

## Results – Enhancer / Suppressor screen

- i) Karst (*kst*) 63D1, a microtubule binding protein involved in zonula adherens assembly and expressed in follicle cells and germ line stem cells. There is a P element insertion allele of this gene available from the stock centre.
- ii) DrgT521-L 63D2, no information regarding this annotation could be found.
- iii) Sprouty (*sty*) 63D3, an inhibitor of EGFR and FGF signaling cascades. Two loss of function alleles available from stock centre.
- iv) Cytoplasmic initiation factor (*cIF2*) 63D3, translation initiation factor. Interacts with Vasa (Carrera et al., 2000). One P element insertion allele of this gene available from stock centre.
- v) Cyclin J (*cycJ*) 63E1, a cyclin dependent kinase which is expressed in the nurse cells. No mutant alleles available.

The enhancer, *Df22/ 63E1-2;64B17*, was tested with another deficiency (*Df(3L) GN24*) region which narrowed down the enhancement region between 63E to 64B17. Although we could reproduce the enhancement with another independent deficiency, there are far too many genes in the interval so smaller deficiencies in the region have to be tested before we can check with single gene alleles (see table below for the genes in the region).

Sl.No	Name of Gene (abb)	Map location	Type of gene coded	Alleles available From Stock centre (number & type)	Other comments
1	encore (enc)	63F1-3	R3H Nucleotide binding	Y (2, one P-element and one EMS)	Nurse cell; oocyte differentiation and number
2	Arrowhead (Awh)	63F4	Transcription factor homeodomain	Y (3, EMS alleles)	Ectoderm development
3	Sc2	63F5-6	Ubiquitin like	Y (4, one EMS, one P)	
4	imaginal discs arrested (ida)	63F6	Anaphase promoting complex	Y (3, one P and two EMS amorphs)	
5	maggie (mge)	63F6	Mitochondrial outer membrane protein translocase	Y (2, EMS alleles)	
6	Ecdysone induced protein (Ep 63F1)	63F6-7	Ca ion binding	N	
7	scratch (scrt)	64A2	Transcription factor	N	
8	Forkhead domain 64A (fd64A)	64A4	Transcription activity	N	
9	Gustatory receptor (Gr64A)	64A4	Taste receptor activity	N	
10	disembodied (dis)	64A5	Electron transport activity	Y (2, one EMS)	
11	wishful thinking (wit)	64A5	TGF- $\beta$ receptor activity	Y (2)	
12	fumarylacetoacetase (faa)	64A5	Fumarylacetoacetase activity	Y (2)	
13	Glutamic acid decarboxylase (GAD1)	64A5	Glutamate decarboxylase	Y (3, one Pelement)	

## Results – Enhancer / Suppressor screen

14	Ack	64A6	Tyrosine kinase activity	N	
15	Chd64	64A6-7	Actin binding	N	
16	Replication factor C40Kd Rfc40	64A7	DNA binding	Y (2)	
17	Ras opposite (Rop)	64A7	SNARE binding	Y (one EMS)	Osk mRNA regulation
18	masquerade (mas)	64A8	endopeptidase	Y (one P element)	
19	Ero1L	64A9	Intracellular protein transport	N	
20	Temperature induced paralytic E (tipE)	64A10	Voltage gated Na channel	N	
21	Ecdysone inducible gene L2 (ImpL2)	64A10	Cell adhesion	Y (one P)	
22	pavorotti (pav)	64A10-11	Microtubule motor activity	Y (one EMS)	
23	archipelago (ago)	64A11-12	Ubiquitin ligase	N	
24	Transcription factor IIE $\beta$ (TfIIE $\beta$ )	64A12	RNA Pol II Transcription activity	N	
25	Hexosaminidase I (Hexo1)	64A12-B1	$\beta$ -N-acetylhexosaminidase activity	N	
26	Cip4	64B1-2	Rho interactor activity	Y (one P)	
27	Syntaxin 17 (Syx17)	64B4-5	T-SNARE activity	N	
28	Tie-like receptor tyrosine kinase	64B9	Tyrosine kinase	N	
29	Src oncogene at 64B	64B11-12	Tyrosine kinase	Y (one P)	Ring canal
30	axotactin (axo)	64B12-13	Cell adhesion	N	
31	Dynein heavy chain 64C (Dhc64C)	64B17-C	Microtubule motor	Y (one EMS allele and one P)	

### 2c.6.3 The Lyra/ senseless region Df42/ 70A2-3;70A5-6

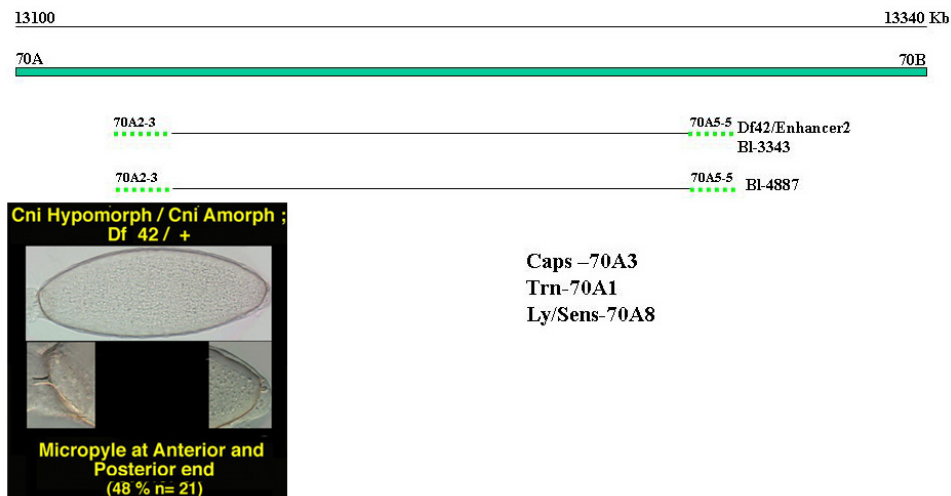


Fig. 41 Schematic representation of the enhancer deficiency region included in Df42

The *Df42* has been annotated as a line which removes the gene *senseless* (*sens*) or Lyra (*Ly*) by Flybase. But *Ly*(70A8) itself lies slightly away from the region that is annotated to be included in the deficiency region. However, *tartan* (*trn*) 70A1 and *capricious* (*caps*) 70A3, are the only two genes in the region included in the deficiency.

### 2c.6.4 The enhancer region (*Df99* /*86F1*;87A9)

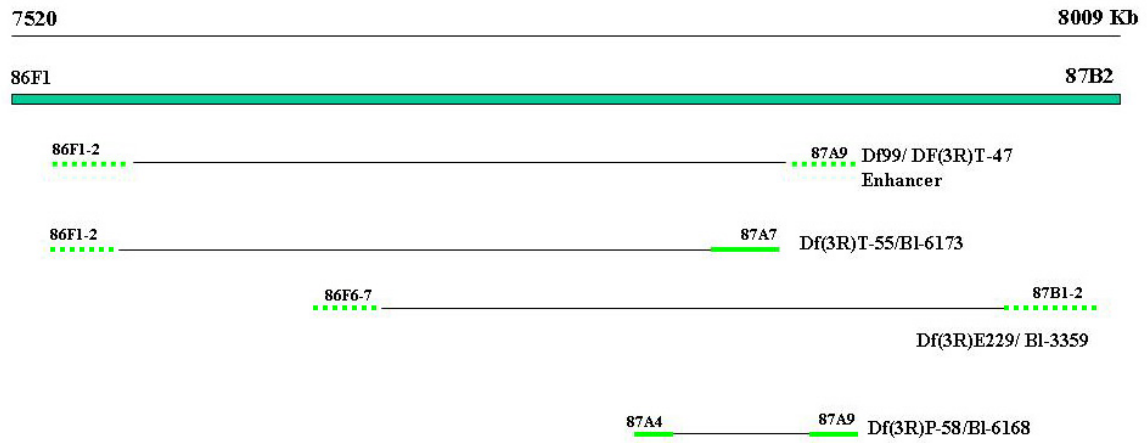


Fig. 42 Schematic representation of the enhancer region included in the *Df99*.

The interaction due to this region are yet to be tested

### **3a Discussion- Cornichon**

#### **3a.1 Cni is an ER to Golgi transport protein**

Subcellular localisation of the Cni-Myc fusion construct expressed in the follicular epithelium shows highest colocalisation with ER markers. Colocalisation with ERGIC and Golgi markers was also observed. Erv14p, the only biochemically and functionally understood member of the Cni family of proteins, functions as an ER to Golgi transport enrichment protein for Axl2p (Powers and Barlowe, 1998). The ERGIC also serves as a sorting station for the retrieval of ER resident proteins (Martinez-Menarguez et al., 1999). This sort of sub-cellular localisation profile fits with the function of an ER to Golgi transport adaptor protein which has to cycle between the ER and the Golgi to carry out its function. There has been only one reported subcellular localisation study, where an HA-tagged Erv14p protein was shown to exhibit a perinuclear distribution (Powers and Barlowe, 1998). No subcellular studies have been reported for any of the members of the Cni family. There are no antibodies raised against this protein and attempts to raise antibodies against this protein in several labs have failed. The protein induces cellular toxicity in bacterial cells when it is expressed as the full length form. The high degree of conservation between members of this family could be another possible reason for the extreme difficulties in the expression of these proteins and in raising antibodies against them.

For the colocalisation experiments the ER and ERGIC markers were visible in the stretched follicle cells. The stretched follicle cells are very flat polarised epithelial cells that are spread like a thin net over the nurse cells. The Golgi markers were not detectable in the stretched follicle cells. The cuboidal follicle cells were the only type of follicle cells, where the Golgi marker could be detected. The Golgi apparatus is a much smaller subcellular organelle compared to the ER, and was much harder to detect in the flat stretched follicle cells.

Two different follicle Gal4 drivers were used to drive the *UAScni5myc* construct in the follicle cells, *CY2Gal4* and *GR1Gal4*. While the expression of *CY2Gal4* gave the highest

consistency in the different follicle cell types, the expression using ***GRIGal4*** was patchy and not consistent to any particular follicle cell type.

### **3a.2 Grk transported via the bulk flow mode of exocytosis can overcome Cni requirement and produces active Grk**

Grk is responsible for initiating both the axes by signaling from the germ line to the somatic follicle cells. Grk transport is highly regulated and shows very strict localisation both at the level of RNA and of protein localisation. Cni is hypothesised to function by specifically enriching Grk into COP-II vesicles during the ER to Golgi transit. To address the question of such a hypothetical role for Cni, the strategy used was to try and shunt massive amounts of Grk through the bulk flow mode of cellular exocytosis. In such a situation of increased amounts of Grk exocytosed, the dependence of Grk on Cni for COP-II mediated enrichment could be overcome. Grk was over/misexpressed from the germ line using germ line specific drivers. The assay was to monitor if there was an increase in the amount of Grk signal from the germ line using the egg shell. The egg shell is very sensitive to the amount of Grk signal from the germ line, an increase in the amount of Grk results in dorsalisation (Nilson and Schupbach, 1999).

Two different germ line specific drivers were used for expression of Grk from the germ line, ***NosGal4VP16*** and ***TubGal4VP16***. Both drivers dorsalise the egg shell when Grk is overexpressed during oogenesis in a cni heterozygous background. Based on the egg shell phenotypes, ***TubGal4VP16*** appeared to be the stronger of the two.

Using a GFP reporter, ***TubGal4VP16*** also has been visualised to initiate GFP expression much earlier than ***NosGal4VP16***. The timing of onset of ***TubGal4VP16*** corresponds to stages much before the first round of Grk signal.

However, the amounts of full length Grk detectable using Western blot analysis were not dramatically different from each other.

When mis/overexpressed in the ***cni*** homozygous background, ***TubGal4VP16*** is able to rescue the axis initiation function but not mis/overexpression using ***NosGal4VP16***. The rescue was assayed by the presence of AP and dorsal egg shell structures on the eggs laid by such females. This indicates that Grk shunted through the bulk flow exocytosis

machinery can overcome the requirement for Cni to specifically enrich it during ER to Golgi transport of the protein.

The ability of one of the Gal4 drivers (which is slightly stronger and is expressed earlier than the other) to overcome the requirement of Cni in Grk signaling could be because of the strength of expression or due to the timing of onset of expression.

In scenario one, where the strength of the expression is the crucial factor, it could be that the small increase in the amount of Grk using *TubGal4VP16* compared to *NosGal4VP16* is enough to overcome the cellular threshold. Due to the excess amounts over this particular threshold, the protein attains concentrations where it can be passively incorporated in the bulk flow exit from the ER. Hence, the requirement for specific cargo enrichment proteins such as Cni can be circumvented.

In scenario two, the rescue could be due to the fact that Grk is expressed by *TubGal4VP16* in stages before the first Grk signaling takes place. Here, the crucial factor is the developmental timing when the expression of Grk is turned on. In such a scenario Grk has to be present to initiate the first round of signaling and the subsequent second round of Grk signaling is dependent on the initiation of the signal in the first round. So, in the absence of Grk expression in time for the first Grk signal even increased amounts of Grk later, do not rescue the function.

There is also a third possibility that it is a combination of both the amounts of Grk expressed and the timing when expression is turned on that is crucial to overcome the requirement for Cni. In this case, not only Grk should be produced in amounts high enough to overcome the concentration thresholds to exit the ER via the bulk flow mode but also this expression has to occur at developmental stages early enough to initiate the first Grk signal from the oocyte.

The issue of whether the rescue is due to the timing or the amounts of Grk expressed can be resolved by checking whether expression of Grk with *TubulinGal4 (TubGal4)* in a cni amorphic is able to rescue the Cni requirement. *Tubgal4* is the version of the tubulin Gal4 driver lacking the VP16 activation domain. This is also a germ line driver and gives a much weaker egg shell dorsalisation phenotype in comparison to both *NosGal4VP16* and *TubGal4VP16*.

In such a case if *TubGal4* is able to rescue the Grk function in a *cni* then it would indicate that the crucial factor is the timing of Grk expression onset and not the amount of Grk expressed.

In case it is unable to bring about the rescue as *TubGal4VP16* does, it would imply that both the timing and amounts of Grk produced are crucial in initiating the signal.

### **3a.3 Grk signaling can be rescued but the regulatory fine tuning is lost**

The ability of the Cni-independent Grk via the bulk flow to produce egg shells with AP polarity and DA material deposition, indicates that Grk is active to signal to the DER. This proves that the function of Cni is only to transport Grk during exocytosis, and not in modifying the structure or activity of Grk. However, regulatory roles in Grk activity by influencing the amount or direction of transport cannot be ruled out.

The EGFR is activated by different ligands in different signaling contexts in a variety of tissues, and the type, structure and the number of ligand molecules are all crucial factors in activating differential signal response due to DER activation. The mammalian EGF-EGFR crystal structure studies have shown 1:1 EGF:EGFR, dimerises by a unique “receptor mediated dimerisation” up on ligand docking (Ogiso et al., 2002). The conformation and number of ligands are crucial factors in this interaction.

The overexpression of Grk using *TubGal4VP16* in a *cni* homozygous background, leads to a rescue in Grk signaling. This can be seen by the presence of a posterior aeropyle like structure and DA material being present in the eggs laid by these flies, indicating that both rounds of Grk signal were initiated. The majority of the rescued eggs however show a ring of DA material deposited around the anterior rim of the egg, a phenotype closer to the dorsalised eggs than the wild type. This phenotype is similar to the egg shell observed due to activation of a constitutively active form of DER (*Atop*) all along the AP axis in the follicle cells (*TI55Gal4*) (Queenan et al., 1997). This indicates that in addition to initiating the Grk signal, Cni mediated Grk transport has also some role in the restriction of the Grk activation domain. Although Grk transport via the bulk flow is able to signal to the receptor, the precision of the signaling achieved by the Cni mediated specific enrichment pathway is not rescued. This also indicates that the point of highest Grk localization at the anterior corner of the oocyte (presumably this is also the same point on

the egg shell where the DAs split) is selected by the precise localization of Grk via the Cni mediated pathway.

Another common phenotype amongst the rescued egg shells were the ones in which DA initiation occurred at multiple points all along the AP axis of the egg shell. These phenotypes are reminiscent of the egg shell phenotype observed due to the activation of a constitutively active form of DER (*λtop*) all along the AP axis in the follicle cells (*T155Gal4*) in a Grk amorphic background (Queenan et al., 1997). Thus Cni mediated routing of Grk has a role in restriction of Grk activation to a small sub domain on the oocyte membrane. The restriction of unregulated EGFR activity is a very important aspect of EGFR regulation. In mammalian systems, constitutive activation of EGFR through autocrine stimulation or other mechanisms is associated with several types of cancer (Burgess and Thumwood, 1994; Sandgren et al., 1990).

A very important question that is still not answered is the post Golgi trafficking of Grk, whether there is still another unknown component involved in the vectorial transport of Grk vesicles to the target subdomain on the oocyte membrane.

### **3a.4 Cni and Star, are both involved in the ER to Golgi transport of Grk**

The function of *S* is to transport EGF ligands from the ER to the Golgi (Lee et al., 2001; Tsruya et al., 2002). *S* is expressed in all stages of the developing egg chambers, first appearing in region 2A of the germarium. In stage 4-7 egg chambers *S* gets concentrated in the oocyte. In later egg chambers (stage 10), it is also detectable in the nurse cells (Pickup and Banerjee, 1999). Germ line clones of *S* result in early germ line arrest phenotypes (Mayer and Nusslein-Volhard, 1988), so addressing the role of *S* for later axis decisions is impossible by conventional loss of function analysis.

*S* and *cni* are synthetically lethal (S. Roth, unpublished observations) making the role of *S* in Grk transport very intriguing. An inducible anti-sense construct of *S* (*UASpStarAS*) was reported which would make it possible to address these questions (Ghiglione et al., 2002). Expression of this construct from the germ line using the *NosGal4VP16* driver resulted in egg shells which showed the initiation of DAs but the absence of the twin DAs. It is interesting as to why the removal of *S* from the germ line results in the inhibition of the Spi mediated EGFR secondary refinement which is responsible for the

DA patterning. Paradoxically, expression of the same construct using *TubGal4VP16* has absolutely no effect on the egg shell. This indicates that the first round of Grk signaling requires only the Cni mediated Grk transport pathway. Whereas for the second round of Grk signaling and subsequent DA patterning requires the cooperation of both Cni and S modes Grk transport. The Grk transport via the S-Rho route is not constitutively active and has to be activated. Whether it is the initiation of the Grk signal by the Cni mediated pathway that activates the subsequent S mediated Grk transport in the oocyte, directly or indirectly, or the induction of the S-Rho pathway transport requires an independent cue is not clear.

In PC12 cells it has been shown that persistent low levels of activation of the EGFR pathway leads to cell fate transitions whereas transient high level activation leads to cell proliferation (Dikic et al., 1994). Similarly, Cni-Grk transport and S-Rho route could be pathways required for low levels and high levels Grk transport requirements.

Another egg phenotype which was seen in very few numbers, was the presence of DA initiation in egg with two micropyles, one on either end. This indicates that under extreme conditions the DV axis polarisation can be initiated in the absence of AP axis initiation. The few egg numbers showing this phenotype makes further analysis of this phenomenon difficult to study.

Overexpression of S and Brho in heterozygous conditions showed no effect on egg shell or the embryos.

Both Gal4 drivers exhibited a series of embryonic defects indicating that the imprecise early Grk signaling during oogenesis can affect several downstream events.

### **3a.5 Cleaved forms of Grk are observed in *cni* homozygous background**

Western blot analysis of the overexpressed protein using both germ line Gal4 drivers in *cni* heterozygous backgrounds resulted in a single band of Grk. This band corresponded to around 60-70 kD and is the full length Grk protein. A smaller band around 30-40 kD band is observed only in conditions where the overexpression is in a *cni* homozygous background. This band is the processed Grk band, processing protease presumably being Rho. The cleaved band being visible only in *cni* homozygous backgrounds indicates that the cleavage mediated by the S-Rho pathway is inhibited in *cni* heterozygous

backgrounds. Further the cleaved band in the *NosGal4VP16* overexpression in a *cni* homozygous was much weaker than the cleaved band in the *TubGal4VP16* under similar expression conditions. This indicates that the S-Rho mediated cleavage of Grk is inhibited in the presence of Cni.

### **3a.6 Regulation may also be at the level of protein stability**

Grk protein at wild type expression levels was not detectable in western blot analysis using Grk1D12 monoclonal as the primary antibody, inspite of several variations in the protein extraction, transfer condition, transfer method and also amounts of protein loaded. This could be because the protein turnover rates are so rapid that the protein is not detectable in wild type expression levels. Grk protein could be detectable only under conditions of mis/overexpression. There is also a difference in the ease with which Grk can be detected, depending upon whether it has a Myc tag or is not tagged, while the Myc tagged Grk is much easier to detect than the non Myc tagged version. The constructs with the Myc tag were detectable within 10-15 minutes of exposure whereas the constructs with no tags were detectable only after 1-3 hours of exposure to the film. Despite these differences in the stability of the proteins observed, the Grk activity assayed by the ability to dorsalise the egg shell using both the germ line Gal4 drivers are the same for both the Myc tagged and non Myc tagged lines.

*UASpGrk* constructs driven by *NosGal4VP16* in a *cni* homozygous background indicated that full length Grk was always present as a doublet band. The cleaved smaller band was very weakly observable in these cases. To test whether the appearance of the second band in the doublet is due to an alternate form of the protein being retained in the ER, the EndoH sensitivity of these bands were tested. EndoH, PNGase and O-glycosidase treatments individually as well as combinations of PNGase and EndoH treatments did not get rid of the doublet band. However, these studies indicated that the mature form of Grk even in the *cni* heterozygous (used as controls) conditions is EndoH sensitive. This indicates that Grk is one of those rare proteins which retains EndoH sensitivity even in the mature form of the protein.

The doublet could still be due to a combination of ER and Golgi glycosylations, as combination of O-glycosidase and EndoH, although attempted, were technically too challenging.

The doublet formation could alternatively be due to some other type of post translational protein modification. *In silico* analysis by using prediction programmes revealed several sites on the cytoplasmic end of Grk which had high probabilities of being modified by phosphorylation.

Alternatively, the doublet could also be because the protein is present in such high amounts that the cellular exocytotic machinery is saturated and the excess protein is consigned to some other cellular structures for degradation. The ER is known to have several mechanisms of quality control for proteins before they exit it.

Grk DC is an allele of Grk where the A249 is mutated to a V. Grk DC (GrkDCMyc) shows the presence of a high molecular weight band at around 60 kD, indicating the mutation results in a non cleavable form of the protein. A deletion construct, which consists only of the extracellular region (GrkdTCMyc) of Grk also results in a similar high molecular weight band. A construct where the cytoplasmic domain of Grk was replaced by five Myc tags showed no signal at all. This indicates that the cytoplasmic tail of Grk has a role in regulating protein stability. These constructs are driven by the endogenous Grk regulatory region so these western blots were assayed using antibodies against the Myc tag as the primary.

### **3a.7 Cni mediated Grk transport prevents hyperactivation of EGFR**

Expression of a deletion construct, lacking the transmembrane and the cytoplasmic domains of Grk (*UASpSecGrk*) is assumed to be the secreted form of Grk (Ghiglione et al., 2002). When this construct is expressed in the germ line using *TubGal4VP16*, it results in the egg chambers being arrested at around stage 6-7. These ovaries have the appearance of bunches of grapes. The reason for the arrest could be due to the hyperactivation of the DER. During the first round of Grk signaling, signal is restricted to the posterior pole and therefore, the follicle cells receiving the signal assume posterior identities. The restriction of the signal is presumably due to the Cni-mediated Grk transport pathway. In case of the overexpression of secreted Grk, it is not restricted only

to the posterior pole and is present in such high amounts that even anterior follicle cells are exposed. This results in the complete reversal of the situation of Grk loss of function, where in the absence of the first Grk signal, the posterior cells assume the default anterior fates. In this case due to the exposure of the anterior follicle cells to Grk, the anterior cells now assume posterior fates, resulting in egg chambers with posterior follicle cells at both the anterior and the posterior end. It would be interesting to check the identity of these cells using markers specific for posterior follicle cells to see if such transformation has occurred.

### **3a.8 Hypothetical Model**

These different lines of observations can be put together in a sketchy and speculative model. The model serves as a frame work to provoke several open questions in the regulation of the Grk mediated DER activation and its regulation during oogenesis.

Initiation of the Grk signal pathway is by the specific ER to Golgi enrichment of small amounts of Grk containing vesicles presumably by Cni. This statement is due to the observation in *cni* amorphic situations there is no signal initiation. These vesicles are directed vectorially to a subdomain on the oocyte which marks the point of highest Grk signal accumulation. This in the later egg is also the point at which the two dorsal appendages separate and the region of highest *aos* expression. This statement is due to the tight localisation of Grk protein observed by immunostaining. Grk is transported in the full length form in this pathway and is stable. The reason for this assumption is because in the mis/over expression of Grk, the full length form is always detectable. S mediated Grk transport is activated only in special conditions requiring higher amounts of Grk, and is inhibited in the presence of the Cni mediated pathway. This presumption is because the secondary refinement may require much more Grk molecules. Cleaved bands of Grk are detectable only in overexpression in *cni* mutant backgrounds. How S mediated overcomes this inhibition is a puzzle. Whether this is just due to the accumulation of increasing amounts of Grk or requires some other signal are just two of several possibilities for the mechanism that induces S-Rho mediated Grk cleavage pathway. Grk transported through this pathway is unstable and degraded very quickly. Star mediated pathway is not an independent pathway and has to be initiated directly or indirectly by

Cni-mediated Grk transport. This assumption is because in *cni* amorphic situations S-Rho pathway does not take over the function of Cni.

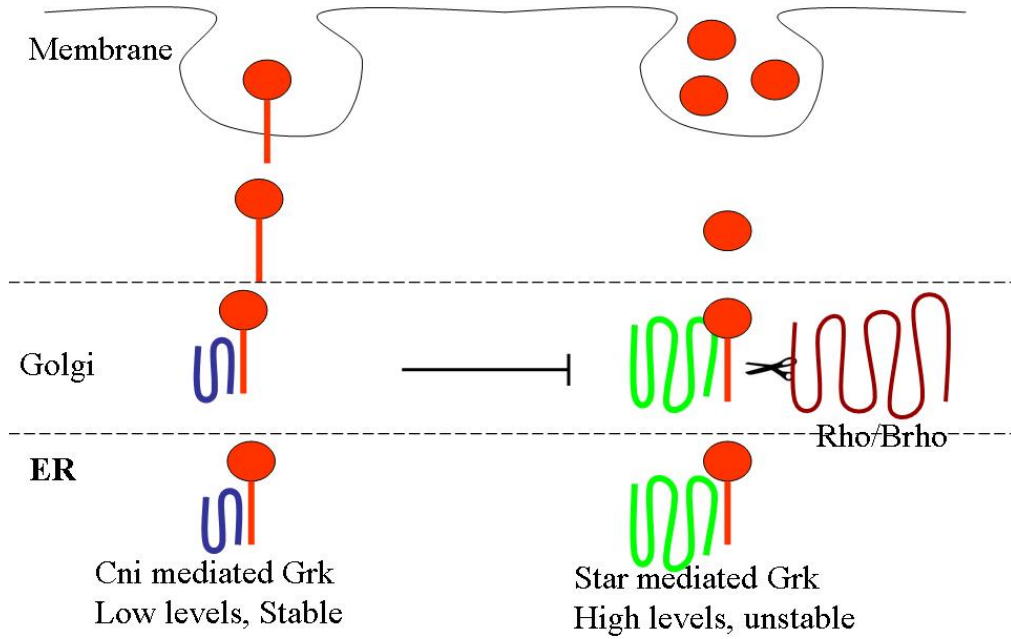


Fig. 43 A hypothetical model for the two modes of Grk transport in the oocyte.

### **3b Discussion – Cornichon related (Cnir)**

Cni and Cnir form the cornichon family of proteins in *Drosophila*, and share a significant degree of homology (45% similar) with each other. An earlier study in the lab indicated that a chromosomal deficiency region including the *cnir* region was synthetically lethal with *cni*. Expression of a construct where the regulatory of *cni* is used to drive Cnir (*PswapcniCnir*), rescues the adult phenotypes of *cni* but does not rescue its oogenesis functions (C. Boekel, Ph.D work). There appears to be some amount of functional redundancy between Cni and Cnir atleast in the somatic tissues, although the germ line function of Cni cannot be replaced by Cnir. Several EMS alleles in the region were available from the lab of Late. Prof Van Eeken, which we screened, to identify one potential candidate allele of *cnir*. Molecular characterization of the allele is in progress. The sequencing of the genomic region including *cnir* from the homozygous lines, indicates a base pair exchange at the 3' end of the *cnir* ORF. This has to be reconfirmed and the sequence information of a 0.7- 1 Kb region just upstream of the ATG has to be obtained. P elements very close to *cnir* have been identified to create new molecularly defined deletions of *cnir*. It is necessary to have a molecularly defined mutant of the gene to investigate the causes of the synthetic lethality with *cni* further and also to understand the cellular roles played by this family of proteins. This will also help in understanding the wing and embryonic lethality phenotypes exhibited by the putative *cnir* allele.

Both Cni and Cnir have a putative phenylalanine doublet (FF) at the C terminal region of the proteins. This motif is a characteristic of the p24 family of proteins. The p24 family of proteins which including the yeast member, Emp24p, are cargo receptor proteins which interact with cargo and coatamers of the COP-I and COP-II in a bimodal interaction (Fiedler et al., 1996). It would also be interesting to know if Cnir also interacts with a specific cargo and if so, what the cargo is?

### **3c Discussion – Enhancer/ suppressor screen**

The effect of gene dosage reduction to bring about enhancement, suppression of synthetic lethality in an already sensitised background was used as the criterion for the design of the screen. The purpose of the enhancer/suppressor genetic screen conducted was to identify new components involved in the Grk-DER mediated DV axis initiation process. As the sensitised background, an allele combination of *cni* which results in the eggs being laid having severely ventralised egg shells (No DAs) and a very small perturbation in posterior follicle cell specification (aeropyle though specified does not appear to be exactly the same as in wild type). To bring about gene dosage reduction a deficiency kit of the third chromosome was used. The screen is not biased to identifying germ line or somatic follicle components and hence has the ability to identify components from both types of cells. This may be crucial in identifying signals such as the back signal which involves components of both cell types to interact with each other. The screen could also identify components that sets up the Grk gradient that is interpreted by downstream components.

#### **3c.1 Screen coverage**

The deficiencies regions of the third chromosome that were considered represents about 16% of the fly genome. This number was arrived at by counting the number of units missing when the break points annotated to each of the deficiency was aligned against the wild type chromosomal map. This would mean a number of around 576 (16%) genes out of the 3600 (100%) genes that have been reported to be essential for viability in *Drosophila* (Spradling et al., 1999). There were 8 regions identified at the end of the pilot screen conducted in this study. Two of these regions were in overlapping regions, so the actual number of interacting chromosomal regions identified, are six. Assuming that in each of the regions identified, the interactions are due to a single gene locus, it would mean that we identified only 1% of the genes analysed, as interactors. The low numbers of the candidates identified would mean that the screen is an efficient means to identify new candidates involved in the initiation of the DV or unmask new roles for components already known to be involved in the process.

### **3c.2 The suppressor was identified as pipe (pip)**

The only region that was identified as a suppressor was the *Df(3L)VW3*, which is a small deficiency which removes the gene *pip* amongst others. Pip codes for a heparan sulphate transferase protein which is activated only in the ventral regions of the embryo downstream of signal initiation by Grk. The ventral restriction of Pip could be directly mediated by the Grk gradient (Peri et al., 2002). *pip* is downstream of *grk* and therefore one of the reasons it was included as the first candidate gene to be tested was to rule out its role. But surprisingly, testing with two different alleles of *pip* resulted in a slightly stronger suppression than those observed with the originally identified deficiency. The DAs appendage initiation and a small DA protusion can be seen in about 70-80% of these, indicating a high penetrance of the suppression.

A coordinate system is set up all along the AP and DV axis by a Grk gradient in the wild type scenario, with highest Grk at the anterior and dorsal and decreasing in amount towards the posterior and ventral. In the sensitised *eni* background, the whole coordinate system is weakened due to decrease in Grk secreted resulting in a decrease in the area specified as anterior and dorsal. Removal of one copy of a component of the ventralising system could be bringing about a corresponding decrease in the area of ventral domain thus pushing the coordinates of the system back towards wild type like situation.

### **3c.3 Sallimus (Sls) and Sprouty (Sty) are amongst the likely candidates**

Three other interacting chromosomal regions have been narrowed down to a region of a few genes.

The synthetic lethality initially observed due to *Df(3L)Aprt-53* (Synthetic lethal 2) was narrowed down to a region containing a single gene using overlapping deficiency. The single region identified in this region is called Sallimus (Sls) and is a protein belonging to the kettin family of Myosin heavy chain proteins. Sls in addition also has a myosin light kinase domain. Loss of function alleles of this genes have been procured from the stock centre to analyse this gene by a candidate approach.

Synthetic lethality due to *Df(3L)HR370* (Synthetic lethal 1) and enhancement due *Df(3L)GN50* (Enhancer1) have been narrowed down to an overlapping region between these two deficiencies. Using these and other overlapping deficiencies, this interaction

## Discussion – Enhancer / Suppressor screen

has been narrowed to a region containing five genes. *sprouty (sty)* is one of the the five candidate genes in this region. Sty is an inhibitor of the the EGFR pathway but so far has not been shown to be implicated in the axis decisions during oogenesis.

*Df42* (Enhancer 2) has been narrowed down to a region of three genes including *senseless (sense)*, *tartan (trn)* and *capricious (cap)*. Candidate approach using alleles of these gene is yet to be done.

The other three interacting regions of the third chromosome has to be analysed further before candidate approaches can be undertaken.

## 4 Materials and Methods

### 4.1 Fly husbandry

All *Drosophila* lines were kept as described by Ashburner (1989). Flies were grown in plastic vials on standard cornmeal agar at 25°C or 17°C. To ensure genetic purity for the progeny of crosses, only none fertilized females were mated with males of the appropriate genotypes. To ensure virginity the vials were emptied and the hatching flies were allowed to grow up to eight hours at 25°C or up to 22h at 17°C before collecting the virgins. Oregon R served as the wildtype strain.

### 4.2 Fly lines used

Besides the various *cni* mutant alleles, alleles for other genes, other interacting deficiencies and overexpression constructs already available in the lab or available from public stock centres, which were used in this study, the following table list other lines from various sources used for conditional expression studies:

Sl No.	Fly Genotype	Source
	<u>Follicle driver Gal4 lines</u>	
1	CY2 Gal4	
2	GR1Gal4	
	<u>Germ line driver Gal4 lines</u>	
3	Nanos Gal4 (NosGal4)	Ephrussi lab
4	Nanos Gal4VP16 (Nos Gal4VP16)	Ephrussi lab
5	Tubulin Gal4 (Tub Gal4)	St.Johnston lab
6	Tubulin Gal4VP16 (Tub Gal4Vp16)	St.Johnston lab
7	pCOG Gal4	C.Ghiglione
	<u>UAST lines</u>	
8	UAS <i>cni</i> -5myc	C.Boekel
	<u>UASp lines</u>	
9	UASpGrk11	Roth lab
10	UASpGrk8A	Roth lab
11	UASpGrk1A	Roth lab
12	UASpGrk3A	Roth lab
13	UASpGrk11	Roth lab
14	UASpGrk8A	Roth lab
15	UASpGrk5Myc (Ist Chr)	C.Ghiglione

16	UAspeGFP	C.Ghiglione
17	UASpSecGrk	C.Ghiglione
18	UAspd19aaGrkMyc (Ist Chr)	C.Ghiglione
19	UAspd19aaGrkMyc (Ist Chr)	C.Ghiglione
	Grk deletion line	
20	Grk DC5Myc,b cni AR55	C.Boekel
21	Grk $\delta$ TC5Myc	C.Boekel
22	Grk $\delta$ TC5Myc	C.Boekel

### 4.3 Preparation of egg shell and embryonic cuticle

For the analysis of the embryonic cuticle, non-hatched larvae were washed in water, dechorionated in 50% NaOCl for 3-5 min, washed rapidly and mounted in a mixture of Hoyer's medium and lactic acid 2:1. Egg shells were simply washed and mounted in the same medium. The mounted samples were incubated at 60°C for at least 24 hours before they were photographed.

### 4.4 Fixation of ovaries for immunostainings

The ovaries were dissected and transferred to heptan fix (200 $\mu$ l 4% paraformaldehyde + 20 $\mu$ L DMSO + 600 $\mu$ l heptan) for 20 min.

The upper heptane phase was removed and replaced with 4% PF and incubated for 5 min more before rinsing several times with PBST.

### 4.5 Antibody staining of ovaries

Immunostaining of ovaries was done as follows

Fixed ovaries were incubated twice in 1% BSA for 30 min to block the non-specific protein binding sites. The incubation the first antibody was done over-night at 4°C. On the next day the antibody solution was removed and ovaries were rinsed twice with PBST (1x PBS + 0.1% Triton-X100) followed by four 30 min washes. Preabsorbed secondary antibody was added for 1.5 h incubation. The antibody was removed and the ovaries were rinsed and washed twice over 45 min. In the case of a secondary antibody coupled with fluorescent label, the ovaries were simply mounted in *Vectashield (Linaris)*.

#### 4.6 In situ hybridisation of ovaries

*In situ* hybridization was done with digoxigenin-labeled RNA probes synthesized using RNA Labelling Mix (Boehringer Mannheim). Detection of single transcripts was performed as outlined in (Tautz and Pfeifle, 1989).

The fixed ovaries were rehydrated in PBST, refixed in 4 % paraformaldehyd in PBST (PF / PBST) for 20 min, washed four times with PBST over 15 min and incubated for 10 min in 50 µg/ml proteinase K. Proteinase was quickly blocked by adding glycine solution (2 mg/ml in PBST) for 2 min. The ovaries were rapidly rinsed 4 times, and refixed with PF/PBST for 20 min and washed three times with PBST all for 15 min. The ovaries were incubated 10 min in 1:1 hybridization solution / PBST and next 10 min only in hybridization solution (hyb. soln.). Prehybridisation required 1 h incubation of embryos in hyb. soln. + 100 µg/mg salmon sperm DNA (Sigma) at 55°C. 1-2 µL of the probe was added per 50 µL of hyb. soln. and allowed to hybridise over night at 55°C. On the next day the probe was removed and the ovaries were rinsed with the prewarmed hyb. soln. and washed 4 times 30 min each at 55°C in hyb. soln. and in a series of hyb. soln. / PBST mixture in proportions 4:1, 3:2, 2:3 and 1:4 for 10 min each at 55°C except the last wash, which was done at room temperature (RT). The hybridization was detected by the immunoreaction. First the ovaries were incubated in PBST + 1%BSA (PBST / BSA) twice for 20 min each to block non-specific immunoreactivity of proteins. After a short wash in PBST, the preabsorbed anti-Digoxigenin-AP conjugated antibody (Dianova) was added at the final dilution 1: 5000 for 1.5 h at RT. The ovaries were washed several times in PBST over 45 min and transferred into alkaline phosphatase staining buffer (APB: 100 mM NaCl, 50 mM MgCl<sub>2</sub>, 100 mM Tris-HCl, pH 9.5, 0.2% Tween). After three 5 min washes in APB, the antibody bound to the epitope was visualised by a blue alkaline phosphatase reaction. X-phosphate / NBT staining solution was added (for 1 ml 79 AP-buffer: 4.4 µL of 75 mg/mL NBT and 3.5 µL of X-phosphate) and the reaction developed in the darkness within 60 min (see Boehringer anti-Dig-AP protocol). The reaction was monitored every 15 min and stopped by washes in PBST. The ovaries were dehydrated and mounted in araldite as described in the section.

For fluorescent *in-situs*, the TSA kit (Molecular Probes) was used. The substrate used in this protocol is a fluorescently labelled Tyramide (labelled with Cy3 or FITC). Tyramide

## Materials & Methods

is a substrate for Horse Radish Peroxidase (HRP). In these cases the secondary antibody used was tagged with HRP (Dianova).

### **4.7 Antibodies used for Immuno-staining**

ER – Bip 1:200 dilution used, Source: C.Boekel

ERGIC- Rat monoclonal MAC 256 1:300 dilution used, Source: Butcher lab, Babrahams Institute, England

Golgi- Anti embryonic Golgi membranes of flies 1:300 dilution used, Source: commercially available.

Anti-Myc antibodies used

Rabbit polyclonal 1:400 dilution used, Source: Santa Cruz Biochemicals

Monoclonal antibodies 1:200 dilution used, Source: Invitrogen Biochemicals

All secondary antibodies were Alexa conjugated antibodies from Molecular Probes.

Phalloidin conjugated with FITC, Rhodamine or Alexa548 was used to detect actin structures in the ovary.

A monoclonal antibody (T-48) against a nuclear lamin was used to mark the nuclei in the egg chambers.

### **4.8 Protein extraction from ovaries for immuno blot analysis**

For preparation of ovarian extracts, 10-15 ovaries were dissected in icecold PBST (1x PBS + 0.1% Triton-X100). The PBST was removed and replaced with hot loading buffer (5x Laemmlis buffer + 10%  $\beta$ -mercaptoethanol ( $\beta$ -SH)). About 5  $\mu$ L of 5x Laemli+  $\beta$ -SH was added / ovariole.

The loading buffer was maintained at 95°C for before ovary dissection

Ovaries were homogenized using a hand held homogenizer, the pestle was moved up and down the tube 50-60 times while maintaining the tube on a 95°C block.

It was then centrifuged at 12K rpm for 5 minutes at 4°C on a table top centrifuge

The soluble protein was transferred to a fresh tube and the pellet discarded.

Protein was stored at -20°C and boiled for 5minutes before loading on the gel.

Usually 20 -25  $\mu$ L was loaded / lane.

10% SDS-PAGE gel under reducing conditions.

## Materials & Methods

Lemmler buffer composition, SDS-PAGE composition, electrophoresis buffer and running conditions were all according to (Maniatis et al., 1982)

### **4.9 Glycosidase assays**

Protein from ovaries was extracted as mentioned above. But before freezing, the buffer and requisite glycosidase was added to the protein and incubated at 37°C for 30-45 minutes. Then the protein was heat denatured by boiling for 5 minutes before loading on a 10% SDS-PAGE gel. EndoH and PNGase were procured from NEB, while O-Glycosidase was from Sigma.

### **4.10 Western Blot Analysis of Proteins**

#### **4.10.1 Electrophoresis and transfer of proteins onto the membrane**

10% SDS-PAGE – Protein gels were cast and electrophoresed according to protocols mentioned in (Maniatis et al., 1982).

After the protein was electrophoresed, the gel was transferred to the cathode buffer (25 mM Tris, 40mM 6-A-Caproic acid, 10% methanol, pH 9.4) for 15 minutes.

Meanwhile piece of Immobilon-P membrane (Millipore) corresponding to the size of the gel was cut, treated with methanol for 30s and then transferred to milli-Q water for 2 minutes.

The membrane was then left in Anode buffer II (25 mM Tris, 10% methanol, pH 10.4) for atleast 5 minutes.

The transfer stack was set up as in the instruction by the manufacturer of the transfer apparatus (Semi dry protein transfer apparatus, Bio-Rad)

Besides the Gel and the membrane 4M filter paper soaked in Anode buffer I (0.3 M Tris, 10% methanol, pH 10.4), Anode buffer II and cathode buffer were used in the creation of the transfer stack.

The transfer was conducted by using a constant current of 1.2 mA/ sq cm of the membrane.

#### **4.10.2 Processing of the transferred membrane and gel**

After transfer the Gel was fixed (10% Acetic acid, 50% methanol for 20 min).

## Materials & Methods

The membrane was treated with MemCode (PerBio), a reversible stain used to check transfer of proteins onto membranes. (This assay for the transfer of Proteins was done only in initial transfer standardisation studies)

The membrane was then treated with Methanol for 2 minutes and dried by air at RT.

### **4.10.3 Primary and secondary antibody treatments**

The transferred membrane was first blocked with 10% Milk Powder in TBST (1x Tris buffered saline + 0.1% triton-X100) for 1-1.5 hrs.

The blocking solution was removed and primary antibodies were added to fresh 10 % MP and the primary the membrane was left overnight at 4°C.

The primary antibody solution was removed and the membranes washed three times for 5 minutes each with TBST solution.

The secondary antibody (Goat anti-mouse-HRP) was added to 10% MP solution, the membrane soaked in it and incubated for 2 hours before detection.

### **4.10.4 Detection of western blots**

The detection of protein was done using the ECL system for chemi-luminescent detection of HRP tagged secondary antibodies. A kit with higher sensitivity in called the ECL-Plus was used for most western blots in this study.

## **4.11 Antibodies used for Immuno-blots**

### **Primary antibodies used**

Grk monoclonal 1D12 , dilution 1:100, Source: DSHB

Anti-acetylated tubulin, dilution 1:2500, Source: Commercially available, Sigma Chemicals

Anti- Myc 1) Monoclonal, dilution 1: 400, Invitrogen

2) Polyclonal, dilution 1: 250, Santa Cruz Biotech

### **Secondary antibodies used**

Goat Anti mouse HRP dilution 1:1500, Source:Dianova

Goat Anti rabbit HRP dilution 1:2500, Source: Dianova

#### 4.12 Genomic DNA extraction from Larvae

This protocol is a modified protocol of the one reported in (Bender et al., 1983).

About 50 larvae was homogenized in 0.5 mL Extraction buffer, using a hand held homogenizer by grinding for a minute.

Around 10  $\mu$ L of Extraction buffer ( 0.1M NaCl, 0.2 M Sucrose, Tris-HCl 0.1 M pH 9.1, EDTA 0.05 M, 0.5% SDS) was taken / larvae.

The extracted was then incubated at 65°C for 30 min to kill nucleases

75  $\mu$ L 8 M potassium acetate was added and incubated for 30 min on ice. Then the extract was spun down at 14K, 4 °C, 4 min . The supernatant was transferred to a fresh tube and spun down once again.

Ethanol was up to 70% concentration the tube and incubated at RT for 5-10 minutes. Pellet was obtained by spinning down at 14K, 5 min, RT. Pellet washed once with 70% ethanol. And air dried for 5 min.

Pellet was resuspended in 200  $\mu$ L (10mM Tris-HCl pH 8, 1 mM EDTA). 20  $\mu$ L of 5M NaCl , 4  $\mu$ L of 0.5 M EDTA and 6  $\mu$ L of 10 mg/ mL RNase A (final con 20  $\mu$ g/mL) was added and incubated at 37 °C for 30 min.

Then 2.1  $\mu$ L of 10 mg/mL Proteinase K was added and incubated at RT for 30 minutes.

The solution was then purified by two rounds of Phenol: Chloroform: IAA mixture.

DNA precipitated by adding two volumes of Ethanol and resuspended in 50  $\mu$ L of TE.

All other DNA cloning protocols were according to (Maniatis et al., 1982).

Primers used to clone and sequence the cnir region are given in the table below

Sl no	Primer name	Primer sequence
1	CG7221ATG	gcatccgcgcattttgtccgagg
2	CnircDNA5p	atgtttctgcccgaacagccacc
3	CnircDNA3p	tcagaaatccgttactatttcgtc
4	CG17262P15p	ttcgaaaacgcagtatgga
5	CG17262P13p	ccgttactatttcgtcgtcctcat
6	Res603p	ccagaaacaggctcgccaaag
7	Res2105	ttcgattccgccccttctga

## 5 Bibliography

Amiri, A. and Stein, D. (2002). Dorsoventral patterning: a direct route from ovary to embryo. *Curr Biol* 12, R532-4.

Bender, W., Spierer, P. and Hogness, D. S. (1983). Chromosomal walking and jumping to isolate DNA from the *Ace* and *rosy* loci and the *bithorax* complex in *Drosophila melanogaster*. *J Mol Biol* 168, 17-33.

Bier, E., Jan, L. Y. and Jan, Y. N. (1990). *rhomboid*, a gene required for dorsoventral axis establishment and peripheral nervous system development in *Drosophila melanogaster*. *Genes Dev* 4, 190-203.

Burgess, A. W. and Thumwood, C. M. (1994). The Sixth George Swanson Christie Memorial Lecture: growth factors and their receptors: new opportunities for cancer treatment. *Pathology* 26, 453-63.

Carrera, P., Johnstone, O., Nakamura, A., Casanova, J., Jackle, H. and Lasko, P. (2000). VASA mediates translation through interaction with a *Drosophila* yIF2 homolog. *Mol Cell* 5, 181-7.

Clifford, R. J. and Schupbach, T. (1989). Coordinately and differentially mutable activities of *torpedo*, the *Drosophila melanogaster* homolog of the vertebrate EGF receptor gene. *Genetics* 123, 771-87.

Davidson, B. and Swalla, B. J. (2001). Isolation of genes involved in ascidian metamorphosis: epidermal growth factor signaling and metamorphic competence. *Dev Genes Evol* 211, 190-4.

DeLotto, Y. and DeLotto, R. (1998). Proteolytic processing of the *Drosophila* Spatzle protein by easter generates a dimeric NGF-like molecule with ventralising activity. *Mech Dev* 72, 141-8.

Dikic, I., Schlessinger, J. and Lax, I. (1994). PC12 cells overexpressing the insulin receptor undergo insulin-dependent neuronal differentiation. *Curr Biol* 4, 702-8.

Fiedler, K., Veit, M., Stamnes, M. A. and Rothman, J. E. (1996). Bimodal interaction of coatamer with the p24 family of putative cargo receptors. *Science* 273, 1396-9.

Gabay, L., Seger, R. and Shilo, B. Z. (1997). In situ activation pattern of *Drosophila* EGF receptor pathway during development. *Science* 277, 1103-6.

## Literature

- Ghiglione, C., Bach, E. A., Paraiso, Y., Carraway, K. L., 3rd, Noselli, S. and Perrimon, N. (2002). Mechanism of activation of the Drosophila EGF Receptor by the TGF $\alpha$  ligand Gurken during oogenesis. *Development* 129, 175-86.
- Ghiglione, C., Carraway, K. L., 3rd, Amundadottir, L. T., Boswell, R. E., Perrimon, N. and Duffy, J. B. (1999). The transmembrane molecule kekkon 1 acts in a feedback loop to negatively regulate the activity of the Drosophila EGF receptor during oogenesis. *Cell* 96, 847-56.
- Godt, D. and Tepass, U. (1998). Drosophila oocyte localization is mediated by differential cadherin-based adhesion. *Nature* 395, 387-91.
- Gonzalez-Reyes, A., Elliott, H. and St Johnston, D. (1995). Polarization of both major body axes in Drosophila by gurken-torpedo signalling. *Nature* 375, 654-8.
- Gonzalez-Reyes, A. and St Johnston, D. (1994). Role of oocyte position in establishment of anterior-posterior polarity in Drosophila. *Science* 266, 639-42.
- Gonzalez-Reyes, A. and St Johnston, D. (1998). The Drosophila AP axis is polarised by the cadherin-mediated positioning of the oocyte. *Development* 125, 3635-44.
- Gonzalez-Reyes, A. and St Johnston, D. (1998). Patterning of the follicle cell epithelium along the anterior-posterior axis during Drosophila oogenesis. *Development* 125, 2837-46.
- Guichard, A., Roark, M., Ronshaugen, M. and Bier, E. (2000). brother of rhomboid, a rhomboid-related gene expressed during early Drosophila oogenesis, promotes EGF-R/MAPK signaling. *Dev Biol* 226, 255-66.
- Guichet, A., Peri, F. and Roth, S. (2001). Stable anterior anchoring of the oocyte nucleus is required to establish dorsoventral polarity of the Drosophila egg. *Dev Biol* 237, 93-106.
- Hashimoto, C., Hudson, K. L. and Anderson, K. V. (1988). The Toll gene of Drosophila, required for dorsal-ventral embryonic polarity, appears to encode a transmembrane protein. *Cell* 52, 269-79.
- Hwang, S. Y., Oh, B., Zhang, Z., Miller, W., Solter, D. and Knowles, B. B. (1999). The mouse cornichon gene family. *Dev Genes Evol* 209, 120-5.
- James, K. E., Dorman, J. B. and Berg, C. A. (2002). Mosaic analyses reveal the function of Drosophila Ras in embryonic dorsoventral patterning and dorsal follicle cell morphogenesis. *Development* 129, 2209-22.

## Literature

- King, R. C. (1970). Ovarian development in *Drosophila melanogaster*. New York: Academic Press.
- Kolodkin, A. L., Pickup, A. T., Lin, D. M., Goodman, C. S. and Banerjee, U. (1994). Characterization of Star and its interactions with sevenless and EGF receptor during photoreceptor cell development in *Drosophila*. *Development* 120, 1731-45.
- Kramer, S., Okabe, M., Hacohen, N., Krasnow, M. A. and Hiromi, Y. (1999). Sprouty: a common antagonist of FGF and EGF signaling pathways in *Drosophila*. *Development* 126, 2515-25.
- Lee, J. R., Urban, S., Garvey, C. F. and Freeman, M. (2001). Regulated intracellular ligand transport and proteolysis control EGF signal activation in *Drosophila*. *Cell* 107, 161-71.
- Lee, M. C., Miller, E. A., Goldberg, J., Orci, L. and Schekman, R. (2004). Bi-Directional Protein Transport Between The Er And Golgi. *Annu Rev Cell Dev Biol* 20, 87-123.
- Livneh, E., Glazer, L., Segal, D., Schlessinger, J. and Shilo, B. Z. (1985). The *Drosophila* EGF receptor gene homolog: conservation of both hormone binding and kinase domains. *Cell* 40, 599-607.
- Lodish, H., Berk, A., Zipursky, S. L., Matsudaira, P., Baltimore, D. and Darnell, J. (1999). Molecular Cell Biology. New York: W.H. Freeman and company.
- Malkus, P., Graham, L. A., Stevens, T. H., Schekman, R., Miller, E. A., Beilharz, T. H., Malkus, P. N., Lee, M. C., Hamamoto, S., Orci, L. et al. (2004). Role of Vma21p in assembly and transport of the yeast vacuolar ATPase. *Mol Biol Cell* 15, 5075-91. Epub 2004 Sep 08.
- Malkus, P., Jiang, F. and Schekman, R. (2002). Concentrative sorting of secretory cargo proteins into COPII-coated vesicles. *J Cell Biol* 159, 915-21. Epub 2002 Dec 23.
- Maniatis, T., Fritsch, E. F. and Sambrook, J. (1982). Molecular cloning: a laboratory manual. Cold Spring Harbor, New York: Cold Spring Harbor Laboratory.
- Martinez-Menarguez, J. A., Geuze, H. J., Slot, J. W. and Klumperman, J. (1999). Vesicular tubular clusters between the ER and Golgi mediate concentration of soluble secretory proteins by exclusion from COPI-coated vesicles. *Cell* 98, 81-90.
- Mayer, U. and Nusslein-Volhard, C. (1988). A group of genes required for pattern formation in the ventral ectoderm of the *Drosophila* embryo. *Genes Dev* 2, 1496-511.

## Literature

- McGregor, J. R., Xi, R. and Harrison, D. A. (2002). JAK signaling is somatically required for follicle cell differentiation in *Drosophila*. *Development* 129, 705-17.
- Micklem, D. R., Dasgupta, R., Elliott, H., Gergely, F., Davidson, C., Brand, A., Gonzalez-Reyes, A. and St Johnston, D. (1997). The mago nashi gene is required for the polarisation of the oocyte and the formation of perpendicular axes in *Drosophila*. *Curr Biol* 7, 468-78.
- Mizuguchi, K., Parker, J. S., Blundell, T. L. and Gay, N. J. (1998). Getting knotted: a model for the structure and activation of Spatzle. *Trends Biochem Sci* 23, 239-42.
- Montell, D. J., Keshishian, H. and Spradling, A. C. (1991). Laser ablation studies of the role of the *Drosophila* oocyte nucleus in pattern formation. *Science* 254, 290-3.
- Morgan, M. M. and Mahowald, A. P. (1996). Multiple signaling pathways establish both the individuation and the polarity of the oocyte follicle in *Drosophila*. *Arch Insect Biochem Physiol* 33, 211-30.
- Morisato, D. and Anderson, K. V. (1994). The spatzle gene encodes a component of the extracellular signaling pathway establishing the dorsal-ventral pattern of the *Drosophila* embryo. *Cell* 76, 677-88.
- Morisato, D. and Anderson, K. V. (1995). Signaling pathways that establish the dorsal-ventral pattern of the *Drosophila* embryo. *Annu Rev Genet* 29, 371-99.
- Neuman-Silberberg, F. S. and Schupbach, T. (1993). The *Drosophila* dorsoventral patterning gene *gurken* produces a dorsally localized RNA and encodes a TGF alpha-like protein. *Cell* 75, 165-74.
- Neuman-Silberberg, F. S. and Schupbach, T. (1994). Dorsoventral axis formation in *Drosophila* depends on the correct dosage of the gene *gurken*. *Development* 120, 2457-63.
- Nilson, L. A. and Schupbach, T. (1998). Localized requirements for *windbeutel* and *pipe* reveal a dorsoventral prepatterning within the follicular epithelium of the *Drosophila* ovary. *Cell* 93, 253-62.
- Nilson, L. A. and Schupbach, T. (1999). EGF receptor signaling in *Drosophila* oogenesis. *Curr Top Dev Biol* 44, 203-43.

## Literature

- Ogiso, H., Ishitani, R., Nureki, O., Fukai, S., Yamanaka, M., Kim, J. H., Saito, K., Sakamoto, A., Inoue, M., Shirouzu, M. et al. (2002). Crystal structure of the complex of human epidermal growth factor and receptor extracellular domains. *Cell* 110, 775-87.
- Pagano, A., Letourneur, F., Garcia-Estefania, D., Carpentier, J. L., Orci, L. and Paccaud, J. P. (1999). Sec24 proteins and sorting at the endoplasmic reticulum. *J Biol Chem* 274, 7833-40.
- Pai, L. M., Barcelo, G. and Schupbach, T. (2000). D-cbl, a negative regulator of the Egfr pathway, is required for dorsoventral patterning in Drosophila oogenesis. *Cell* 103, 51-61.
- Peri, F., Bokel, C. and Roth, S. (1999). Local Gurken signaling and dynamic MAPK activation during Drosophila oogenesis. *Mechanisms of Development* 81, 75-88.
- Peri, F. and Roth, S. (2000). Combined activities of Gurken and decapentaplegic specify dorsal chorion structures of the Drosophila egg. *Development* 127, 841-50.
- Peri, F., Technau, M. and Roth, S. (2002). Mechanisms of Gurken-dependent pipe regulation and the robustness of dorsoventral patterning in Drosophila. *Development* 129, 2965-75.
- Pickup, A. T. and Banerjee, U. (1999). The role of star in the production of an activated ligand for the EGF receptor signaling pathway. *Dev Biol* 205, 254-9.
- Powers, J. and Barlowe, C. (1998). Transport of axl2p depends on erv14p, an ER-vesicle protein related to the Drosophila cornichon gene product. *J Cell Biol* 142, 1209-22.
- Powers, J. and Barlowe, C. (2002). Erv14p directs a transmembrane secretory protein into COPII-coated transport vesicles. *Mol Biol Cell* 13, 880-91.
- Queenan, A. M., Barcelo, G., Van Buskirk, C. and Schupbach, T. (1999). The transmembrane region of Gurken is not required for biological activity, but is necessary for transport to the oocyte membrane in Drosophila. *Mech Dev* 89, 35-42.
- Queenan, A. M., Ghabrial, A. and Schupbach, T. (1997). Ectopic activation of torpedo/Egfr, a Drosophila receptor tyrosine kinase, dorsalizes both the eggshell and the embryo. *Development* 124, 3871-80.
- Ray, R. P. and Schupbach, T. (1996). Intercellular signaling and the polarization of body axes during Drosophila oogenesis. *Genes Dev* 10, 1711-23.
- Reich, A. and Shilo, B. Z. (2002). Keren, a new ligand of the Drosophila epidermal growth factor receptor, undergoes two modes of cleavage. *Embo J* 21, 4287-96.

## Literature

Riechmann, V. and Ephrussi, A. (2001). Axis formation during *Drosophila* oogenesis. *Curr Opin Genet Dev* 11, 374-83.

Roth, S. (2003). The origin of dorsoventral polarity in *Drosophila*. *Philos Trans R Soc Lond B Biol Sci* 358, 1317-29; discussion 1329.

Roth, S., Jordan, P. and Karess, R. (1999). Binuclear *Drosophila* oocytes: consequences and implications for dorsal-ventral patterning in oogenesis and embryogenesis. *Development* 126, 927-34.

Roth, S., Neuman-Silberberg, F. S., Barcelo, G. and Schupbach, T. (1995). *cornichon* and the EGF receptor signaling process are necessary for both anterior-posterior and dorsal-ventral pattern formation in *Drosophila*. *Cell* 81, 967-78.

Sandgren, E. P., Luetkeke, N. C., Palmiter, R. D., Brinster, R. L. and Lee, D. C. (1990). Overexpression of TGF alpha in transgenic mice: induction of epithelial hyperplasia, pancreatic metaplasia, and carcinoma of the breast. *Cell* 61, 1121-35.

Sapir, A., Schweitzer, R. and Shilo, B. Z. (1998). Sequential activation of the EGF receptor pathway during *Drosophila* oogenesis establishes the dorsoventral axis. *Development* 125, 191-200.

Schejter, E. D., Segal, D., Glazer, L. and Shilo, B. Z. (1986). Alternative 5' exons and tissue-specific expression of the *Drosophila* EGF receptor homolog transcripts. *Cell* 46, 1091-101.

Schneider, D. S., Jin, Y., Morisato, D. and Anderson, K. V. (1994). A processed form of the Spatzle protein defines dorsal-ventral polarity in the *Drosophila* embryo. *Development* 120, 1243-50.

Schnepp, B., Donaldson, T., Grumblin, G., Ostrowski, S., Schweitzer, R., Shilo, B. Z. and Simcox, A. (1998). EGF domain swap converts a *Drosophila* EGF receptor activator into an inhibitor. *Genes Dev* 12, 908-13.

Schnepp, B., Grumblin, G., Donaldson, T. and Simcox, A. (1996). *Vein* is a novel component in the *Drosophila* epidermal growth factor receptor pathway with similarity to the neuregulins. *Genes Dev* 10, 2302-13.

Schulz, C., Wood, C. G., Jones, D. L., Tazuke, S. I. and Fuller, M. T. (2002). Signaling from germ cells mediated by the rhomboid homolog *stet* organizes encapsulation by somatic support cells. *Development* 129, 4523-34.

## Literature

Schweitzer, R., Shaharabany, M., Seger, R. and Shilo, B. Z. (1995). Secreted Spitz triggers the DER signaling pathway and is a limiting component in embryonic ventral ectoderm determination. *Genes Dev* 9, 1518-29.

Sen, J., Goltz, J. S., Konsolaki, M., Schupbach, T. and Stein, D. (2000). Windbeutel is required for function and correct subcellular localization of the Drosophila patterning protein Pipe. *Development* 127, 5541-50.

Sen, J., Goltz, J. S., Stevens, L. and Stein, D. (1998). Spatially restricted expression of pipe in the Drosophila egg chamber defines embryonic dorsal-ventral polarity. *Cell* 95, 471-81.

Shilo, B. Z. (2003). Signaling by the Drosophila epidermal growth factor receptor pathway during development. *Exp Cell Res* 284, 140-9.

Spradling, A. C. (1993). Developmental genetics of oogenesis. In *The development of Drosophila melanogaster*, vol. 1 (ed. M. Bate and A. Martinez-Arias), pp. 1-70. New York: Cold Spring Harbor Laboratory Press.

Spradling, A. C., Stern, D., Beaton, A., Rhem, E. J., Laverty, T., Mozden, N., Misra, S. and Rubin, G. M. (1999). The Berkeley Drosophila Genome Project gene disruption project: Single P-element insertions mutating 25% of vital Drosophila genes. *Genetics* 153, 135-77.

Steiner, G. and Smolen, J. (2002). Autoantibodies in rheumatoid arthritis and their clinical significance. *Arthritis Res* 4, S1-5. Epub 2002 Apr 26.

Tautz, D. and Pfeifle, C. (1989). A non-radioactive in situ hybridization method for the localization of specific RNAs in Drosophila embryos reveals translational control of the segmentation gene hunchback. *Chromosoma* 98, 81-5.

Theurkauf, W. E., Smiley, S., Wong, M. L. and Alberts, B. M. (1992). Reorganization of the cytoskeleton during Drosophila oogenesis: implications for axis specification and intercellular transport. *Development* 115, 923-36.

Tsruya, R., Schlesinger, A., Reich, A., Gabay, L., Sapir, A. and Shilo, B. Z. (2002). Intracellular trafficking by Star regulates cleavage of the Drosophila EGF receptor ligand Spitz. *Genes Dev* 16, 222-34.

## Literature

Twombly, V., Blackman, R. K., Jin, H., Graff, J. M., Padgett, R. W. and Gelbart, W. M. (1996). The TGF-beta signaling pathway is essential for *Drosophila* oogenesis. *Development* 122, 1555-65.

Urban, S., Lee, J. R. and Freeman, M. (2001). *Drosophila* rhomboid-1 defines a family of putative intramembrane serine proteases. *Cell* 107, 173-82.

Utku, N., Bulwin, G. C., Beinke, S., Heinemann, T., Beato, F., Randall, J., Schnieders, B., Sandhoff, K., Volk, H. D., Milford, E. et al. (1999). The human homolog of *Drosophila* cornichon protein is differentially expressed in alloactivated T-cells. *Biochim Biophys Acta* 1449, 203-10.

Vaux, D., Tooze, J. and Fuller, S. (1990). Identification by anti-idiotypic antibodies of an intracellular membrane protein that recognizes a mammalian endoplasmic reticulum retention signal. *Nature* 345, 495-502.

Wasserman, J. D. and Freeman, M. (1998). An autoregulatory cascade of EGF receptor signaling patterns the *Drosophila* egg. *Cell* 95, 355-64.

Xi, R., McGregor, J. R. and Harrison, D. A. (2003). A gradient of JAK pathway activity patterns the anterior-posterior axis of the follicular epithelium. *Dev Cell* 4, 167-77.

Zak, N. B., Wides, R. J., Schejter, E. D., Raz, E. and Shilo, B. Z. (1990). Localization of the DER/flb protein in embryos: implications on the faint little ball lethal phenotype. *Development* 109, 865-74.

Zhang, Q. H., Ye, M., Wu, X. Y., Ren, S. X., Zhao, M., Zhao, C. J., Fu, G., Shen, Y., Fan, H. Y., Lu, G. et al. (2000). Cloning and functional analysis of cDNAs with open reading frames for 300 previously undefined genes expressed in CD34+ hematopoietic stem/progenitor cells. *Genome Res* 10, 1546-60.

## 6 Summary

During oogenesis, in *Drosophila melanogaster*, the exchange of signals between the oocyte and the surrounding follicle cells govern both the polarization of the maturing egg and the subsequent establishment of the future embryonic body axes. Gurken (Grk), a TGF- $\alpha$ -like molecule signaling twice from the oocyte to the overlying follicle cells brings about the polarisation of both axes, the anterior-posterior (AP) and the dorsal-ventral (DV). The signal is perceived by the *Drosophila* EGF receptor (DER) present in abutting follicle cells. Cornichon (Cni) is a small hydrophobic protein which is absolutely required for Grk signaling. Earlier studies, in the lab, has shown a protein-protein interaction between the ER-luminal domain of Cni and the juxtamembrane domain (JMD) domain of Grk. In this study, it has been shown that the subcellular localisation of Cni is in line with an ER to Golgi cycling function. By inducing Grk transit through the bulk flow pathway of cellular exocytosis it could be shown that the requirement for Cni in enrichment of Grk vesicles can be overcome. Grk secreted via the bulk flow pathway in absence of Cni is active and signals to the DER. This demonstrates that Cni function is restricted to the transport of Grk from the ER to the Golgi and is not required for modification and/or proteolytic activation of Grk. This mode of ligand trafficking is a new component of the EGF ligand regulatory system. *cni* is not only required in the oocyte, it has also a somatic functions as indicated by head and wing phenotypes and decreased viability which result from amorphic *cni* mutations. The somatic, but not the ovarian functions of *cni* can be rescued by *cornichon related (cnir)*. An earlier study in the lab revealed that a chromosomal deficiency removing regions including *cnir* is synthetically lethal with *cni*. A genetic screen was conducted to identify a putative loss of function allele of *cnir*, from an existing collection of EMS allele in this region. The molecular characterisation of the allele is not yet completed. In addition, an enhancer/suppressor screen in a sensitized genetic background to identify new components or new unidentified roles for known components, in the initiation of the DV axis was conducted. As the sensitized background, a *cni* hypomorphic allele combination which leads to strongly ventralized eggs with a weak defect in posterior follicle cell specification was used. Deficiencies on the third chromosome were assayed for suppression or enhancement of the *cni* egg

## Summary

phenotype or for synthetic lethality, upon gene dosage reduction . Eight candidate regions of the third chromosome consisting of one suppressor, four enhancers and three synthetic lethal were identified. The suppression was narrowed down to a single gene namely, *pipe*. *pipe* is a gene which is activated directly by the Grk gradient and its activity defines the ventral side of the egg and embryo. Of the other interactors, four of them have been narrowed down to regions containing a few genes.

## 7 Zusammenfassung

Während der Oogenese Drosophilas bestimmt der Austausch von Signalen zwischen der Oozyte und den umgebenden Follikelzellen sowohl die Polarisation des reifenden Eies als auch die folgende Etablierung der zukünftigen embryonalen Körperachsen. Das in der Oozyte exprimierte Signalprotein Gurken (Grk) induziert die Polarisierung beider Körperachsen durch die Aktivierung des Drosophila EGF-Rezeptors (DER) im darüber liegenden Follikel epithel. Cornichon (Cni) ist ein kleines hydrophobes Protein, das für die Aktivierung des DER durch Grk notwendig ist. Frühere Arbeiten in unserem Labor konnten eine Protein-Protein Interaktion zwischen der ER-luminalen Domäne von Cni und der juxtamembranen Domäne (JMD) von Grk nachweisen. Die vorliegende Arbeit zeigt, dass Cni im ER und im Golgi lokalisiert ist, was auf eine mögliche Transportfunktion von Cni zwischen diesen beiden Endomembransystemen hinweist. Durch Überexpression von Grk wurde der „bulk flow“ Exocytoseweg induziert. Dadurch konnte demonstriert werden, dass die Cni Funktion durch eine Überexpression von Grk umgangen werden kann. Das durch die „bulk flow“ Exocytose sezernierte Grk ist in der Lage den EGF Rezeptor zu aktivieren. Dies zeigt, dass Cni eine Transportfunktion erfüllt und nicht für die posttranslationelle Modifikation oder proteolytische Aktivierung von Grk verantwortlich ist. Dieser Cni vermittelte Transport von Gurken postuliert ein neues Regulationssystem für EGF-Liganden. *cni* wird nicht nur in der Oozyte, sondern auch in somatischen Zellen benötigt wie eine amorphe Mutation des Gens beweist, die vermindert lebensfähig ist und einen Phänotyp des Kopfes und Flügels zeigt. Die somatische, doch nicht die Keimbahn Funktion von *cni* kann durch *cornichon related (cnir)* gerettet werden. Frühere Arbeiten in unserem Labor haben gezeigt, dass eine chromosomale Defizienz, die auch die *cnir* Region umfasst, in Kombination mit *cni* synthetisch lethal ist. Unter Zuhilfenahme existierender EMS Allele in der genomischen *cnir* Region wurde versucht mögliche funktionelle Verlustallele des Gens zu identifizieren. Die molekulare Charakterisierung eines gefundenen *cnir* Allels steht noch aus. Zusätzlich wurde ein „Enhancer/Supressor Screen“ in einem sensitivierten genetischen Hintergrund durchgeführt, um entweder neue Komponenten oder bisher nicht charakterisierte Funktionen bekannter Komponenten, die an der Bildung der dorsoventralen Achse beteiligt sind, zu identifizieren. In diesem Ansatz wurde eine Kombination hypomorpher *cni* Allele verwendet, deren Phänotypen sich in stark ventralisierten Eiern mit schwachen Defekten bei der Spezifizierung der posterioren Follikelzellen äußert. Defizienzen auf dem dritten Chromosom wurden auf Abschwächung oder Verstärkung des *cni* Ei-Phänotyps oder auf synthetische Lethalität hin

untersucht, die als Folge einer Gen Dosis Reduktion auftreten können. Acht mögliche Regionen wurden identifiziert, darunter eine Supressorregion, vier Enhancerregionen und drei Regionen synthetischer Lethalität. Als Supressor wurde pipe identifiziert, ein Gen, dessen Expression direkt durch den Grk Gradienten reguliert wird und dessen Aktivität für die Induktion der ventralen Seite des Embryos benötigt wird. Vier der verbleibenden Kandidaten konnten bereits auf eine Region mit wenigen Genen begrenzt werden.

## **8 Erklärung**

Ich versichere hiermit, dass ich die von mir vorgelegte Dissertation selbstständig angefertigt, die benutzten Quellen und Hilfsmittel vollständig angegeben und die Stellen der Arbeit – einschließlich Tabelle, Karten und Abbildungen -, die anderen Werken im Wortlaut oder dem Sinn nach entnommen sind, in jedem Einzelfall als Entlehnungen kenntlich gemacht habe; dass diese Dissertation keiner anderen Fakultät oder Universität zur Prüfung vorgelegen hat; dass sie noch nicht veröffentlicht worden ist, sowie, dass ich eine solche Veröffentlichung vor Abschluss des Promotionsverfahrens nicht vornehmen werde.

Die Bestimmungen der geltenden Promotionsordnung sind mir bekannt. Die von mir vorgelegte Dissertation ist von Herrn Prof. Dr. Siegfried Roth betreut worden.

Ich versichere, dass ich alle Angaben nach bestem Wissen und Gewissen gemacht habe und verpflichte mich, jedmögliche, die obigen Angaben betreffende Veränderung, dem Dekanat unverzüglich mitzuteilen.

Köln, den 12.12.2004

Sajith Dass

## 9 Lebenslauf

Sajith Dass	Staatsangehörigkeit: Indien  Geboren am 09.07.1972 in Thopuzha, Bundestaat: Kerala, Land: Indien  Eltern: Mr. Thulasi Dass and Mrs:Lalitha Dass
1978-1988	Primary and secondary School education, St.Xaviers Boys High School, Bangalore, Indien.
1988-1990	Pre-University Course (PUC), St.Josephs college of Arts and Science, Bangalore, Indien.
1990-1993	Bachelor of Science (B.Sc) St.Josephs college of Arts and Science, Bangalore, Indien.
1993-1995	Master of Science (M.Sc) - Biochemie Maharaja Sayajirao University (MSU) of Baroda, Gujarat, Indien.  M.Sc thesis bei Herrn Dr. Naresh Kumar am Department für Biochemie der MSU, Baroda, Indien.  Titel: Role of „Nif A” in the excision of the “nif-D element” of <i>Anabaena Sp. Strain PCC 7120</i> in <i>Rhizobium</i> .
1996 – 2000	Wissenschaftlicher Mitarbeiter 1996-1998 Centre for Biotechnology, Department of Microbiology, MSU, Baroda, Indien.  1999-2000 National Centre for Biological Sciences (NCBS), Bangalore, Indien.
Seit 2001	Doktorarbeit bei Herrn Prof. Dr. Siegfried Roth, am Institut für Entwicklungsbiologie der Universität zu Köln

## 10 Acknowledgements

It was both a honour and privilege to have had the opportunity to be in the same building even as the Late Prof. Jose Campos Ortega.

I would like to express my gratitude to Prof. Siegfried Roth for his guidance and mentorship during my thesis time here. Prof. Maria Leptin for having given me an opportunity to be in Koeln as part of the Graduiertenkolleg.

Gratitude to Prof.Martin Huelskamp, Dr. Thomas Klein and Dr.Veit Riechmann for being members of the examination committee.

Thanks to Dr.Christian Boekel, Dr.Christian Ghiglione and Frau Andrea Klaes, for sharing scientific reagents with me.

Warm regards to Claudia Wunderlich, Martin Technau and Bhupendra Shrivage for being more than just wonderful colleagues, for being great friends.

Thanks is also due to Dr. Thomas Wunderlich for being a wonderful friend and a great house mate.

Best regards to all the past and present members of Roth AG in particular, and of the entire Institut für Entwicklungsbiologie in general for providing a very good atmosphere.

I shall not list the people by names because the list tends to be endless.

Last but not least I would also like to express my gratitude to my family who have always been there for me, good times and bad, especially my mother who has been my source of strength.

Finally thanks to my Cologne exposure I am now aware of the three Ks of life:

Karneval, Kicken und Koelsch....in that order.